



REFERENCE ONLY

UNIVERSITY OF LONDON THESIS

Degree *PhD*

Year *2006*

Name of Author *Jones, R M*

COPYRIGHT

This is a thesis accepted for a Higher Degree of the University of London. It is an unpublished typescript and the copyright is held by the author. All persons consulting the thesis must read and abide by the Copyright Declaration below.

COPYRIGHT DECLARATION

I recognise that the copyright of the above-described thesis rests with the author and that no quotation from it or information derived from it may be published without the prior written consent of the author.

LOANS

Theses may not be lent to individuals, but the Senate House Library may lend a copy to approved libraries within the United Kingdom, for consultation solely on the premises of those libraries. Application should be made to: Inter-Library Loans, Senate House Library, Senate House, Malet Street, London WC1E 7HU.

REPRODUCTION

University of London theses may not be reproduced without explicit written permission from the Senate House Library. Enquiries should be addressed to the Theses Section of the Library. Regulations concerning reproduction vary according to the date of acceptance of the thesis and are listed below as guidelines.

- A. Before 1962. Permission granted only upon the prior written consent of the author. (The Senate House Library will provide addresses where possible).
- B. 1962 - 1974. In many cases the author has agreed to permit copying upon completion of a Copyright Declaration.
- C. 1975 - 1988. Most theses may be copied upon completion of a Copyright Declaration.
- D. 1989 onwards. Most theses may be copied.

This thesis comes within category D.

This copy has been deposited in the Library of

UCL

This copy has been deposited in the Senate House Library, Senate House, Malet Street, London WC1E 7HU.

**Regulation and function of the *INK4a/ARF* tumour suppressor
locus**

Rebecca Jones

Thesis submitted towards the degree of Doctor of Philosophy

University of London

2005

University College London

Gower Street

London

Cancer Research UK

Lincoln's Inn Fields

London

UMI Number: U592119

All rights reserved

INFORMATION TO ALL USERS

The quality of this reproduction is dependent upon the quality of the copy submitted.

In the unlikely event that the author did not send a complete manuscript and there are missing pages, these will be noted. Also, if material had to be removed, a note will indicate the deletion.



UMI U592119

Published by ProQuest LLC 2013. Copyright in the Dissertation held by the Author.
Microform Edition © ProQuest LLC.

All rights reserved. This work is protected against
unauthorized copying under Title 17, United States Code.



ProQuest LLC
789 East Eisenhower Parkway
P.O. Box 1346
Ann Arbor, MI 48106-1346

Summary

The *CDKN2a* locus encodes two important tumour suppressors, p16^{INK4a} and ARF. The two genes share a common exon which is translated in different reading frames. p16^{INK4a} binds to CDK4 and CDK6, preventing them from forming active complexes with D cyclins. As a result, pRb does not undergo the phosphorylation necessary for the transition from the G1 to S phase of the cell cycle. ARF inhibits the ubiquitination of p53 by MDM2, thereby causing the accumulation of p53.

There is a growing awareness that the *CDKN2a* locus plays a central role in the cellular defences against transformation, and in the cellular response to stress. For example, p16^{INK4a} is involved in senescence, a permanent cell cycle arrest triggered in primary human fibroblasts in response to many stresses, including the overexpression of oncogenes. However, little is known about the regulation of p16^{INK4a} under these circumstances, and work in this thesis investigates this issue using overexpression of Myc as a model.

The thesis also describes the characterisation of human diploid fibroblasts (Milan cells) from a patient homozygous for the R24P mutation of p16^{INK4a}. As this mutation is in exon 1 α , ARF is unaffected. The mutant p16^{INK4a} cannot bind to CDK4, but retains some capacity to bind to CDK6. Milan cells have also been used in combination with shRNA targeting ARF to investigate the relative roles of p16^{INK4a} and ARF in the prevention of transformation. A panel of Milan cells were produced expressing telomerase, with combinations

of Myc, Ras and shRNA targeting ARF, and the ability of the cells to grow in soft agar was assessed. A similar panel of Milan expressing p53 shRNA was also built up. These cells were used to investigate whether ablation of ARF can substitute for the loss of p53 function often associated with transformation, and to help identify which aspects of the p53 pathway are activated in the defence against transformation.

Acknowledgments

Many thanks to my supervisor Gordon Peters, for the opportunity to work in his lab, and for all his help and support during the last four years.

Thanks to all members of the lab, past and present that I have had the opportunity to work with, with special thanks to the following people:

To Janice and Sharon, who run an exceptionally organised lab and have patiently provided seemingly endless amounts of wisdom, practical help and support.

To Helen and Elaine, for giggling with me through the good times, and providing me with tea and a sympathetic ear through the bad times. It was fun.

For my many friends and family, who have understood it was correct etiquette to ask after the health of my cells, and who have patiently listened to tales of mould and experiments gone wrong, and for the most part managed to look interested.

To Tim, for many things, not least for technical IT support, and providing portable internet access. There are pluses to having your very own 'IT expert', and I appreciate it greatly.

Finally, and most importantly to Mum, Dad, Mark (and Quang), for supporting me for many years, allowing me to reach this point, and helping me through the whole PhD process. I promise I will leave home eventually.

Table of contents

Title Page	1
Summary	2
Acknowledgments	4
Table of contents	5
List of figures and tables	9
Abbreviations	13
Introduction	18
1.1 General	18
1.2 <i>CDKN2a</i> locus	20
1.3 Functions of ARF	22
1.4 Functions of p16 ^{INK4a}	25
1.5 Senescence and stasis	32
1.6 Regulation of <i>INK4a</i> and <i>ARF</i>	42
1.7 Relative roles of <i>INK4a</i> and <i>ARF</i>	45
Materials and Methods	53
2.1 Solutions	53

2.2	Cell culture	58
2.3	Protein biochemistry	65
2.4	DNA techniques	72
2.5	RNA techniques	80
Regulation of the <i>CDKN2a</i> locus in response to Myc		83
3.1	The effect of Myc overexpression on p16 ^{INK4a} and ARF	84
3.2	The role of p16 ^{INK4a} in the arrest of HDFs in response to overexpressed Myc	87
3.3	Factors affecting the ability of Myc to activate p16 ^{INK4a} transcription	90
3.4	The contribution of Myc to the endogenous levels of p16 ^{INK4a} in fibroblasts	92
3.5	Is the <i>CDKN2a</i> locus co-ordinately regulated in response to Myc?	94
3.6	Timecourse of p16 ^{INK4a} induction by Raf-ER	101
3.7	Increase in p16 ^{INK4a} protein levels in response to Myc and Raf at an individual cell level	103
3.8	Is cell division necessary for the induction of <i>INK4a</i> expression in response to Myc?	110
3.9	The effects of 5-azacytidine on p16 ^{INK4a} expression	112
3.10	Discussion	115

Characterisation of the Milan fibroblast strain	119
4.1 Investigating the functionality of ARF in Milan cells	122
4.2 Ability of the R24P variant of p16 ^{INK4a} to bind to CDK4 and CDK6	124
4.3 Composition of p16 ^{INK4a} and cyclin D1 complexes in senescent Milan cells	126
4.4 Analysis of the function of the R24P variant of p16 ^{INK4a}	128
4.5 Effects of pRb and p53 ablation on the lifespan of Milan fibroblasts	131
4.6 The effects of Bmi-1 on the lifespan of Milan fibroblasts	135
4.7 The effects of expression of exogenous CDK4 and CDK6 on the lifespan of Milan fibroblasts	137
4.8 The ability of kinase dead CDK4 and CDK6 to extend the lifespan of HDFs	139
Transformation of p16^{INK4a}-deficient Milan fibroblasts	144
5.1 The effect of oncogenic Ras on the proliferation of Milan fibroblasts	144
5.2 The transformation potential of p16 ^{INK4a} -deficient fibroblasts	146
5.3 Generation of a panel of Milan Tert cells expressing combinations of Myc, Ras and shRNA targeting ARF	147
5.4 Generation of a panel of Milan Tert cells expressing combinations of Myc, Ras and shRNA targeting p53	150
5.5 The effect of ARF knockdown on the proliferation of	153

	Milan fibroblasts	
5.6	Requirement for anchorage independent growth of Milan fibroblasts	153
5.7	The effects of ARF knockdown on the anchorage independent growth of Milan cells	155
5.8	Effects of shRNA against p53 on the anchorage independent growth of Milan cells	158
	Discussion	162
6.1	The significance of the R24P variant of p16 ^{INK4a}	162
6.2	The role of CDK4 and CDK6 inhibition at senescence	165
6.3	The importance of p16 ^{INK4a} and ARF in the cellular defences against transformation	166
6.4	Senescence as a tumour suppressive mechanism <i>in vivo</i>	175
6.5	Concluding remarks	177
	References	178

List of Figures and Tables

Introduction

Figure 1.1	Structure of the <i>CDKN2a</i> and <i>CDKN2b</i> loci	21
Figure 1.2	p53-MDM2 loop	24
Figure 1.3	G ₀ to S phase transition in mammalian cells	26
Figure 1.4	Diagrammatic representation of subunit rearrangement triggered at senescence	29
Figure 1.5	Summary of the pRb and p53 pathways	31
Figure 1.6	Curves showing the behaviour of HDFs, MEFs and HMECs while undergoing growth in tissue culture	37
Figure 1.7	Senescence can be invoked by a variety of stimuli	40
Figure 1.8	Schematic illustrating the p16 ^{INK4a} -ARF proteins expressed by the Leiden and Q34 cells	50

Materials and Methods

Table 2.1	Antibodies	70
Table 2.2	Oligonucleotide primers used for sequencing	78
Table 2.3	Oligonucleotides used as Q-PCR primers	81

Regulation of the *CDKN2a* locus in response to Myc

Figure 3.1	Induction of p16 ^{INK4a} and ARF at the RNA and protein	85
------------	--	----

	level in response to retroviral expression of Myc	
Figure 3.2	The response of HDFs to the overexpression of Myc	88
Figure 3.3	The effects of Max and a MadMyc fusion protein on the induction of p16 ^{INK4a} by Myc	91
Figure 3.4	The contribution of Myc to the basal level of p16 ^{INK4a} in Hs68 fibroblasts nearing the end of their replicative lifespan	93
Figure 3.5	The effects of Myc-ER induction on <i>INK4a</i> and <i>ARF</i> RNA levels over a 24 hour timecourse	95
Figure 3.6	The response of HDFs to the induction of Myc-ER over a timecourse of 11 days	99
Figure 3.7	The effects of Raf-ER induction on <i>INK4a</i> and <i>ARF</i> RNA levels over a timecourse of 11 days	102
Figure 3.8	Induction of p16 ^{INK4a} in response to Myc-ER at the individual cell level over a timecourse of 11 days	104
Figure 3.9	Induction of p16 ^{INK4a} at the single cell level in response to the induction of Raf-ER	108
Figure 3.10	The effects of contact inhibition on the induction of p16 ^{INK4a} in response to Myc-ER	111
Figure 3.11	The effects of treatment with 5-azacytidine on the induction of p16 ^{INK4a} by Myc-ER	113

Characterisation of the Milan fibroblast strain

Figure 4.1	Binding of the R24P variant of p16 ^{INK4a} to CDK4 and CDK6	120
Figure 4.2	Pedigree of the family from which the homozygous carrier	121

of R24P was identified

Figure 4.3	ARF function in Milan fibroblasts	123
Figure 4.4	Binding properties of the R24P variant of p16 ^{INK4a}	125
Figure 4.5	Composition of cyclin D1 and p16 ^{INK4a} complexes in senescent Milan and UZU fibroblasts	127
Figure 4.6	The ability of the R24P variant of p16 ^{INK4a} to inhibit the proliferation of HDFs	129
Figure 4.7	Immunoblot analysis of the expression of exogenous proteins in Milan cells	132
Figure 4.8	The effects of the viral oncoproteins E6 and LT on the behaviour of Milan cells at senescence	134
Figure 4.9	The effects of Bmi-1 on the lifespan of Milan fibroblasts	136
Figure 4.10	The effects of exogenous CDK4 and CDK6 on the lifespan of Milan fibroblasts	138
Figure 4.11	The affinity of kinase dead CDK4 and CDK6 for cyclin D1, p21 ^{CIP1} and p16 ^{INK4a}	140
Figure 4.12	The role of the kinase activity of CDK4 and CDK6 in the lifespan extension caused by exogenous expression of the kinases	143

Transformation of p16^{INK4a}-deficient Milan fibroblasts

Figure 5.1	The response of Milan fibroblasts to the overexpression of oncogenic Ras	145
Figure 5.2	Generation of a panel of Milan cells expressing telomerase, Myc, Ras and shRNA against ARF	148
Figure 5.3	Immunoblot analysis of Milan tert cells expressing	149

combinations of Myc, Ras and ARF shRNA

Figure 5.4	Immunoblot analysis of MT cells expressing combinations of Myc, Ras and p53 shRNA	151
Figure 5.5	Effects of ARF or p53 knockdown on Milan cell proliferation	152
Table 5.1	Anchorage independent growth of Milan Tert cells expressing combination of ARF shRNA, Myc and Ras	154
Figure 5.6	Effect of ARF knockdown on the size of anchorage independent colonies formed by Milan Tert cells	156
Figure 5.7	Effects of ARF knockdown on the anchorage independent growth of Leiden Tert cells	157
Table 5.2	Anchorage independent growth of Milan Tert cells expressing combinations of p53 shRNA, Myc and Ras	159
Figure 5.8	Effects of p53 shRNA on the size of anchorage independent colonies formed by Milan Tert cells	161

Discussion

Table 6.1	Published protocols for the neoplastic transformation of primary human fibroblasts	168
-----------	--	-----

Abbreviations

A_{nm}	absorbance of light (nm)
ATCC	American tissue culture collection
ATP	adenosine 5'-triphosphate
BCA	bicinchoninic acid
blast	blasticidin
bleo	bleomycin
bp	base pair(s)
BrdU	5-bromo-2'-deoxyuridine
BSA	bovine serum albumin
°C	degrees centigrade
CDK	cyclin dependent kinase
cDNA	complementary DNA
CIP	CDK interacting protein
CO ₂	carbon dioxide
DAPI	4',6-diamidine-2-phenylindole dihydrochloride
DMSO	dimethyl sulphoxide
DNA	deoxyribonucleic acid
dNTP	deoxynucleoside 5-triphosphate
E4	Dulbecco's modified Eagle medium
E6	human papilloma virus type 16 E6 protein
E7	human papilloma virus type 16 E7 protein

ECL	enhanced chemiluminescence
EDTA	ethylenediaminetetraacetic acid (sodium salt)
ER	oestrogen receptor
FBS	foetal bovine serum
<i>g</i>	gravity
G ₁	gap phase 1 of the cell cycle
G ₂	gap phase 2 of the cell cycle
H ₂ O ₂	hydrogen peroxide
HA	hemagglutinin
HBS	HEPES buffered saline
HDAC	histone deacetylase
HDF	human diploid fibroblast
HEPES	N-(2-hydroxyethyl)piperazine-N'-(2-ethanesulfonic acid)
HMEC	human mammary epithelial cell
HRP	horseradish peroxidase
hTERT	human telomerase reverse transcriptase
hygro	hygromycin
INK4	inhibitor of CDK4
IP	immunoprecipitation
kb	kilobase
kDa	kilo Dalton
LT	SV40 Large T antigen
LTR	long terminal repeat
M ₀	mortality stage 0

M ₁	mortality stage 1
M ₂	mortality stage 2
MAPK	mitogen-activated protein kinase
MEF	mouse embryonic fibroblast
MEK	MAPK/ERK kinase
M phase	mitosis phase of the cell cycle
NP40	nonidet P40 (octylphenoxy polyoxy ethanol)
PAGE	polyacrylamide gel electrophoresis
PBSA	phosphate buffered saline A
PCR	polymerase chain reaction
PD	population doublings
puro	puromycin
Rb	retinoblastoma protein
RNA	ribonucleic acid
ROS	reactive oxygen species
rpm	revolutions per minute
RT-PCR	reverse transcriptase PCR
SA-βgal	senescence associated β-galactosidase
SAHF	senescence associated heterochromatin formation
SDS	sodium dodecyl sulphate
siRNA	small interfering RNA
shRNA	small hairpin RNA
S phase	DNA synthesis phase of the cell cycle
ss	single stranded
st	SV40 small t antigen

SV40	Simian Virus 40
TEMED	N,N,N',N'-tetramethylethylenediamine
T _m	melting temperature
TRAP	Telomeric Repeat Amplification Protocol
Tris	tris(hydroxymethyl)aminomethane
Tween-20	polyoxyethylenesorbitan monolaurate
UK	United Kingdom
UTR	untranslated region
UV	ultra violet
v/v	volume per volume
WB	western blot
WT	wild-type
w/v	weight per volume
X-gal	5-bromo-5-chloro-3-indolyl-β-D-galactosidase

A	amps
c	centi
g	gram
k	kilo
L	litre
m	metres
m	milli
M	molar (moles per litre)
n	nano
μ	micro

p

pico

Chapter 1

Introduction

1.1 General

Cell proliferation is a tightly regulated process, and a cell integrates many signals both internal and external before committing to divide. Cancer arises when this process becomes deregulated and a clone of cells becomes capable of proliferation in inappropriate circumstances. The evolution of a cancer is often viewed as a Darwinian process, with cells sustaining random mutations, followed by selection for those that are advantageous to the cell. For cancer to occur it has been argued that a cell needs to accumulate between four and seven mutations (Hanahan and Weinberg 2000). These mutations can either inactivate tumour suppressor genes and overcome barriers to proliferation, or activate proto-oncogenes allowing the cell to gain a beneficial characteristic. Mutations in tumour suppressor genes are usually recessive, and in most cases both copies of the gene need to be inactivated before the gained characteristic becomes apparent. However, with some tumour suppressor genes, a mutation in one copy of the gene results in haploinsufficiency with the remaining wild-type allele producing insufficient gene product to maintain a normal phenotype. In contrast, mutation which activate proto-oncogenes are always dominant and have effects on the cell irrespective of the presence of a normal allele.

It has been suggested that cancer-promoting mutations allow a cell to gain six characteristics; a self sufficiency in growth signals, evasion of apoptosis, insensitivity to anti-growth signals, sustained angiogenesis, limitless replicative potential, and tissue invasion and metastasis (Hanahan and Weinberg 2000; Hahn and Weinberg 2002). Other mutations can be regarded as permissive rather than causative and give rise to cancer by promoting the accumulation of advantageous mutations, for example through genomic instability. Formation of a tumour may also be influenced not only by changes to the clone of cells forming the tumour, but also to the surrounding cells which can undergo changes to support the tumour formation for example by neo-vascularisation of the tumour.

While a fascinating subject to study in its own right, it is necessary to understand the process of cancer evolution in order to design appropriate and targeted treatments. Many cancer cells are aneuploid, and have sustained multiple mutations, some of which are necessary for the formation of the cancer, while others may have arisen as a consequence of tumorigenic events. This makes it very difficult to deduce from a cancer cell which mutations are incidental and which are essential. It is therefore attractive to approach the problem from the opposite direction and to investigate the barriers to tumorigenesis present in normal cells and to determine what combination of genetic alterations allows a normal cell to become tumorigenic. Interest in this approach has been renewed as new techniques and resources have become available making it possible to sustain the proliferation of normal cells. This thesis describes an approach using fibroblasts from rare individuals whose

cells are genetically predisposed to form cancers via the loss of a tumour suppressor gene.

1.2 CDKN2a locus

The *CDKN2a*, or *INK4a/ARF* locus, is located on chromosome 9p21 in humans and was first discovered by linkage studies searching for a melanoma susceptibility gene known to be located in this region (Kamb et al. 1994; Nobori et al. 1994; Okamoto et al. 1994; Wainwright 1994; Ranade et al. 1995). As well as being involved in familial melanoma, the locus was subsequently found to be frequently mutated in spontaneous tumours (discussed in more detail below). The product of the locus was initially found to be a 16 kDa protein which had been previously described as an inhibitor of CDK4 (INK4) (Serrano et al. 1993; Xiong et al. 1993), and the protein was named p16^{INK4a}. The locus was officially designated *CDKN2a*, and p16^{INK4a} was found to be encoded by three exons, 1 α , 2 and 3 (1.1). Unusually, the locus was also found to contain another transcript with a separate promoter and first exon, exon 1 β , which was also encoded by exon 2 using a different reading frame (Figure 1.1)(Stone et al. 1995). While initially thought to be another variant of p16^{INK4a}, this transcript was later found to encode a functional protein (Quelle et al. 1995b) which bears no similarity to p16^{INK4a} at the amino acid level. This unusual protein was named ARF, for its use of the alternative reading frame. Within 30 kb of the *INK4a* gene is the *INK4b* gene encoding p15^{INK4b}, another member of the same gene family as *INK4a*, which was first observed during the positional cloning of *INK4a* (Kamb et al.

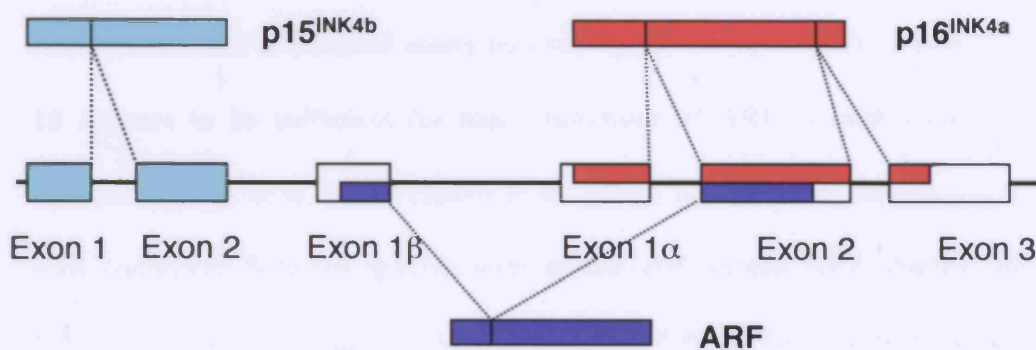


Figure 1.1 Structure of the *CDKN2a* and *CDKN2b* loci

The *CDKN2a* locus encodes the tumour suppressors p16^{INK4a} and ARF. p16^{INK4a} is encoded by exons 1 α , 2 and 3, while ARF is encoded by exons 1 β , and exon 2. The genes have separate promoters, while the common second exon is translated in different reading frames. The *CDKN2b* locus lies upstream of exon 1 β and comprises two exons, exon 1 and exon 2, which encode p15^{INK4b}, a member of the same protein family as p16^{INK4a}.

1994). *INK4b* is encoded by two exons (Figure 1.1), and though to have arisen by gene duplication, accounting for the presence of two members of the gene family within the same chromosomal region.

The structure of the locus is conserved between mouse and humans, but interestingly it was found that while chickens express p15^{INK4b} and ARF, they lack an *INK4a* gene (Kim et al. 2003). It was also observed that differences in the splicing of the chicken gene result in the production of an 60 amino acid ARF protein that is encoded solely by exon 1 β (Kim et al. 2003). Indeed, exon 1 β appears to be sufficient for many functions of ARF in both mouse and humans (Quelle et al. 1997; Llanos et al. 2001), but the gene sequence is not well conserved between species with mouse and human ARF sharing only 50% identity at the amino acid level (Stott et al. 1998). The origin of the ARF protein remains obscure as it bears little resemblance to any known proteins, and any possible advantages of the unusual structure of the *CDKN2a* locus are not immediately apparent.

1.3 Functions of ARF

ARF is a highly basic protein comprising 169 amino acids in mice, (19kDa), and 132 amino acids (14kDa) in humans. ARF is reputed to bind to a variety of cellular proteins including the transcription factors E2F-1, DP1, and Myc (Eymin et al. 2001; Martelli et al. 2001; Datta et al. 2002; Mason et al. 2002; Qi et al. 2004). ARF has also been reported to bind to a wide range of other proteins such as B23, Topoisomerase I, WRN, Ubc9, HIF1- α , TBP-1, Bcl-6, and Pex19p (in mice), and affect a number of cellular processes such as ribosome biogenesis, apoptosis, the response to irradiation and the activity of

the ATR and ATM pathways (Fatyol and Szalay 2001; Karayan et al. 2001; Wadhwa et al. 2002; Itahana et al. 2003a; Sugimoto et al. 2003; Suzuki et al. 2003; Ayrault et al. 2004; Li et al. 2004b; Pollice et al. 2004; Woods et al. 2004; Andrique et al. 2005; Korgaonkar et al. 2005; Rizos et al. 2005; Rocha et al. 2005; Suzuki et al. 2005).

However, the most functionally relevant activity of ARF is to bind to MDM2¹ causing activation of the p53 pathway. In the absence of ARF, MDM2 binds to p53 and acts as an E3 ubiquitin ligase marking p53 for proteasomal degradation. MDM2 also causes relocation of p53 from the nucleoplasm to the cytosol where it is degraded. ARF stabilises p53 by binding to and inhibiting MDM2 (Figure 1.2) (Stott et al. 1998; Sharpless and DePinho 1999; Sherr and Weber 2000; Brooks and Gu 2004) resulting in an accumulation of p53 and the activation of downstream effectors of p53 such as p21^{CIP1}. Several feedback loops govern this pathway, with p53 activating expression of MDM2 and inhibiting the expression of ARF.

However, mice deficient in both p53 and ARF exhibit a different spectrum of tumours than either of the single knockouts alone, and p53 deficient MEFs still arrest in response to overexpressed ARF (Carnero et al. 2000; Weber et al. 2000a). It has been suggested that this provides evidence that ARF can

¹ MDM2 or Murine double minute protein, is often referred to as HDM2 in human cells. However for ease of understanding, during this text it will be referred to as MDM2 regardless of the cell type of origin.

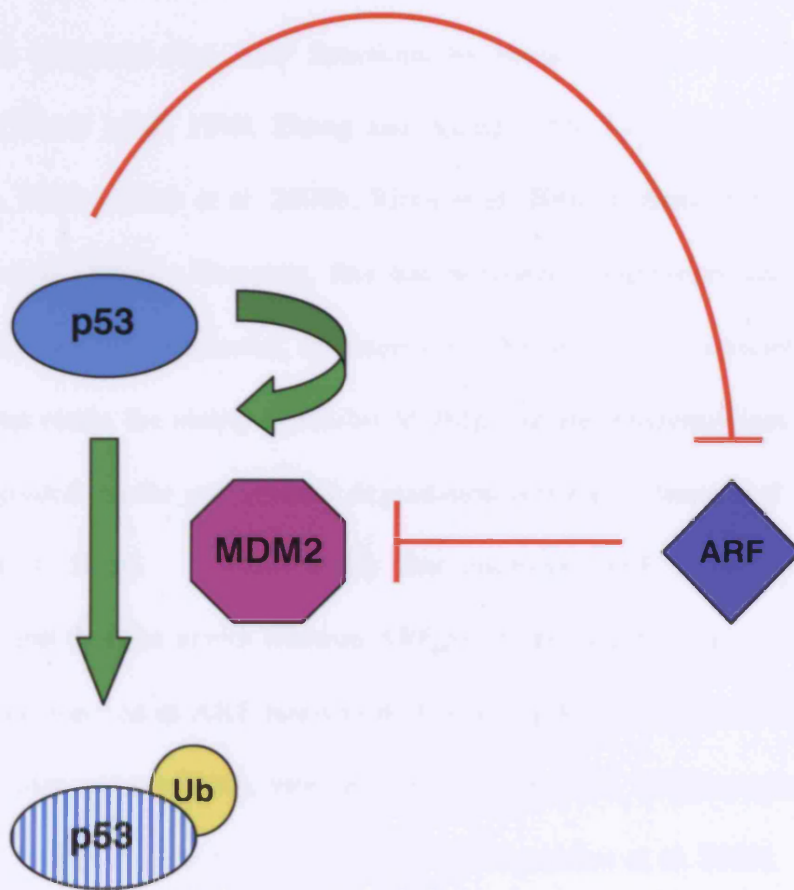
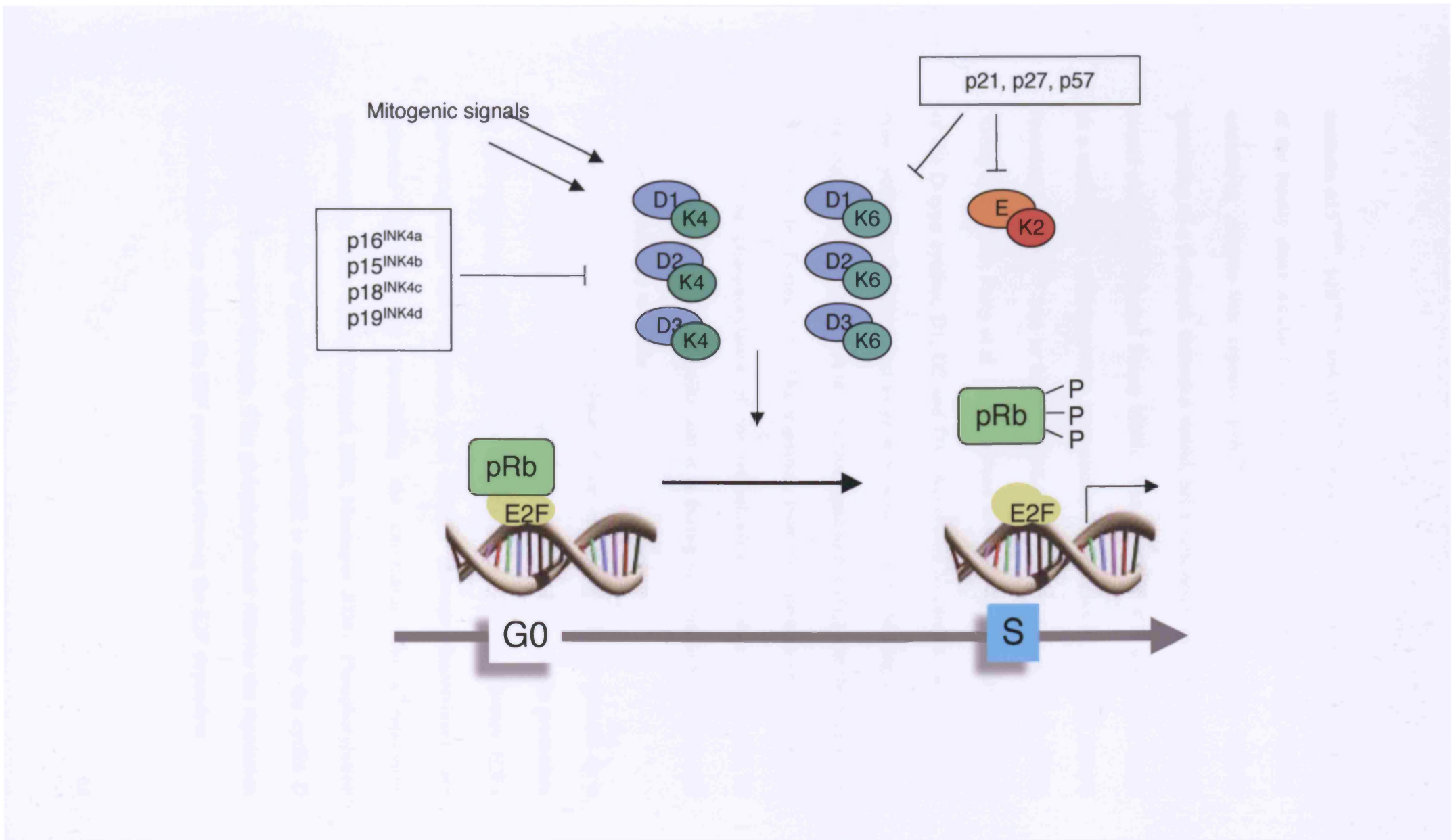


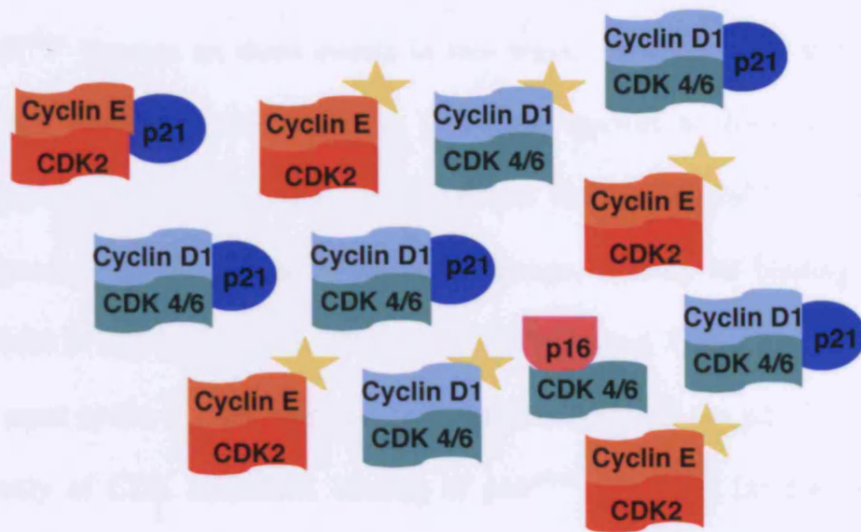
Figure 1.2 p53-MDM2 loop

MDM2 ubiquitinates p53 marking it for degradation. This ubiquitination is inhibited by the binding of ARF to MDM2, causing an accumulation of p53 in response to increased levels of ARF. In turn, p53 negatively regulates the expression of ARF, and positively regulates the expression of MDM2



contains p15^{INK4b}, p18^{INK4c}, and p19^{INK4d} (Ruas and Peters 1998). All members of the family share similar functional properties and are structurally similar, containing ankyrin-like repeats. p16^{INK4a} contains 4 ankyrin-like repeats consisting of a β -strand, extended strand, helix-turn-helix, extended strand, β -strand element (Ruas and Peters 1998). This structure is hypothesised to act as a scaffold for protein-protein interactions. Until recently, the only known function of p16^{INK4a} was to bind to CDK4 and CDK6 (Serrano et al. 1993; Xiong et al. 1993; Parry et al. 1995; Serrano et al. 1995), the catalytic partners of the D-type cyclins, D1, D2 and D3. According to current models, the D-type cyclins are thought to act as growth factor sensors (Massague 2004), and are required for the transition of cells from quiescence (G_0) into the S-phase of the cell cycle (Figure 1.3). The transition from G_0 , through G_1 , to S phase involves the phosphorylation of the retinoblastoma protein (pRb), and its family members, p107 and p130, and it is during this transition that the cell becomes committed to divide.

At the beginning of the G_1 phase of the cell cycle, pRb is present in a hypophosphorylated state. In this state, the protein is present at the promoters of E2F responsive genes bound to E2F proteins. This inactivates E2Fs converting them into repressors, and HDACs (histone deacetylases) are recruited to these loci remodelling the chromatin into a repressive conformation (Sherr and McCormick 2002; Massague 2004). Phosphorylation of the pRb family of proteins by cyclin/CDK is undertaken by the cyclin D and cyclin E dependent kinases. This phosphorylation relieves the repression by causing pRb to release the E2F proteins, allowing the E2F-dependent



Increased p16

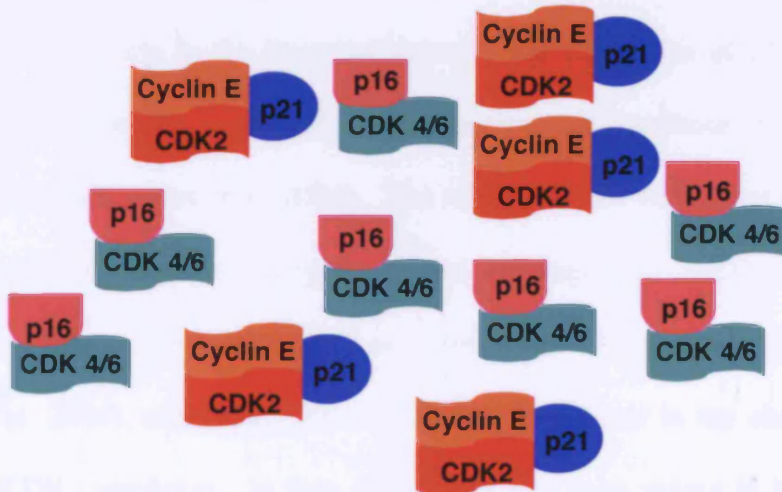


Figure 1.4 Diagrammatic representation of subunit rearrangement triggered at senescence

When levels of p16^{INK4a} increase, the binding of p16^{INK4a} to CDK4 and CDK6 displaces p21^{CIP1} which is then free to bind to Cyclin E/CDK2 complexes inhibiting their function. (Active Cyclin-CDK complexes are denoted by the presence of a yellow star.)

transcription which is required for cell cycle progression.

p16^{INK4a} impacts on these events in two ways. p16^{INK4a} binds to CDK4 and CDK6 preventing their binding to D-type cyclins to form active kinase complexes. This inhibition occurs because binding of p16^{INK4a} to the cyclin-dependent kinase causes an allosteric change, altering its binding site with Cyclin D and reducing its affinity for ATP (Pei and Xiong 2005). However, as most cyclin D-CDK complexes contain members of the p21^{CIP1} and p27^{KIP1} family of CDK inhibitors, binding of p16^{INK4a} to Cyclin D/CDK complexes displaces p21^{CIP1} and p27^{KIP1}. In turn, these CDK inhibitors are redistributed to CDK2/Cyclin E complexes and CDK2/Cyclin A complexes respectively, causing inhibition of these complexes (Figure 1.4) (Ortega et al. 2002).

However, this is a simplistic view of the regulation of the G₁ to S phase transition, and recent observations suggest that the situation is more complex. Recent reports in the literature describe the generation of CDK4 and CDK6 double-knockout mice, and D-type cyclin triple knockout mice (Kozar et al. 2004; Malumbres et al. 2004). The mice were not viable, but died after many organs had already undergone normal development. MEFs from these mice were able to proliferate, albeit at a slower rate (Kozar et al. 2004; Malumbres et al. 2004), suggesting that cell division can occur in the absence of Cyclin D/CDK complexes. In turn, CDK2 has also been shown to be non-essential for cell proliferation (Berthet et al. 2003). While some compensation by the remaining Cyclin/CDK complexes has been observed in cells from these knockout mice, some evidence suggests that there may be other mechanisms that can control the G₁ to S phase progression. However, the consensus model still forms a relevant framework for considering new advances.

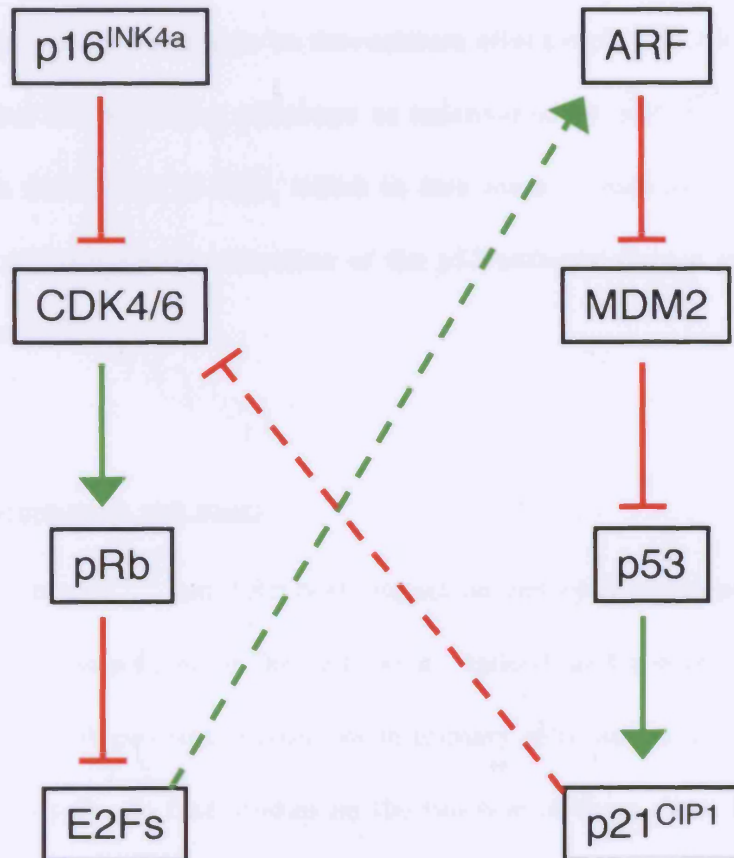


Figure 1.5 Summary of the pRb and p53 pathways

The pRb and p53 pathways are linked by the activation of ARF transcription by E2F-1, and the inhibition of CDK4 and CDK6 by p21^{CIP1}. (Inhibitory interactions are shown in red, and interactions which promote the function of a protein are shown in green.)

Thus, elevated expression of p16^{INK4a} causes cells to arrest in the G₁ phase of the cell cycle, an arrest which is dependent on the presence of functional pRb. Overexpression of ARF also causes a cell cycle arrest by stabilising p53 resulting in an increase in its downstream effector p21^{CIP1}. ARF also links the p53 and Rb signalling pathways as inactivation of pRb by phosphorylation causes the release of E2F, which in turn leads to increased transcription of ARF and subsequent activation of the p53 pathway (James and Peters 2000) (Figure 1.5).

1.5 Senescence and stasis

Although p16^{INK4a} and ARF both impact on cell cycle regulation, they are not essential components of the cell cycle. Indeed, under normal circumstances levels of both proteins remain low in primary cells and do not fluctuate during the cell cycle. In fact, studies on the function of these genes in primary cells led to the realisation that the *CDKN2a* locus was implicated in senescence and the cellular defences against stress (Ruas and Peters 1998; Drayton and Peters 2002).

Tumour cell lines containing genetic aberrations are immortal and their growth in tissue culture can be continued indefinitely. In the 1960s it became apparent that in contrast, cultures of primary human diploid fibroblasts (HDFs) which were genetically 'normal' had a finite lifespan (Hayflick and Moorhead 1961; Hayflick 1965). Depending on the individual and tissue from which the fibroblasts were derived, cultures of HDFs typically undergo between 60 and 80 divisions before undergoing an irreversible arrest in the G₁ phase of the cell cycle (Mathon and Lloyd 2001). This arrest is named

replicative senescence or Mortality Stage 1 (M1) (Figure 1.6). Cells which have undergone senescence are metabolically stable and continue to be viable. The arrest is accompanied by phenotypic changes in the cell, which becomes larger taking on a flattened appearance. The arrest is also accompanied by an increase in endogenous β -galactosidase activity (which is commonly used as a marker of senescence), increased production of extracellular matrix, a more prominent nucleolus and an altered gene expression profile (Ruas and Peters 1998; Mathon and Lloyd 2001). Senescence in HDFs can also be accompanied by the formation of senescence associated heterochromatin foci (SAHF) suggesting widespread changes in gene expression that are controlled at the level of chromatin structure (Narita et al. 2003). The formation of SAHF is dependent on pRb and may silence E2F responsive promoters.

Strains of fibroblasts seem to retain a 'memory' of the number of cell divisions they have undergone, as they always undergo senescence after a predetermined number of cell divisions even if the replication of the cells has been temporarily halted. This suggests that fibroblasts must have an intrinsic counting mechanism which triggers senescence, and the most likely candidate for this internal clock is the telomeres. The telomeres comprise units of TTAGGG repeats located on the ends of all chromosomes, which are bound by specialised binding proteins (Stewart and Weinberg 2002). The telomere consists of several kilobases of double stranded DNA with a 3' overhang comprising several hundred bases of single-stranded (ss) DNA (Ben-Porath and Weinberg 2004). This single-stranded DNA is protected from the cellular machinery which recognises ssDNA as damaged DNA, by the formation of a protective T-loop structure where the ssDNA invades the double-stranded

DNA 5' of the stretch of single-stranded DNA (Ben-Porath and Weinberg 2004). This structure is stabilised by the binding of telomere binding proteins such as TRF1, TRF2 and POT1.

During DNA replication, the lagging strand is replicated by the use of Okazaki fragments to prime the replication of this strand. However, this strategy cannot completely replicate the telomeres, and due to this end replication problem, successive cell divisions lead to erosion of the telomeres (Stewart and Weinberg 2002). It is thought that senescence is not triggered by telomeres reaching a critically short length, rather it is the 'uncapping' of the telomere or the disruption of the structure at the end of the telomere which is responsible for triggering the arrest (Karlseder et al. 2002; Ben-Porath and Weinberg 2004). This has been confirmed using oligonucleotides homologous to the telomere 3' overhang to mimic disruption of the telomere structure which results in a senescence-like arrest (Li et al. 2003; Li et al. 2004a). The structure of the T loop can also be disturbed using a dominant negative form of the telomere binding protein TRF2, which triggers senescence in HDFs (de Lange 2002). After disruption of the T loop structure the unprotected telomere end is seen as damaged DNA, and this triggers a DNA damage checkpoint response.

As cells reach senescence they accumulate DNA damage foci at the telomeres. These foci are similar to those seen at the site of DNA double strand breaks and contain several markers of DNA damage including phosphorylated histone H2AX, 53BP1, MDC1, NBS1, Rad17, Mre11 and ATM (d'Adda di Fagagna et al. 2003; Takai et al. 2003). Subsequent signalling occurs through the ATM/Chk2 DNA damage pathway activating

the p53 and p21^{CIP1} pathway, although signalling can occur through the ATR pathway at a lower efficiency if ATM is disabled (d'Adda di Fagagna et al. 2003; Takai et al. 2003; Gire et al. 2004; Herbig et al. 2004).

In addition to the accumulation of p21^{CIP1} observed at senescence there is also an increase in p16^{INK4a} at senescence (Alcorta et al. 1996; Hara et al. 1996). Whilst the involvement of p21^{CIP1} in the arrest triggered by a signal from the telomeres is universally agreed upon, the involvement of p16^{INK4a} is more controversial. Several reports in the literature demonstrate that p16^{INK4a} expression is upregulated via an unidentified pathway in response to a signal from the telomeres at senescence (de Lange 2002; Smogorzewska and de Lange 2002; Jacobs and de Lange 2004), but other labs present conflicting evidence (Herbig et al. 2004). The differences between different reports may be due to the kinetics of the response, with p16^{INK4a} being activated significantly after p21^{CIP1} (Alcorta et al. 1996), or may be due to the difference in oxygen levels in which the cells were cultured in different studies, with p16^{INK4a} playing a more prominent role under conditions in which the cells are oxidatively stressed.

The arrest of HDFs at replicative senescence can be overcome, for example by expression of the viral oncoprotein SV40 Large T antigen, or a combination of the Human Papilloma virus oncoproteins E6 and E7. Both strategies disable the pRb and p53 pathways, and the culture continues to divide before entering a second stage termed crisis or Mortality stage 2, M2 (Figure 1.6). Here cells attempt to replicate but unsuccessful cell division results in cell death (Wright et al. 1989; Bond et al. 1999; Wei and Sedivy 1999). This is due to continued telomere erosion resulting in the formation of chromosomal fusions and the

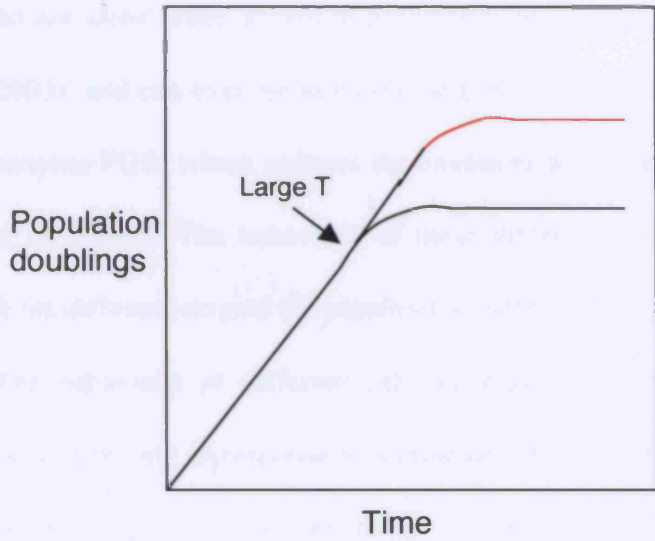
breakage of chromosomes, which eventually trigger apoptosis. The role of the telomeres in senescence is confirmed by the ability of exogenous hTERT, the catalytic subunit of the telomerase gene, to allow fibroblasts to bypass the senescence arrest (Bodnar et al. 1998; Vaziri and Benchimol 1998).

However, not all cell types can be immortalised by expression of hTERT. Human epithelial cells such as mammary or prostate epithelial cells undergo an arrest before reaching senescence, termed M0. Cells escaping this arrest are found to have silenced p16^{INK4a} expression by methylation (Brenner et al. 1998; Foster et al. 1998; Huschtscha et al. 1998; Jarrad et al. 1999). After overcoming this arrest, cultures continue growing until they undergo a telomere-based arrest which has been proposed to be M2 (Romanov et al. 2001) (Figure 1.6). Human epithelial cells can be immortalised by the expression of hTERT providing they have bypassed M0. Unlike human cells, mouse somatic cells express telomerase and have relatively long telomeres (Sherr and DePinho 2000). However, mouse embryonic fibroblasts undergo only a few population doublings in culture before undergoing an arrest (Figure 1.6), suggesting that telomere attrition is not responsible for this arrest. The spontaneous outgrowth of immortal clones happens with a much higher frequency than in cultures of human cells, and usually results from the loss of ARF or p53.

These observations suggest that cells grown using conventional tissue culture techniques are being subjected to stress causing activation of cell cycle inhibitors such as p16^{INK4a} and ARF. If this was true, the arrest could be avoided by reducing the stress to which the cells are subjected. The M0 arrest of human epithelial cells can be bypassed by growing cells on feeder layers

Figure 1.6 Curves showing the behaviour of HDFs, MEFS, and HMECS while undergoing growth in tissue culture

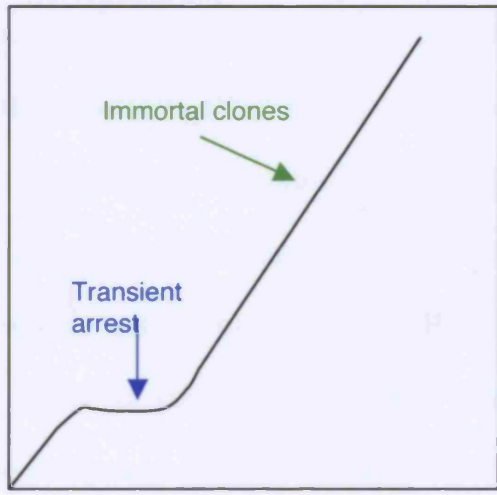
Human diploid fibroblasts (HDFs) arrest at M1, but upon ablation of the p53 and pRb pathways can continue growing until they reach crisis. Mouse embryonic fibroblasts (MEFs) undergo a stress induced arrest from which immortal clones arise with a high frequency, while human mammary epithelial cells (HMECs) undergo a stress induced arrest called M0 which can be overcome by methylation of p16^{INK4a}, or growth in more favourable culture conditions. This allows HMECs to continue growing until they undergo a telomere based arrest.



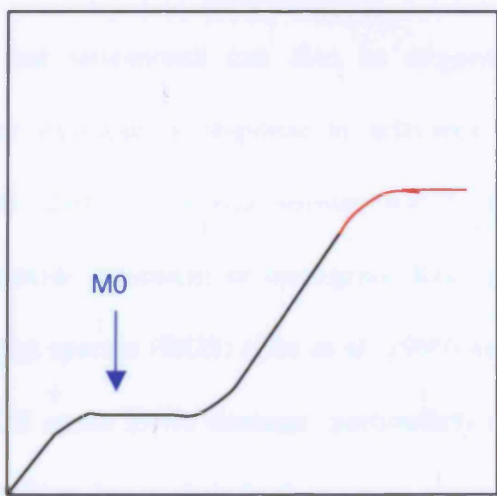
Crisis (M2)

M1

HDFs



MEFs



M1/M2?

HMECs

(Herbert et al. 2002). Senescence in MEFs is due to oxygen sensitivity as they do not arrest when grown in physiological oxygen conditions (Parrinello et al. 2003), and can even be immortalised by increased expression of the glycolytic enzyme PGM which reduces the oxidative stress suffered by the cells (Kondoh et al. 2005). The behaviour of these different cell types illustrates that cells from different origins are sensitive to differing sources of stress.

The behaviour of different cell types in culture shows that senescence can occur not only in response to a critically short telomere, but also in response to other triggers. It is becoming increasingly clear that the induction of senescence is a programme which can be put into action in response to a variety of cellular stresses (Figure 1.7). When cells suffer from stress or damage, they can decide to undergo a transient cell cycle arrest, apoptosis or stasis (a senescence-like arrest triggered by stress) (Ben-Porath and Weinberg 2004). Senescence can be triggered in young cells by a variety of acute stresses such as culture shock, DNA damage, histone deacetylase inhibitors, and by oxidative damage such as treatment with H₂O₂ or hyperoxia (Figure 1.7) (Campisi 2001). More relevant for a role in tumour suppression is the observation that senescence can also be triggered by aberrant oncogenic signalling, for example in response to activated Ras (Serrano et al. 1997; Drayton et al. 2003). Several stimuli which trigger senescence such as hydrogen peroxide treatment or oncogenic Ras can cause the production of reactive oxygen species (ROS) (Lee et al. 1999) and it has been hypothesised that these ROS cause DNA damage, particularly in the telomeres which are especially sensitive due to their high guanine content (Wright and Shay 2002).

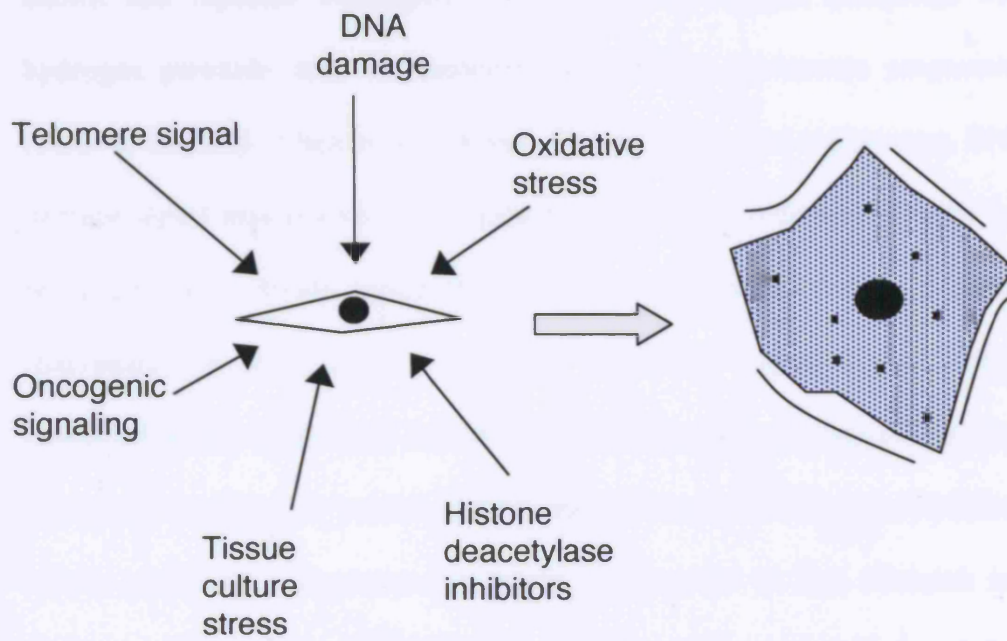


Figure 1.7 Senescence can be invoked by a variety of stimuli

Indeed long telomeres increase the sensitivity of cells to hydrogen peroxide treatment (Rubio et al. 2004).

It is becoming clear that exposure to more than one form of stress, or repeated exposure to stress, is necessary to trigger senescence. Some studies have shown that repeated onslaughts, such as two subsequent treatments with hydrogen peroxide, may be needed to activate the senescence programme (Chen et al. 2001; Chen et al. 2004a). During replicative senescence, DNA damage signal may need to be coupled to mitogenic stimulation with the cell being primed to divide before the senescence programme can be triggered (Satyanarayana et al. 2004). A recent report has suggested that freshly explanted human fibroblasts do not arrest in response to oncogenic Ras, and that previous culture or oxidative stress may be needed to sensitise fibroblasts before premature senescence can occur in response to Ras (Benanti and Galloway 2004). This suggests that cellular stress may need to reach a threshold level before a programme of senescence is implemented. It has been shown that within a culture cells undergo senescence at different times, probably in response to different stimuli, and this would reflect the differing levels of stress that individual cells have been subjected to (Brookes et al. 2004; Herbig et al. 2004; Martin-Ruiz et al. 2004).

Whilst many of the circumstances leading to activation of the senescence programme are known, it is unknown how the senescence programme is triggered at the biological level. It has been proposed that stimuli could converge on a common pathway which triggers senescence and one candidate for this is the MAPK p38 (Iwasa et al. 2003). However, it remains clear that implementation of the arrest involves p16^{INK4a} and ARF.

1.6 Regulation of *INK4a* and *ARF*

The *CDKN2a* locus obviously responds to stress signals, but the mechanism by which the locus is regulated remains unclear. ARF expression is activated in mouse and human cells in response to a variety of factors including Myc, β -catenin, AP-1 dimers, and the viral oncoprotein E1A, while Dmp1, Abl and oncogenic Ras can cause expression of ARF in mouse cells (de Stanchina et al. 1998; Palmero et al. 1998; Radfar et al. 1998; Zindy et al. 1998; Inoue et al. 1999; Schmitt et al. 1999; Damalas et al. 2001; Ameyar-Zazoua et al. 2005; Sreeramaneni et al. 2005). Most intriguing is the activation of ARF expression by E2F-1 (Bates et al. 1998; Dimri et al. 2000) which links the p53 and Rb signalling pathways (Figure 1.5). Inactivation of pRb by phosphorylation causes the release of E2F, which in turn leads to increased transcription of ARF and subsequent activation of the p53 pathway (James and Peters 2000). This may have implications for viruses which would need to disable the pRb pathway to drive cell proliferation, but may also need to disable the p53 response which would be consequently activated. New work has shown that in addition to the activation of ARF expression by E2F1, another member of the E2F family, E2F3b, may repress ARF expression in normally proliferating mouse fibroblasts (Aslanian et al. 2004), and ARF expression is activated in cells in which E2F3b is lost. However, it remains clear that aberrant E2F activity results in the activation of ARF.

ARF expression in mouse and human cells can also be repressed by a variety of agents in addition to pRb and E2F3b, including feedback by p53, Twist, Tbx2, Tbx3 and the polycomb group genes Cbx7 and Bmi1, while ARF repression by Twist has been demonstrated in mouse cells (Robertson and

Jones 1998; Jacobs et al. 1999a; Maestro et al. 1999; Jacobs et al. 2000; Lingbeek et al. 2002; Aslanian et al. 2004; Gil et al. 2004; Maeda et al. 2005).

Indeed the ability of Bmi1 to cooperate with Myc in mouse lymphomagenesis has been attributed to its effects on ARF expression (Jacobs et al. 1999b).

Expression of *INK4a* is also repressed by the polycomb group proteins Bmi-1, and Cbx7 (Jacobs et al. 1999a; Itahana et al. 2003b; Gil et al. 2004). The *CDKN2a* locus is clearly subject to epigenetic silencing by DNA methylation during cancer (Herman et al. 1995; Merlo et al. 1995; Otterson et al. 1995; Costello et al. 1996; Lo et al. 1996) and this, in combination with the involvement of polycomb group proteins, suggests that repression of the locus is mediated by chromatin remodelling. Consistent with this suggestion, it has been proposed that cells exposed to histone deacetylase inhibitors undergo accelerated senescence, and a senescence specific form of HDAC-2 has been described (Wagner et al. 2001; Munro et al. 2004). The physiological importance of repression of the locus is demonstrated by the proliferative defects observed in Bmi1-deficient haematopoietic stem cells which is due to derepression of the *CDKN2a* locus in these cells (Leesard and Sauvageau 2003; Park et al. 2003). There is also evidence that p16^{INK4a} is repressed by pRb in human cells (Hara et al. 1996), and the direct binding of Tbx2, Tbx3 and TAL1-SCL to the *INK4a* promoter represses transcription (Jacobs et al. 2000; Lingbeek et al. 2002; Hansson et al. 2003).

It is well established that expression of oncogenic Ras activates p16^{INK4a} expression both by activation of the MKK3/6-p38 MAPK pathway (Wang et al. 2002; Deng et al. 2004), and by the well documented activation of the Ras-Raf-MEK pathway (Serrano et al. 1997; Ohtani et al. 2001), resulting in

binding of Ets2 to the *INK4a* promoter and subsequent activation of transcription. Ets proteins are also implicated in the control of p16^{INK4a} expression at senescence. In older fibroblasts Ets1 replaces Ets2 at the p16^{INK4a} promoter, and Ets1 has been reported to increase in aging rodent cells causing transcription of both p16 and ARF (Krishnamurthy et al. 2004). The activation of p16^{INK4a} transcription by the Ets proteins is antagonised by Id1, which is downregulated at senescence, as is its affinity of binding to E47 which itself binds to an E box region in the p16^{INK4a} promoter (Alani et al. 2001; Ohtani et al. 2001; Zheng et al. 2004). Several other factors have also been reported to activate p16^{INK4a} transcription including junB, Snf5, Myc, p21^{CIP1} and Sp1, 14-3-3 σ , and a dominant negative form of the telomere binding protein TRF2 (Dellambra et al. 2000; Passegue and Wagner 2000; Betz et al. 2002; Smogorzewska and de Lange 2002; Drayton et al. 2003; Oruetebarria et al. 2004; Xue et al. 2004).

p16^{INK4a} RNA is known to be very stable (Hara et al. 1996), and recent evidence suggests the RNA may be even more stable at senescence due to a decrease in the binding of AUF1, a protein implicated in decreasing mRNA stability, to a region in the 3' UTR of the mRNA (Hara et al. 1996; Wang et al. 2002). Recent research has suggested that in addition to regulation at the level of *INK4a* transcription, p16^{INK4a} can also be post-translationally modified. p16^{INK4a} can be phosphorylated on serines 7, 8, 140 and 152. Endogenous p16^{INK4a} associated with CDK4 was shown to be phosphorylated on position 152, although this does not affect its ability to bind to CDK4 (Gump et al. 2003). Although, p16^{INK4a} is naturally lysine-less, it can be

degraded by the ubiquitin system, potentially via N terminal ubiquitination (Ben-Saadon et al. 2004).

1.7 Relative roles of *INK4a* and *ARF*

The structure of the *CDKN2a* locus is conserved between humans and mice. This led to the use of mouse knockout experiments to address the relative contributions of the *INK4a* and *ARF* genes to tumour suppression. The initial mouse model lacked exon 2, which therefore affected both products of the locus (Serrano et al. 1996). These mice were viable, but developed tumours at an early age (average 29 weeks), and had an increased sensitivity to carcinogenic treatment. The fibroblasts from these knockout mice did not undergo senescence and were transformed by the expression of a single oncogene, H-Ras, in contrast to wild-type MEFs which require the expression of two cooperating oncogenes for transformation. However, although exon 1 β is sufficient for many functions of ARF (Quelle et al. 1997), the knockout of exon 2 did not delineate the separate functions of these two genes. Knockouts of exon 1 β (Kamijo et al. 1997; Kamijo et al. 1999), and exon 1 α (Sharpless et al. 2001), in combination with a mouse model expressing a truncated form of p16^{INK4a} (Krimpenfort et al. 2001) attempted to address this problem. MEFs from mice deficient solely in *ARF* were transformed by the expression of oncogenic Ras, whereas MEFs deficient in *INK4a* arrested. This implies that ARF and p53 play a central role in stasis in MEFs. From these experiments it was also clear that *ARF*-null mice were highly tumour prone, similar to p53 knockout mice, while *INK4a*-deficient mice were not tumour prone without the addition of carcinogens. These experiments were conducted in different

genetic backgrounds and experiments looking at the individual knockouts of *INK4a* and *ARF* in the same genetic background suggested that mice deficient in both genes had a greater tumour predisposition than either of the single knockouts alone (Sharpless et al. 2004). This suggested that *INK4a* also plays a role in tumour suppression in mice, an idea which was supported by further studies using a Ras-induced model of melanoma (Sharpless et al. 2003). The role of *ARF* has also been studied by engineering mice in which the coding sequence of exon 1 β was replaced by a sequence encoding GFP (Zindy et al. 2003). In MEFs from these mice, an accumulation of green cells was observed upon serial passaging, and tumours formed in these mice were green showing that expression of ARF had been activated as a tumour suppressive mechanism (Zindy et al. 2003). The importance of the *CDKN2a* locus in tumour suppression was confirmed by a reciprocal experiment in which ‘*super INK4a/ARF*’ mice expressing an extra copy of the entire locus were generated. These mice were found to have a higher cancer resistance than normal mice, and an increased resistance to in vitro immortalisation and transformation, while retaining normal aging (Matheu et al. 2004).

Experiments to address the relative contributions of *INK4a* and *ARF* in human cells have, through necessity, taken different approaches. Initially, the relative roles of the pRb and p53 pathways in the senescence of human cells were addressed using viral oncoproteins. Overcoming the p53 pathway using the viral oncoprotein HPV E6 allows cells to grow to an intermediate stage between senescence and crisis known as M1.5 (Bond et al. 1999; Morris et al. 2002). In contrast, overcoming the pRb pathway using HPV E7 (which also disables p21^{CIP1} and activates ARF), allows cultures to reach a stage which

more closely resembles crisis than senescence (Bond et al. 1999), although it occurs after fewer population doublings. Experiments have also been undertaken to look at the role of the *CDKN2a* locus in the transformation of human cells. Initial experiments were carried out using viral oncoproteins such as SV40 Large T antigen and a combination of HPV E6 and E7 to disable the pRb and p53 pathways. This allowed the cells to be transformed by a combination of hTERT (to bypass the telomere dependent arrest), H-Ras and SV40 small t antigen (Hahn et al. 1999; Hahn et al. 2002).

Overexpression of CDK4 and CDK6 insensitive to p16^{INK4a} allows cells to bypass senescence and continue growing before arresting at M1.5 (Morris et al. 2002). The R24C variant of CDK4 that is insensitive to p16^{INK4a} in combination with cyclin D1 has also been used to model loss of p16^{INK4a} during transformation, and has been used in combination with a dominant negative form of p53 to overcome the p53 pathway (Hahn et al. 2002; Wei et al. 2003b).

Another approach has used gene targeting in HDFs to produce fibroblasts deficient in p21^{CIP1}. These cells are reported to continue dividing until they reach crisis (Wei and Sedivy 1999), and fibroblasts heterozygous for p21^{CIP1}, p53 or pRb have been shown to undergo spontaneous loss of heterozygosity, silencing the remaining copy of the gene before continuing to divide until they reach crisis (Wei et al. 2003a). Fibroblasts deficient in p53 and p21^{CIP1} were used to investigate the role of these genes in transformation (Wei et al. 2003b), and loss of p16^{INK4a} was modelled in these experiments using a cyclin D1-CDK4^{R24C} fusion protein which is resistant to p16^{INK4a}. These experiments also found that deletion of p53 combined with loss of p16^{INK4a} function was

necessary for transformation. The construction of fibroblasts deficient in p16^{INK4a} using gene targeting has not been possible due to the structure of the locus and its proximity to the p16^{INK4a} homologue p15^{INK4b}.

The recent advent of siRNA technology has allowed the specific ablation of p16^{INK4a} and ARF in human cells. Loss of p16^{INK4a} allows an extension of the lifespan of HDFs (Bond et al. 2003; Wei et al. 2003a), while there is still no evidence for the involvement of ARF during the replicative senescence of human cells (Wei et al. 2001). The role of p16^{INK4a} in the defences of human cells against transformation was confirmed using siRNA targeting p53 in combination with siRNA targeting p16^{INK4a} or pRb (Voorhoeve and Agami 2003). This report also looked at the tumour suppressive role of ARF in human cells, and confirmed that in contrast to the situation in mice, p16^{INK4a} was the major tumour suppressor of the human *CDKN2a* locus.

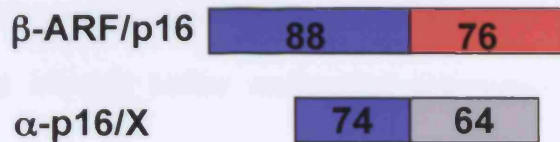
This observation is confirmed by the epidemiological evidence from human cancer. Germline mutations of this locus are predominantly associated with familial melanoma, although patients carrying mutations in this locus are also predisposed to other tumour types including glioma, HNSCC, bladder, cervical, breast, pancreatic cancer, NSCLC and NHL (Ruas and Peters 1998). Most of the mutations have been found to affect *INK4a*, or both of the genes, and mutations affecting only *ARF* are very rare. A germline mutation of *ARF* has been described, but this is thought to confer less susceptibility to melanoma than germline mutation of *INK4a*, and mutation of both genes may be needed for melanoma to develop in these patients (Hewitt et al. 2002).

This locus is also frequently mutated in spontaneous human tumours. Mutations usually affect both genes, but many mutations have been described

affecting only *INK4a*, and there are a few recorded mutations where only *ARF* is affected. Mutations of the locus include point mutations, deletions and insertions, with some deletions causing a frameshift with the resulting protein continuing in a different reading frame. Mutations in exon 2 change the coding sequence of both genes, but may leave ARF functionally unimpaired, as exon 1 β appears to be sufficient for many functions of ARF (Llanos et al. 2001). The *CDKN2a* locus is also frequently affected by promoter methylation, and loss of heterozygosity at this locus is frequently accompanied by methylation of the remaining allele (Ruas and Peters 1998).

Our laboratory has investigated the relative roles of *INK4a* and *ARF* in senescence and transformation by exploiting two strains of human dermal fibroblasts, Q34 and Leiden, from rare patients who carry germline mutations in both alleles of the *CDKN2a* locus. These cell strains are operationally p16-deficient, whilst retaining functional ARF. Q34 cells come from a patient with a familial history of cancer, including melanoma (Huot et al. 2002). The cells are heterozygous for two independent missense mutations (Figure 1.8). The first mutation causes a Met to Thr change at amino acid 53 of p16^{INK4a} whilst the second mutation causes an Asp to Asn mutation at amino acid 108. Only the second mutation affects ARF, causing a change near its carboxy terminus which does not appear to affect the function of the protein. The Leiden patient comes from a melanoma-prone family and is homozygous for a 19 base pair deletion in exon 2 (Brookes et al. 2002). This causes the deletion of 6 amino acids, and also results in a frame-shift. As a result, the cells express

Leiden homozygous for 19 bp deletion in exon 2



Q34 compound heterozygote

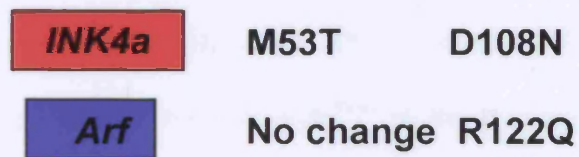


Figure 1.8 Schematic illustrating the p16^{INK4a} and ARF proteins expressed by the Leiden and Q34 cells

The Leiden patient is homozygous for a 19bp deletion which causes a frameshift. As a result, Leiden cells express an ARF/p16^{INK4a} fusion protein which retains known functions of ARF, and a p16^{INK4a}/X fusion protein that is non-functional. The Q34 patient is a compound heterozygote, carrying two point mutations affecting the *CDKN2a* locus. Q34 cells are also operationally deficient in p16^{INK4a} and retain functional ARF.

two fusion proteins, α -p16/X comprising the 74 residues of p16^{INK4a} followed by a further 74 residues in the +1 reading frame, and β -ARF/p16 containing the first 88 amino acids of ARF fused to the last 76 amino acids of p16^{INK4a} (Figure 1.8). α -p16/X is non-functional, but β -ARF/p16 seems to retain the known functions of ARF.

The Leiden and Q34 strains of p16^{INK4a}-deficient fibroblasts have a partially extended lifespan before undergoing senescence at M1.5 (Brookes et al. 2004). This can be explained using the subunit rearrangement model. Loss of functional p16^{INK4a} prevents the displacement of p21^{CIP1} from CDK4 and CDK6 complexes onto CDK2 complexes which would otherwise occur at senescence and inhibit the function of CDK2. p16-deficient fibroblasts, unlike 'normal' human diploid fibroblasts, do not arrest in response to oncogenic Ras, Ets1, or Ets2 (Brookes et al. 2002; Huot et al. 2002; Drayton et al. 2003), suggesting a central role for p16^{INK4a} in the response to aberrant oncogenic signalling. Expression of exogenous Myc or Ras in p16-deficient fibroblasts expressing telomerase partially transforms the fibroblasts, making them capable of anchorage independent growth. Leiden cells expressing exogenous telomerase and Myc and Ras in combination form larger anchorage independent colonies in soft agar than the cells expressing either Myc or Ras alone. The cells expressing a combination of Myc and Ras are also capable of tumorigenicity in nude mice (Drayton et al. 2003). This is in contrast to the findings of other groups where loss of p53 function was necessary for transformation. However tumour formation was inefficient and occurred after a significant time-lag, and analysis of the karyotypes of the tumours showed that the tumours were formed from three clones of cells which had been

present in the parental population. Although the tumours had wild-type p53, several had silenced ARF.

However, some residual concerns remain about the ARF proteins expressed in Leiden and Q34 cells, and it has been suggested that the ARF expressed in Leiden cells is overactive (Wei et al. 2003b), while that expressed in Q34 cells is partially impaired. This thesis describes the characterisation of a novel strain of fibroblasts from a patient with a family history of melanoma. These cells are homozygous for a point mutation in exon 1 α , and express the R24P variant of p16^{INK4a}, while ARF is completely unaffected in these cells.

Chapter 2

Materials and Methods

2.1 Solutions

Media, some commonly used solutions, and clean glassware were provided by Cancer Research UK Cell Services. Electrophoresis buffers were kept as a common laboratory stock. Some plasmid DNA preparations were kindly donated by members of the laboratory. Chemicals were usually purchased from Sigma or VWR International (BDH Merck Eurolab). Water was purified using a Millipore reverse osmosis system and autoclaved. Solutions were made up in water (unless otherwise stated), before being autoclaved or filtered through a 0.22 μ M filter where appropriate.

Solutions used in this thesis are described below:

6x agarose gel loading buffer	30% (v/v) glycerol
	0.1% (w/v) bromophenol blue
20x agarose gel electrophoresis buffer	0.8M Trizma base
	0.1M sodium acetate
	0.02M EDTA
	5% (v/v) glacial acetic acid
	adjust pH to 7.6

Annealing buffer	100mM potassium acetate 30mM HEPES-KOH pH7.4 2mM magnesium acetate
Blocking solution	PBSA 0.2% (v/v) Tween-20 5% (w/v) dried milk (Marvel)
Citric acid/ Na ₂ HPO ₄ buffer	36.85% (v/v) 0.1M citric acid 63.15% (v/v) 0.2M Na ₂ HPO ₄ verify pH is 6.0
2x Hepes Buffered Saline (HBS)	280 mM NaCl 10mM KCl 1.5mM Na ₂ HPO ₄ 12mM dextrose 50mM Hepes adjust pH to 7.05
High salt buffer	0.5M NaCl 50mM Tris pH8.0 1% (v/v) NP40
L-Broth	1% (w/v) NaCl

	1% (w/v) bacto-tryptone
	0.5% (w/v) yeast extract
NP40 lysis buffer	150mM NaCl
	50mM Tris-HCl (pH 8.0)
	1% (v/v) NP40
PBSA	8.06mM Na ₂ HPO ₄
	0.8% (w/v) NaCl
	1.47mM KH ₂ PO ₄
	0.025% (w/v) KCl (pH 7.2)
1000x Protease inhibitor cocktail	AEBSF 20mM
	10 mM EDTA
	Bestatin 1.3mM
	E-64 140μM
	Leupeptin 10μM
	Aprotinin 3μM
10x Protein gel electrophoresis buffer	3.8M glycine
	0.5M Trizma base
	0.07M SDS
Protein gel transfer buffer	10% (v/v) protein gel electrophoresis buffer

	20% (v/v) methanol
SA-βgal staining solution	1mg/ml X-gal in dimethylformamide 20% (v/v) 0.2M citric acid/ Na ₂ HPO ₄ buffer 5mM potassium ferrocyanide 5mM potassium ferricyanide 150mM NaCl 2mM MgCl ₂
1x Sample buffer	62.5mM Tris-HCl (pH 6.8) 2% (w/v) SDS 5% (v/v) 2-mercaptoethanol 0.002% (v/v) glycerol
2x Sample buffer	125mM Tris (pH 6.8) 4% (w/v) SDS 10% (v/v) 2-mercaptoethanol 0.04% (w/v) bromophenol blue solution 0.004% (v/v) glycerol
SOC medium	2% (w/v) tryptone 0.05% (w/v) yeast extract

	0.006% (w/v) NaCl
	0.002% (w/v) KCl
	0.02% (w/v) MgCl ₂
	0.025% (w/v) MgSO ₄
	0.036% (w/v) D-Glucose
TE buffer	10mM Tris-HCl (pH8.0)
	1mM EDTA (pH8.0)
Trypsin	0.8% (w/v) NaCl
	0.01% (w/v) Na ₂ HPO ₄
	0.1% (w/v) D-Glucose
	0.3% (w/v) Trizma base
	0.2% (v/v) KCl (19% stock)
	0.15% (v/v) phenol red (1% stock)
	0.006% (w/v) Penicillin
	0.01% (w/v) Streptomycin
	0.25% (w/v) trypsin (Difco 1:250 stock)
	HCl to pH 7.7
Versene	0.02% (w/v) EDTA in PBSA (pH 7.2)
	0.0015% (w/v) phenol red

2.2 Cell culture

2.2.1 Human cell strains

BOSC 23	Ad5-transformed human embryonic kidney 293 cell line expressing gag-pol and env genes for ecotropic retrovirus packaging (Pear et al. 1993)
Hs68	Neonatal foreskin fibroblast strain (ATCC number CRL-1635)
Leiden	Adult dermal fibroblast, p16 ^{INK4a} deficient (Brookes et al. 2002)
Milan	Adult dermal fibroblast, p16 ^{INK4a} compromised (characterised in the thesis)
Q34	Adult dermal fibroblast, p16 ^{INK4a} deficient (Huot et al. 2002)
Ras GP+E	GP+E cell line stably producing retrovirus encoding H-Ras G12V
TIG3	Foetal lung fibroblast strain (Provided by E Hara)
UZU	Child fibroblast strain (Ian Kerr, Cancer Research UK)
U2OS	Human osteosarcoma cell line (ATCC number HTB-96)
904	Adult dermal fibroblast strain

Fibroblast strains were infected with an amphotropic retrovirus (pWXL-Neo-Eco) encoding the murine basic amino acid receptor, and selected in 200µg/ml G418 (McConnell et al. 1998). Expression of this cell surface receptor allows subsequent infection of the fibroblasts using ecotropic retroviruses.

2.2.2 General cell growth conditions

Cells were grown as monolayers in 10cm dishes (Corning) at a constant temperature of 37°C, and maintained in 5-6% carbon dioxide. Cells were fed every two to three days with fresh warmed 'medium', consisting of E4 (Dulbecco's modified eagles medium), supplemented with 10% foetal bovine serum (PAA Clone). Cells were grown until confluent and then passaged. To passage, cells were rinsed with 4 mls versene, and incubated at 37°C with 1 ml trypsin/versene (1:3 mix) until all cells were detached. A fraction of the cells, (usually a half, a quarter, or an eighth) were then replated in 10 mls of fresh medium. A 1:2 split was taken to be equivalent to 1 population doubling (PD).

2.2.3 Storage and recovery of cells

Cell monolayers were washed once with versene, and incubated with 1 ml trypsin/versene (1:3) mix at 37°C until the cells were detached. Cells were resuspended in fresh medium and centrifuged for 5 minutes at 1500g. The supernatant was removed, and the cell pellet resuspended in 1 ml of E4, supplemented with 20% foetal bovine serum and 10% DMSO. Cells were wrapped in multi-layered tissue and cooled slowly to -70°C. Cells were then placed in liquid nitrogen for long term storage.

Cells were recovered by thawing quickly in a waterbath at 37°C, before the dropwise addition of cold medium. Cells were spun down for 5 minutes at 1500g, and the supernatant removed. The pellet was resuspended in fresh medium, and plated out.

2.2.4 Production of retroviral stocks

(i) Transient transfection of BOSC23 cells

Retroviral stocks were produced using the BOSC23 packaging cell line. After transient transfection with a plasmid containing retroviral LTR sequences and the gene of interest, this cell line produces ecotropic virus encoding the gene. BOSC23 cells were plated out at a density of 6×10^6 cells per 10cm dish. 24 hours later, the medium on the BOSC23 cells was changed to 5 mls medium supplemented with $25 \mu\text{M}$ chloroquine. $10 \mu\text{g}$ of plasmid DNA in $440 \mu\text{l}$ of $0.1 \times \text{TE}$ was added to $60 \mu\text{l}$ of CaCl_2 solution. Whilst air was being bubbled through the DNA solution, $500 \mu\text{l}$ of $2 \times \text{HBS}$ was added in a dropwise fashion. This solution was then added to the BOSC23 cells. After 7 hours, the medium was replaced with 10 mls of fresh medium. At least 7 hours before taking a retroviral harvest, the medium on the plate of BOSC23 cells was decreased to 5 mls. To harvest, the virus-containing medium was collected and filtered through a $0.45 \mu\text{M}$ PVDF membrane (Millipore).

(ii) GP+E cells

For experiments using pBabe^{bleo} retrovirus expressing H-Ras, better infectivity was obtained when stably transfected GP+E cells were used. These cells were grown in medium containing 200g/ml zeocin, to maintain selection for the H-Ras plasmid. At least 7 hours before

infection, the medium on these cells was replaced with 5 mls of fresh medium. To harvest, the virus-containing medium was collected and filtered through a 0.45 μ M filter.

2.2.5 Infection of fibroblasts with ecotropic retrovirus

The day before infection, fibroblasts were split appropriately to reach between 50 and 75% confluence the next day. To infect, the medium on the cells was replaced with filtered viral harvest containing 4 μ g/ml polybrene. For multiple infections, additional harvests were made from the virus producing cells and added to the fibroblasts during the day of infection. The following day, the medium on the fibroblasts was replaced and 24 to 48 hours after infection, selection was initiated in medium containing the appropriate antibiotic. (Puromycin 1.25 μ g/ml, zeocin 50-200 μ g/ml, hygromycin B 50 μ g/ml, blasticidin 1.25-2.5 μ g/ml.)

2.2.6 Senescence-associated beta-galactosidase staining (SA- β gal staining)

Endogenous SA- β gal staining at pH 6.0 is used to identify senescent cells. In the presence of a suitable substrate, X-gal, this activity produces a characteristic 'blue' colour, allowing the identification of senescent cells. Cell monolayers were washed twice with PBSA before fixing with 2% formaldehyde and 0.2% glutaraldehyde in PBSA for 5 minutes at room temperature. Cells were washed twice with PBSA before the addition of sufficient staining solution to cover the cell monolayer. The cells were then incubated overnight at 37°C in normal atmospheric conditions.

2.2.7 Immunofluorescence

Immunofluorescence was used to follow the induction of proteins at an individual cell level, and was performed using the Molecular Probes Image-iT FX kit with Alexa Fluor secondary detection conjugates according to the manufacturer's protocol. Briefly, cells were plated on glass chamber slides (LabTek), and treated as required. At the appropriate timepoint, the media was removed and cells were washed in PBSA before being fixed in warm (37°C) 3.7% formaldehyde for 10-15 minutes at room temperature. Cells were rinsed 3-4 times in PBSA, and the cells were permeabilised using 0.2% Triton in PBSA for 5 minutes at room temperature. Cells were then rinsed 3-4 times in PBSA, and the samples were covered with several drops of Image-iT FX signal enhancer, before being left for 30 minutes at room temperature. Samples were rinsed 3-4 times in PBSA, before the addition of primary antibody diluted in blocking solution to the concentration used for western blotting (detailed below). Samples were then incubated with primary antibody at 4°C overnight. Samples were rinsed thoroughly before the addition of the secondary conjugate (Alexa Fluor goat anti rabbit 555nm, or goat anti-mouse 488nm) diluted to 5µg/ml in blocking solution. After 90 minutes at room temperature, samples were rinsed in PBSA before being mounted using the ProLong Gold antifade reagent with DAPI (Molecular Probes) to stain the cell nuclei. Slides were stored at -20°C, until cells were visualised using microscopy.

2.2.8 Immunohistochemistry

Immunohistochemistry was performed using the DakoCytomation EnVision System-AP kit according to the manufacturer's protocol. Cells grown in chamber slides (LabTek), were rinsed 3-4 times in PBSA before fixing in a 1:1 mixture of methanol and acetone for 20 minutes at -20°C. Cells were rinsed 3-4 times in PBSA, and incubated overnight at 4°C with primary antibody diluted in blocking solution to the concentration used for western blotting (detailed below). Cells were then rinsed 3-4 times in PBSA before the addition of alkaline phosphatase labelled polymer for 30 minutes. Samples were then washed thoroughly in PBSA as before, before the addition of substrate chromogen solution for 30 minutes. Samples were then washed in distilled water, before mounting using ProLong Gold AntiFade reagent with DAPI (Molecular Probes) to stain the cell nuclei. Slides were stored at -20°C, until microscopy was used to visualise the cells.

2.2.9 Incorporation of BrdU

Cells were seeded in 35mm glass-bottomed dishes (MatTek Corporation). When cells reached approximately 50% confluency, the medium was replaced with BrdU labelling medium. After 18-24 hours growth in the labelling medium, the cells were washed twice with PBSA before fixing for at least 20 minutes at -20°C using 70% ethanol in 50mM glycine buffer pH 2.0. BrdU incorporation was then assayed using the Boehringer Mannheim kit following the manufacturers adherent cell protocol. Briefly, the cells were incubated with an anti-BrdU monoclonal antibody in the presence of nucleases to allow access of the antibody to the DNA. The cells were then incubated with anti-

mouse-Ig-alkaline phosphatase. In the presence of colour substrate solution, a brown product was produced indicating the presence of incorporated BrdU in the DNA. The percentage of cells with incorporated BrdU was scored using a light microscope. Several fields of view were counted, with a minimum of 300 cells being assayed.

2.2.10 Proliferation assay using crystal violet staining

The relative proliferation rate of different cell cultures was monitored over a period of time by staining viable cells with crystal violet. Triplicate samples of 5×10^3 cells per well were plated out in a 24 well plate. For each timepoint, one plate was required. At the specified time, each well was washed twice with 1 ml PBSA and fixed with 500 μ l of 10% (v/v) formaldehyde. After five minutes, the wells were washed twice with 1 ml water, and stained with 250 μ l 0.1%(w/v) crystal violet. After 30 minutes, the cells were washed four times with 1 ml water, and the stain was extracted from the cells using 1 ml 10% (v/v) acetic acid. This was then diluted with an equal volume of water, and the $A_{590\text{nm}}$ of this solution measured. This value was averaged for the triplicates of each cell type, and normalised to the $A_{590\text{nm}}$ at day 1. The first reading taken to be day 1, was usually made 18- 24 hours after the cells were plated.

2.2.11 Anchorage independence assay

The ability of cells to grow in 0.2% agarose was used as a measure of transformation. An agarose base was formed using 2 mls of a 1:1 mixture of

2xE4 (supplemented with 20% FBS), and 2% agarose, warmed to 60°C, in each well of a six well plate. Samples of 1×10^4 cells were prepared in 1 ml of 2xE4 supplemented with 20% FBS. 1 ml of 0.4% agarose, warmed to 55°C, was added and the mixture plated into a well. Duplicate wells of each cell type were set up. Cells were fed weekly with 2 mls of a 1:1 mixture of 2xE4 with 20% FBS, and 0.4% agarose per well. After 4 to 6 weeks the percentage of cells forming colonies was counted using a light microscope.

2.2.12 Giemsa staining of anchorage independent colonies

To improve photographic imaging, anchorage independent colonies were stained with Giemsa stain. Giemsa stain (Fluka) was diluted 1:5 in a 5:24 mix of glycerol and methanol. Six well plates containing anchorage independent colonies were incubated with the solution for 20 minutes whilst agitating. Excess dye was removed by repeated rinsing with distilled water.

2.3 Protein biochemistry

2.3.1 Preparation of total cell lysates

(i) Lysis in SDS sample buffer

Cells were lysed in SDS lysis buffer to provide total protein samples for western blotting. Cell monolayers were washed twice with PBSA, before the addition of 100µl of 1x sample buffer (without bromophenol blue or 2-mercaptoethanol). Cells were scraped using a cell scraper (Corning), and the lysate collected into a 1.5ml centrifuge tube.

Samples were boiled for 10 minutes, and aliquots taken to determine the protein concentration. Samples containing a fixed amount of protein were aliquotted. A quarter of the sample volume was calculated and this amount of bromophenol blue and 2-mercaptoethanol mixture was added to the protein sample to form 1 x sample buffer. Samples were stored at -20°C .

(ii) Lysis in NP40 buffer

NP40 lysis buffer was used when protein samples were required for immunoprecipitation, or when the status of protein phosphorylation was to be determined by western blotting. Cells were trypsinised and resuspended in medium. Cells were spun down for 5 minutes at 1500g, the supernatant removed, and the cells resuspended in cold PBSA. This was repeated, and the supernatant removed. Cells were resuspended in 150 μl cold NP40 lysis buffer containing freshly added protease inhibitors (at 1 in 1000 dilution). Lysates were snap frozen in dry ice and stored at -70°C . Before protein quantification, samples were centrifuged for 15 minutes at 18000g and 4°C to clear the lysate. The supernatant was collected on ice before aliquots were taken for protein quantification.

2.3.2 Protein quantification

Protein concentration was determined using the Pierce BCA system. This system uses a copper sulphate solution as a source of Cu^{2+} ions. In the presence of protein and under alkaline conditions, these ions are reduced to form Cu^{1+} ions which then react with the BCA reagent, exhibiting absorbance

at 562nm. 10µl duplicates of total protein sample were assayed according to the manufacturers instructions, against a series of standards of known protein concentration.

2.3.3 Immunoprecipitation

Depending on the experiment, fixed amounts (500µg – 1mg) of total protein were aliquotted and made up to a total volume of 500µl-1 ml of NP40 lysis buffer containing protease inhibitors (at 1 in 1000). Antibody (2-20µl) and 20µl of protein A or G beads were added. (Protein A beads were used in conjunction with a rabbit polyclonal antibody and Protein G beads with a mouse monoclonal antibody). The samples were rotated at 4°C overnight. The beads were washed 4 times with 1 ml of cold NP40 lysis buffer containing protease inhibitors. The beads were then boiled for 10 minutes in the presence of 25µl of 2x sample buffer to release bound proteins from the beads. The released proteins in 2x sample buffer were then separated using SDS-PAGE.

2.3.4 Separation of proteins by SDS-PAGE

Polyacrylamide gels (13x14x0.075cm) were poured using the Hoeffer HIS vertical slab gel system. The resolving gel contained 30% acrylamide mix (37.5:1 acrylamide:bis-acrylamide, Anachem) diluted in 375mM Trizma base (pH 8.8), 0.1% (w/v) SDS, 0.1% (w/v) ammonium persulphate and 0.04% (v/v) TEMED. The acrylamide mixture was protected from the air with isopropanol while polymerisation occurred. When the gel was polymerised, the isopropanol was removed and the gel was rinsed with water to remove

residual alcohol. A stacking gel was then poured containing 5% acrylamide in 125mM Trizma base (pH 6.8), 0.1% (w/v) SDS, 0.1% (w/v) ammonium persulphate and 0.1% (v/v) TEMED. Samples of 15-35 μ g of total protein in 1x sample buffer, or immunoprecipitated proteins in 2x sample buffer were applied to the gel along with 14 C labelled rainbow markers (Amersham) to facilitate gel orientation and protein size determination. Electrophoresis was performed in 1x protein electrophoresis buffer in water-cooled tanks at a constant current of 35mA with unlimited voltage. Gels were run until the dye front reached the bottom of the gel.

2.3.5 Immunoblotting for proteins (western blotting)

After separation by SDS-PAGE, proteins were transferred from the gel to a PVDF Immobilon-P membrane (Millipore), using the Atta semi-dry blotting method. The membrane was cut to the size of the gel, pre-treated with methanol for 30 seconds, rinsed with water for 2 minutes, and equilibrated in transfer buffer for at least 5 minutes prior to use. 6 pieces of 3MM filter paper cut to 13x14cm were soaked in transfer buffer. The gel was placed on the membrane, between a sandwich of 3MM in the transfer cassette. Bubbles were removed by 'rolling' a plastic pipette across the sandwich, and spare transfer buffer was poured on to keep the membrane wet. A constant current of 0.27mA was passed through the electrodes for 1 hour. The membrane was rinsed in PBSA, before rocking in blocking buffer for 1 hour at room temperature, or overnight at 4°C.

To detect proteins by immunoblotting, the membrane was sealed in a plastic bag with primary antibody diluted in 10 mls of blocking buffer and rocked for

either 1 hour at room temperature or overnight at 4°C. Primary antibodies were usually used at 1 in 1000 dilution if purified, or 1 in 5 for monoclonal antibodies obtained as tissue culture supernatant. The membrane was washed with 6x200 mls of PBSA containing 0.2% (v/v) Tween-20 to remove excess antibody, whilst rocking for at least 1 hour in total. The membrane was then incubated for 45 minutes at room temperature with the appropriate HRP-linked secondary antibody (Amersham) diluted to 1 in 2000 in 10 mls of blocking buffer. After washing as before, the bound antibody was visualised using enhanced chemiluminescence (ECL, Amersham Pharmacia Biotech) to detect the presence of HRP. The membrane was incubated for 1 minute in a 1:1 mix of detection reagents 1 and 2. Hyperfilm MP (Amersham Pharmacia Biotech) was exposed to the blot in a Hypercassette (Amersham Pharmacia Biotech) for an appropriate length of time (between 1 second and overnight) before developing the film.

To reprobe, membranes were rinsed in PBSA to remove ECL before incubating with a different primary antibody. Membranes were stored in Saran wrap at -20° C. Membranes were stripped by rocking for 15 minutes at room temperature in 30mls of Restore western blotting stripping buffer (Pierce). Membranes were rinsed twice in PBSA, before reblocking for 1 hour at room temperature in blocking buffer.

2.3.6 Antibodies

Target protein	Name	Type	Source
Arf	54-75	Rabbit polyclonal	David Parry, DNAX
CDK4	SC601	Rabbit polyclonal	Santa Cruz
CDK4	DCS31	Mouse monoclonal	Neomarkers
CDK6	SC177	Rabbit polyclonal	Santa Cruz
CDK6	K6.83	Mouse monoclonal	Neomarkers
Cyclin D1	287.3	Rabbit polyclonal	David MacAllan, our laboratory
Cyclin D1	DCS6	Mouse monoclonal	Neomarkers
Cyclin D2	SC754	Rabbit polyclonal	Santa Cruz
HA tag	12CA5	Mouse monoclonal	Central services, Cancer Research UK
MDM2	4B11	Mouse monoclonal	Oncogene Science
MEK1/2		Rabbit	Cell Signalling Technology

		polyclonal	
Myc	9E10	Mouse monoclonal	Central Services, Cancer Research UK
p16 ^{INK4a}	JC8	Mouse monoclonal	Cancer Research UK (originally from Jim Koh and Ed Harlow)
p16 ^{INK4a}	DCS50	Mouse monoclonal	Cancer Research UK (Jiri Bartek)
p16 ^{INK4a}	DPAR12	Rabbit polyclonal	David Parry, our laboratory
p16 ^{INK4a}	SC468	Rabbit polyclonal	Santa Cruz
p21 ^{CIP1}	SC397	Rabbit polyclonal	Santa Cruz
p53	DO-1	Mouse monoclonal	Santa Cruz
Ras	Pan-Ras	Mouse monoclonal	Oncogene Research Products

Table 2.1 Antibodies

JC8 recognises an epitope in the N-terminal half of p16^{INK4a} and was routinely used to detect the protein by western blotting. However, JC8 was incapable of detecting the Milan (R24P) form of p16^{INK4a}. This was detected using either the Santa Cruz rabbit polyclonal raised against p16^{INK4a}, or DCS50. DCS50 recognises the C terminus of p16^{INK4a} and was also capable of detecting the Leiden ARF/p16^{INK4a} fusion protein by western blotting. DPAR12 was a

polyclonal antibody raised against full length His-tagged p16^{INK4A} and was used for immunoprecipitation.

2.4 DNA techniques

2.4.1 Plasmid vectors

pBabe This vector allows the production of ecotropic retroviruses when transiently transfected into an appropriate packaging cell line. It is based on the Moloney murine leukaemia virus (Morgenstern and Land 1990). The gene of interest is expressed from a promoter contained in the LTR region, and an antibiotic resistance gene is expressed from an SV40 early region promoter. The plasmid also contains an ampicillin resistance gene for selection in bacteria.

pRetroSuper This vector is based on the pMSCV retroviral plasmid and the pSUPER shRNA expressing plasmid (Brummelkamp et al. 2002b). An shRNA hairpin targeting the gene of interest is expressed from the RNA polymerase-III promoter (Brummelkamp et al. 2002a). The plasmid contains an antibiotic resistance gene for selection in eukaryotic cells, and an ampicillin resistance gene allowing selection in bacteria.

pWZL

This vector allows the production of ecotropic retroviruses when transiently transfected into an appropriate packaging cell line.

2.4.2 Transformation of chemically competent bacteria

To obtain bacterial vectors containing the requisite plasmid, the DNA was introduced into One Shot TOP10 chemically competent cells (Invitrogen) were used. Bacteria were stored at -70°C and thawed on ice prior to transfection. DNA ($1\mu\text{l}$ of plasmid preparation or $5\mu\text{l}$ of ligation mixture) was added to the cells and they were incubated on ice for 30 minutes. Cells were heat shocked in a waterbath at 42°C for 30 seconds. $250\mu\text{l}$ of SOC medium was added to the cells and they were incubated at 37°C and 200rpm for one hour, before plating out on L-agar plates containing $100\mu\text{g/ml}$ ampicillin. Plates were incubated overnight at 37°C .

2.4.3 Small scale preparation of plasmid DNA (minipreps)

Small scale DNA purification was used to screen bacterial colonies to identify clones expressing the correct plasmid. 4 ml cultures of L-broth with $100\mu\text{g/ml}$ ampicillin were inoculated with single colonies picked from the transformation plate. Cultures were incubated at 37°C overnight in a shaking incubator. Bacteria were pelleted by centrifugation and the supernatant discarded. The pellets were then processed by the staff of the London Research Institute Equipment Park, and the DNA was purified using the

Qiagen DNA purification system (described below), and a Qiagen liquid handling robot.

2.4.4 Large scale preparation of plasmid DNA (maxipreps)

200ml cultures of L-broth containing 100µg/ml ampicillin were inoculated with a single colony picked from a transformation plate, and incubated at 37°C in an incubator (Innova 4430) which rotates the cultures at 200rpm. Bacterial cells were harvested by centrifuging for 15 minutes at 4°C and 6000g in a Beckman Coulter Advanti J-20 XP centrifuge. Plasmid DNA was then purified using the Qiagen Maxiprep kit according to the manufacturers protocol. Briefly, bacterial cells were lysed in NaOH-SDS buffer in the presence of RNase A, before neutralising the lysate by the addition of acidic potassium acetate. The lysate was cleared by running through a QIAfilter cartridge to remove insoluble complexes formed by protein-DNA aggregates. The cleared lysate was then passed through a QIAGEN-tip to enable the DNA to bind to the matrix. The tip was washed with a medium salt buffer, before elution of the DNA in a high salt buffer. The DNA was then desalted and concentrated by isopropanol precipitation. After centrifugation, the DNA pellet was washed in 70% ethanol, before re-centrifuging. The DNA pellet was then dried and resuspended in TE buffer. and plasmid DNA preparations were stored at 4°C. The concentration of the DNA preparation was quantified using a spectrophotometer. The absorbance of the DNA solution at a wavelength of 260nm was measured, and the DNA concentration was calculated based on the information that a measurement of 1.0 is equivalent to

50µg/ml of double stranded DNA. A measurement of absorbance at 280nm was also made to check the purity of the DNA.

2.4.5 Restriction enzyme digests of plasmid DNA

Plasmid DNA was digested by restriction enzymes to check its identity, or to isolate a DNA fragment for use in cloning. 1µg or 10µg of DNA respectively, were digested in a final volume of 20µl or 50µl. 20-100 units of restriction enzyme (New England Biolabs) were used with less than 10% of the final volume being enzyme. The digestion buffer supplied with the enzyme was used to provide suitable salt conditions. BSA was added when suggested by the manufacturer. Digests were incubated in a waterbath at 37°C for between 2 and 4 hours, and the DNA fragments were then resolved by agarose gel electrophoresis.

2.4.6 Agarose gel electrophoresis of DNA fragments

1% (w/v) agarose (SeaKem) in 1x DNA electrophoresis buffer, was boiled in a microwave until completely dissolved. After the addition of ethidium bromide at 0.5µg/ml, the gel was cast using the Hoeffer system. DNA loading buffer was added to the DNA samples at a ratio of 1:6. Once set, the gel was placed in a tank containing 1xDNA electrode buffer. DNA samples were loaded on the gel alongside 1µg of commercially supplied size markers (1kb and 100bp ladders) from New England Biolabs. Electrophoresis was performed at a constant voltage of 80-100V for between 30 minutes and 1 hour. DNA fragments were visualised using a UV transilluminator.

To purify DNA fragments for use in a ligation reaction the appropriate fragments were excised from the gel under UV light, and DNA was isolated using the QIAquick gel extraction kit following the manufacturers microcentrifuge protocol to remove the enzyme and salts present in the restriction enzyme digests. The DNA fragments were separated by electrophoresis in a 1% agarose gel as described and visualised to verify the fragment size.

2.4.7 Ligation of plasmids

A small aliquot (2 μ l) of purified plasmid and insert DNA were used to estimate the relative amounts of DNA present based on the intensity of the bands under UV light and the size of the fragments. Between four and six times more insert than vector was used in the ligation reaction. Ligation reactions were set up containing the DNA, 1 μ l T4 DNA ligase (New England Biolabs) and 2 μ l 10xT4 DNA ligase buffer (New England Biolabs) in a total volume of 20 μ l. The reactions were incubated at 16°C overnight in a DNA thermal cycler (MJ Research).

2.4.8 Generation of plasmid constructs

(i) Retroviral vectors for shRNA expression

Oligonucleotides containing a hairpin targeting human Myc were cloned into the retroviral expression vector pRetroSuper. The oligonucleotides contained a 20bp unique sequence and the reverse complement sequence separated by a loop (7bp). The oligonucleotides also contained BamHI and XhoI restriction sites for cloning into the

vector. Transcription of the insert from the vector would result in the synthesis of a positive strand transcript which would fold to form an shRNA hairpin structure. The oligonucleotides were synthesised as forward and reverse 64-mers and are described below:

Forward:GATCCCCGATGAGGAAGAAATCGATGTTCAAGAGA
CATCGATTTCTTCCTCATCTTTTTGGAAA

Reverse:AGCTTTTCCAAAAGATGAGGAAGAAATCGATGTCT
CTTGAACATCGATTTCTTCCTCATCGGG

1µl of each oligonucleotide (200µM in water) and 48µl of annealing buffer were incubated for 4 mins at 95°C and 10 mins at 70°C before slowly cooling to 4°C to allow the oligonucleotides to anneal. Oligonucleotides were phosphorylated using T4 Polynucleotide kinase (New England Biolabs), and ligated into vector which had previously been digested with EcoRI and HindIII and purified. Successfully ligated plasmids were isolated as described above and sequence verified.

2.4.9 Oligonucleotides

Oligonucleotides were used as primers for sequencing. Primers were synthesised by the ICRF/Cancer Research UK oligonucleotide synthesis service, and were supplied purified with a calculated T_m . Oligonucleotides were diluted in water to form stocks of 1µg/µl. Sequences of primers used are contained in the table below:

Name	Sequence
pBabeF1	CGTCTCTCCCCCTTGAACC
pBabeF2	CCCCGCCTCAATCCTCC
pBabeR1	CCTGGGGACTTTCCACACC
pBabeR2	CTGCCTGCTGGGGAGCC
K4SEQ1	TGTAGACCAGGACCTAAGGAC
K4SEQ2	CCGTGGTTGTTACACTCTGG
pRSF	TACATCGTGACCTGGGAAGC
pRSR	TAAAGCGCATGCTCCAGACT

Table 2.2 Oligonucleotide primers used for sequencing

2.4.10 Sequencing

Sequencing was carried out using the ABI PRISM Dye Terminator Cycle sequencing kit (Applied Biosystems). The DNA to be sequenced is used as a template for a PCR reaction incorporating dye-labelled dNTPs into the product. Sequencing reactions contained 150-300ng of template DNA, 8 μ l of Big Dye Terminator mix (Applied Biosystems), and 1 μ l primer (0.01 μ g/ μ l) in a final volume of 20 μ l. These were initially heated in a DNA thermal cycler (MJ Research) to 96°C for 1 minute to separate the DNA strands. The reaction was then subjected to 25 cycles of melting at 96°C for 10 seconds, annealing at x°C for 5 seconds, and elongation at 60°C for 4 minutes. The annealing temperature was calculated by using a temperature 4°C below the estimated melting temperature of the oligonucleotide. If the template DNA contained hairpin sequences, (for example if shRNA vectors were being

sequenced), 5% DMSO was added to the sequencing reaction and the melting temperature was increased to 98°C.

The DNA product was purified to remove excess labelled dNTPs using the DyeEx 2.0 kit (Qiagen) according to the manufacturer's protocol. The products of the sequencing reaction were applied to a gel bed and centrifuged for 3 minutes at 750g in a microcentrifuge. The eluate containing the purified DNA was concentrated in a vacuum centrifuge (DNA Speed Vac Savant). The pellets were frozen at -20°C. Samples were then handled by the staff of the Equipment Park (London Research Institute, Cancer Research UK) who separated the DNA products by electrophoresis through a capillary using the Applied Biosystems Prism 3730 system, and collected and analysed the data.

2.4.11 ELISA based TRAP assay

So-called TRAP assays (Telomere repeat amplification protocol) were used to assess the telomerase activity in fibroblast cell strains immortalised by the expression of exogenous hTERT. TRAP assays were performed using the TeloTAGGG Telomerase PCR ELISA^{PLUS} kit (Roche), according to the manufacturer's protocol. In the first elongation and amplification step, telomerase adds telomeric TTAGGG repeats to the 3'-end of a biotin-labelled synthetic primer (P1-TS). The products of the PCR reaction are then denatured and hybridised to digoxigenin-labelled detection probes specific for the synthesised telomeric repeats. The products are then immobilised via the biotin label to a streptavidin-coated plate and visualised using an anti-digoxigenin antibody conjugated to HRP and a suitable peroxidase substrate.

2.5 RNA techniques

2.5.1 Preparation of total cellular RNA

Total cellular RNA was prepared using the Qiagen RNeasy kit, according to the manufacturer's protocol for animal cells. Cell monolayers were rinsed twice with PBSA, before the addition of 600µl of lysis buffer containing 2-mercaptoethanol to inactivate RNases. The cells were detached using a cell scraper (Corning), and lysate collected in an Eppendorf tube. The lysate was then snap frozen on dry ice before storing at -70°C .

To purify RNA, the lysates were thawed in a waterbath at 37°C for 20 minutes, and homogenised by passing through a QIAshredder spin column (Qiagen). Ethanol was added to the sample, and RNA recovered by binding to an RNeasy silica-gel membrane. The membrane was then washed to remove contaminants, and the RNA eluted in RNase-free water. RNA samples were stored at -70°C . A spectrophotometer was used to measure the absorbance of the RNA solution at a wavelength of 260nm, and the RNA concentration was calculated based on the information that a measurement of 1.0 is equivalent to 40µg/ml of RNA. A measurement of absorbance at 280nm was also made to check the purity of the RNA.

2.5.2 Reverse transcription

RT (Reverse transcription) was performed using the Applied Biosystems/Roche kit according to the manufacturer's instructions. Random hexamers were used to prime the reaction which contained 2-3µg of total RNA template in a volume of 50µl. The reaction mixture was placed in a

DNA thermal cycler (MJ Research) and incubated at 25°C for 10 minutes initially, then at 48°C for 30 minutes for the reverse transcription to occur, and finally at 95°C for 5 minutes to inactivate the enzyme. The cDNA products were then stored at -20°C.

2.5.3 Quantitative (Real-time) PCR

RNA was transcribed into cDNA as described above. Quantitative (Q) PCR was performed using the Applied Biosystems system, in which SYBR green fluourophore is incorporated into the DNA products as they are synthesised. The progress of the PCR reaction is followed by measuring the fluorescence of the incorporated SYBR green. The initial amount of RNA template present can be deduced from the progress of the PCR reaction.

Oligonucleotide primers were synthesised by the Cancer Research UK oligonucleotide synthesis service, and were provided purified and quantified.

Target gene	Forward primer sequence	Reverse primer sequence
p16 ^{INK4A}	GAAGGTCCCTCAGACATCCCC	CCCTGTAGGACCTTCGGTGAC
Arf	CCCTCGTGCTGATGCTACTG	ACCTGGTCTTCTAGGAAGCGG
β-Actin	TGCAGGTTGGATGGTCAGACAC	GCCAAGACCACCAGCACG
Cyclin D2	GGAACCTGGCAGCTGTCACTC	ACATGGCAAACCTTAAAGTCGGTG

Table 2.3 Oligonucleotides used as Q-PCR primers.

To minimise pipetting errors, mastermixes of the primers for each gene, and the cDNA samples were set up in triplicate. Aliquots from these mastermixes

were used to establish 50 μ l reactions containing 1 μ l cDNA, 1 μ l primer mix (forward and reverse, 10 μ M), and 15 μ l SYBR green (Applied Biosystems). For each cDNA mastermix, a control reaction was set up containing β -actin primers. 23 μ l duplicates of this mix were dispensed into wells of a 96 well ABI PRISM optical reaction plate (Applied Biosystems). The plate was sealed with an ABI PRISM Optical Cap (Applied Biosystems), centrifuged to remove any bubbles, and then placed in an ABI PRISM 7700 sequence detector machine and run on the following programme: 50°C for 2 minutes, 95°C for 10 minutes, followed by 40 cycles of 95°C for 15 seconds, and 60°C for 1 minute. Data were collected and analysed using the sequence detector v1.7a software. The data were normalised to the β -actin value for each cDNA sample.

Chapter 3

Regulation of the *CDKN2a* locus in response to Myc

p16^{INK4a} plays a pivotal and well-documented role in the defences of HDFs against cellular stresses and oncogenic insults, while the alternative product of the *CDKN2a* locus, ARF, also plays a potential role in the prevention of transformation in HDFs. This places the *CDKN2a* locus at the centre of cellular defences against oncogenic insults. However, the regulation of the *CDKN2a* locus is still poorly understood.

Aberrant Ras activity promotes signalling via the Ras/Raf/MEK signalling pathway and the p38 MAPK pathway, leading to increased transcription of p16^{INK4a} and cell cycle arrest (Serrano et al. 1997; Zhu et al. 1998; Ohtani et al. 2001; Wang et al. 2002; Drayton et al. 2003; Deng et al. 2004). Previous work in this laboratory had shown that expression of exogenous Myc in HDFs also causes a cell cycle arrest accompanied by an increase in the protein levels of p16^{INK4a} and ARF (Drayton et al. 2003). Interestingly, this arrest is not observed in the Q34 and Leiden fibroblast strains. These cells are derived from patients with mutations in both copies of the *CDKN2a* locus, and are functionally p16^{INK4a}-deficient, whilst retaining functional ARF (Brookes et al. 2002; Huot et al. 2002). Further experiments utilising a tamoxifen regulated Myc-ER fusion protein (Littlewood et al. 1995) showed that a modest increase in *INK4a* RNA levels could be observed over a timecourse of 24 hours. This induction was not blocked by cycloheximide suggesting it was a direct effect

of Myc on the *INK4a* locus (S. Drayton, personal communication). These preliminary findings suggested that it would be informative to investigate the regulation of the *INK4a/ARF* locus by Myc and in particular to consider whether *INK4a* and *ARF* were responding independently via elements in their respective promoters or as part of a co-ordinated response to oncogenic challenge.

3.1 The effects of Myc overexpression on p16^{INK4a} and ARF

As a starting point, we wanted to confirm the induction of p16^{INK4a} and ARF at the protein and RNA level in response to retrovirally expressed c-Myc. To simplify interpretation of the results by removing any confounding effects of senescence or cell cycle arrest, the experiments were performed in the p16^{INK4a}-deficient Q34 cell strain that had been transduced with hTERT. For comparison, parallel cultures were infected with a retrovirus encoding H-Ras, a known activator of p16^{INK4a}, or an empty vector control. Pools of infected cells were selected in bleomycin for two weeks, and separate lysates were prepared for RNA and protein analysis to look at the induction of *INK4a* and *ARF* at the protein and RNA levels. Relative protein levels were determined by western blotting, and RNA levels were analysed by quantitative PCR.

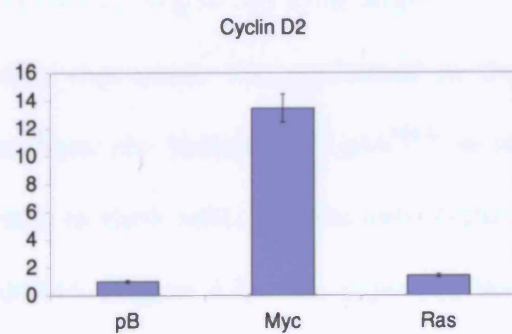
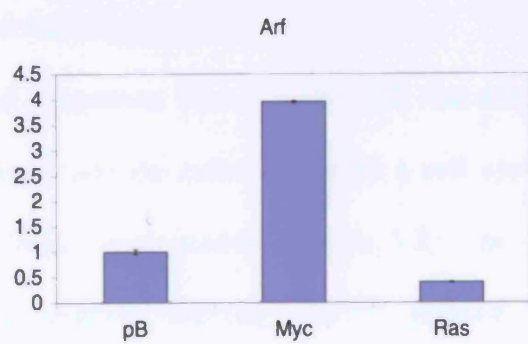
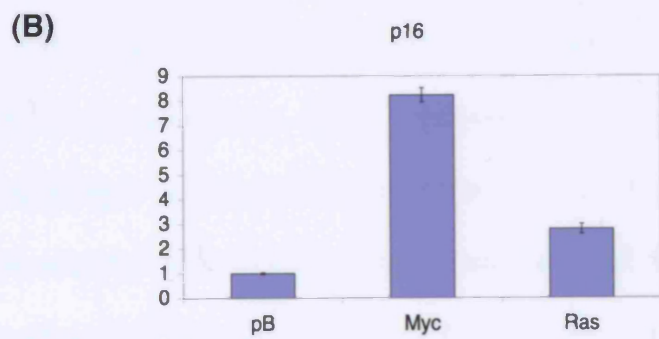
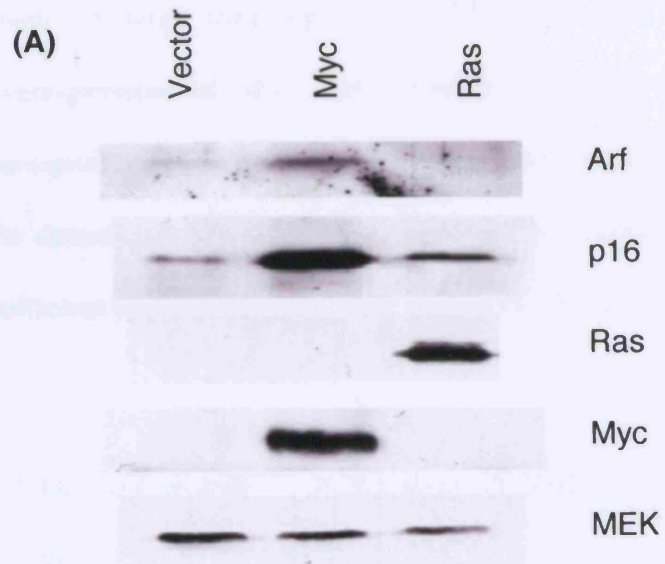
In response to Myc overexpression, *INK4a* RNA was induced 8-fold, and *ARF* RNA was induced 4-fold (Figure 3.1). For comparison, cyclin D2, a direct Myc target (Bouchard et al. 1999), was induced 13-fold at the RNA level (Figure 3.1). Interestingly, *INK4a* RNA was induced only 3-fold and *ARF* RNA was not induced at all in response to the overexpression of oncogenic Ras. The induction of genes at the RNA level was mirrored at the protein

Figure 3.1 Induction of p16^{INK4a} and ARF at the RNA and protein level in response to retroviral expression of Myc

Q34 cells expressing telomerase were infected with a retrovirus expressing Myc, Ras or an empty vector control virus (pBabe^{puro}). Pools of cells were recovered by selection in the appropriate drug

(A) Samples (16µg) of total protein were fractionated by SDS-PAGE in 12% and 15% gels, transferred to membrane, and the immunoblots were developed with antibodies against the indicated proteins followed by ECL.

(B) Samples of RNA (2µg) RNA were reverse transcribed into cDNA which was then used as a template for Quantitative PCR. The data were normalised to Beta-Actin. Cyclin D2 was used as an example of a gene which is directly induced by Myc at the RNA level.



level. A large induction of p16^{INK4a} protein was seen in response to the overexpression of Myc, and a smaller induction was seen in response to oncogenic Ras (Figure 3.1). Although basal levels of ARF are usually below the detection limits by western blotting, the overexpression of Myc caused a sufficient increase to make ARF detectable (Figure 3.1).

3.2 The role of p16^{INK4a} in the arrest of HDFs in response to overexpressed Myc

The crucial role of p16^{INK4a} in implementing an arrest in response to Myc was confirmed using wild-type fibroblasts in which p16^{INK4a} expression had been specifically ablated by RNA interference. A pRetroSuper based plasmid containing a validated short hairpin sequence (shRNA) against human *INK4a* was obtained from Reuven Agami (Voorhoeve and Agami 2003) and was used to ablate p16^{INK4a} expression in Hs68 fibroblasts, a strain of normal fibroblasts obtained from neonatal foreskin.

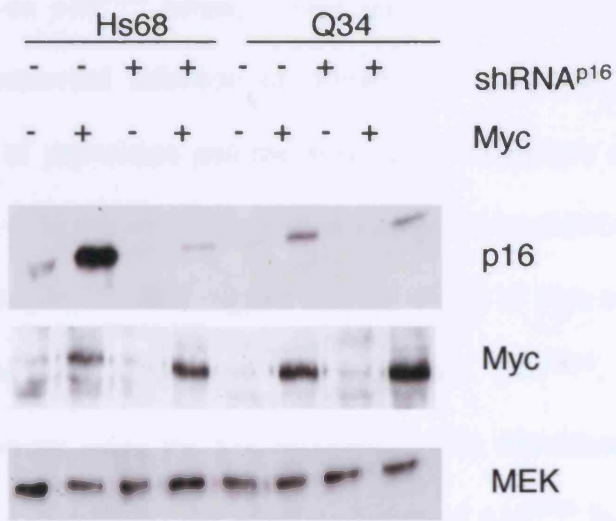
Expression of exogenous Myc in Hs68 cells was accompanied by an increase in p16^{INK4a} levels and the cells underwent a cell cycle arrest, as shown by a decrease in BrdU incorporation (Figure 3.2). In contrast, the Hs68 cells expressing an shRNA targeting p16^{INK4a} showed a reduced induction of p16^{INK4a} and did not undergo a cell cycle arrest.

When a similar experiment was performed in the Q34 strain of p16^{INK4a}-deficient fibroblasts the induction of p16^{INK4a} in response to Myc was less pronounced than in Hs68 cells, and was only slightly reduced by the presence of p16^{INK4a} shRNA (Figure 3.2). As expected, these cells did not arrest as demonstrated by the sustained BrdU incorporation. Although this is in line

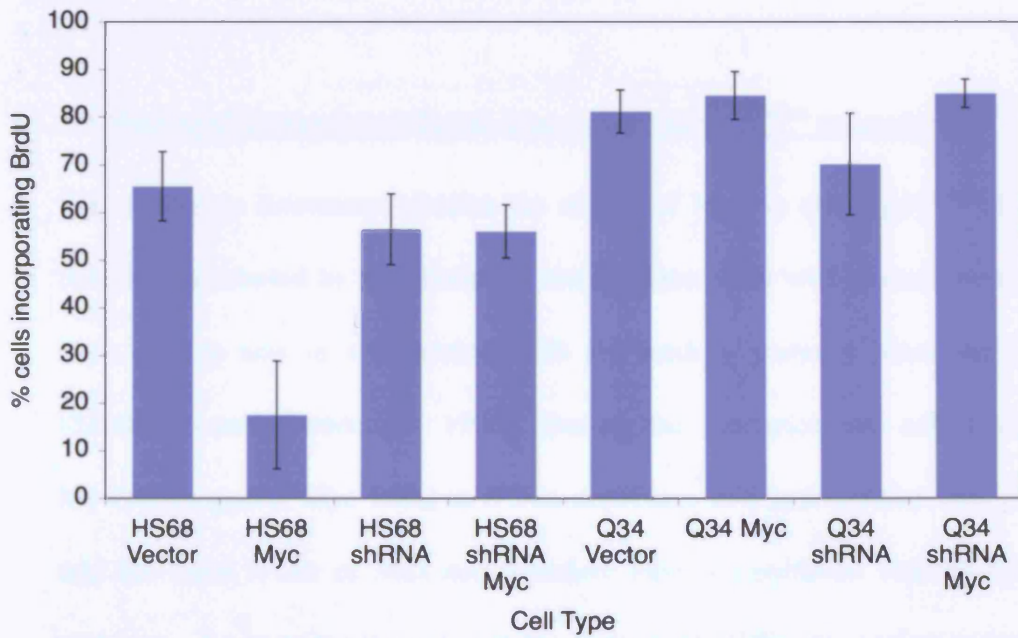
Figure 3.5 The effects of Myc-ER induction on *INK4a* and *ARF* RNA levels over a 24 hour timecourse

Hs68 cells expressing the Myc-ER fusion protein were treated with 4-OH tamoxifen for the indicated times. Samples of RNA (3µg) were reverse transcribed into cDNA which was then used as a template for Quantitative PCR. The data were normalised to Beta-Actin. The Quantitative PCR was repeated three times, and the average value for each timepoint is shown. The error bar corresponds to the standard deviation between these three separate repeats. Cyclin D2 was used as an example of a gene which is directly induced by Myc at the RNA level.

(A)



(B)



with the fact that both p16^{INK4a} alleles in the Q34 cells are functionally impaired (Huot et al. 2002), the interpretation is complicated by the modest effects on p16^{INK4a} levels. These results highlight one of the difficulties in using retroviral infection of primary cell pools as a standard procedure. Levels of expression and the ensuing consequences can be highly variable, and the effectiveness of knockdown achieved by shRNA is also variable.

Nevertheless, the data suggest that the ability of Myc to arrest primary human fibroblasts is dependent on functional p16^{INK4a}, confirming previous observations using the p16-deficient Leiden fibroblast strain (Drayton et al. 2003). Intriguingly, the small induction of p16^{INK4a} in response to oncogenic stress observed in the Q34 cells, was later observed in the p16-compromised Milan fibroblasts (Chapters 4 and 5) suggesting that the p16-status of the cells may affect the ability of oncogenes to induce p16^{INK4a}.

3.3 Factors affecting the ability of Myc to activate p16^{INK4a} transcription

We wanted to determine whether the ability of Myc to affect p16^{INK4a} levels could be attributed to its effects on transcription. It is well documented that Myc always acts in conjunction with its binding partners Max and Mad (Sakamuro and Prendergast 1999). During the transcriptional activation of Myc target genes, Myc binds to E box sequences as a heterodimer with Max, and the basal levels of Max can therefore have a significant bearing on the response. To examine this issue in the context of HDFs, the coding sequence for Max was cloned into the pBabe retroviral vector and introduced into Q34 fibroblasts expressing telomerase and Myc. Levels of p16^{INK4a} in the control

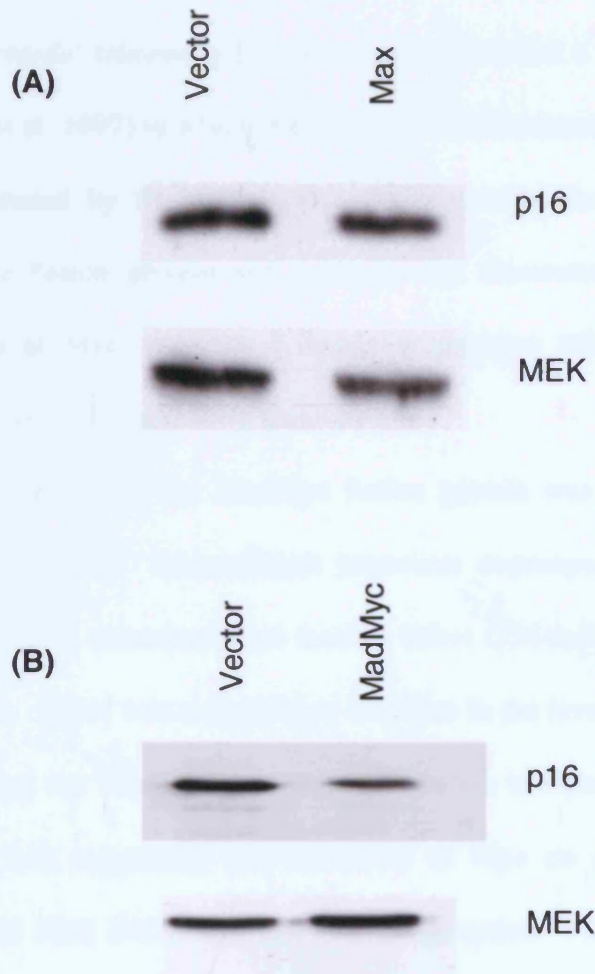


Figure 3.3 The effects of Max and a MadMyc fusion protein on the induction of p16^{INK4a} by Myc

Q34 cells expressing telomerase and Myc were infected with an empty retrovirus control (pBabe^{bleo}) and retrovirus expressing Max (A) or a MadMyc fusion protein (B). Pools of cells were recovered by selection in the appropriate drug.

(A) Samples (16µg) of total protein were fractionated by SDS-PAGE in an 15% gel, transferred to membrane and the immunoblot was developed with antibodies against the indicated proteins followed by ECL

(B) Samples (30µg) of total protein were fractionated by SDS-PAGE in an 15% gel, transferred to membrane and the immunoblot was developed with antibodies against the indicated proteins followed by ECL.

and Max expressing cells were identical (Figure 3.3) suggesting that Max is not limiting for the induction of p16^{INK4a} expression in this system.

The Bernards' laboratory had previously described a MadMyc fusion protein (Berns et al. 1997) in which the amino terminal transactivation domain of Myc was replaced by the transcriptionally repressive domain of Mad. As the MadMyc fusion protein still contains the dimerisation and DNA binding domains of Myc, it exerts a dominant negative effect by binding to Myc binding sites and repressing transcription.

A cDNA encoding the MadMyc fusion protein was cloned into the pBabe retroviral vector. Recombinant retrovirus expressing MadMyc and empty vector control retrovirus were used to infect Q34 cells expressing telomerase and Myc. There was a significant decrease in the level of p16^{INK4a} in the cells expressing the MadMyc fusion protein when compared to the control cells (Figure 3.3) suggesting that the effect of Myc on p16^{INK4a} depends on its ability to bind DNA and activate transcription. However, this does not confirm that Myc is binding to the *INK4a* promoter, as Myc could be acting indirectly via another target gene.

3.4 The contribution of Myc to the endogenous levels of p16^{INK4a} in fibroblasts

Myc is known to be present, and presumably functional, in exponentially growing cell cultures. As Myc activates p16^{INK4a} transcription, we thought it was interesting to investigate whether Myc was contributing to the basal level of p16^{INK4a} protein in human diploid fibroblasts. Cells nearing the end of their replicative lifespan were used for these studies to maximise the endogenous levels of p16^{INK4a}. Having become aware that the Q34 fibroblast strain is

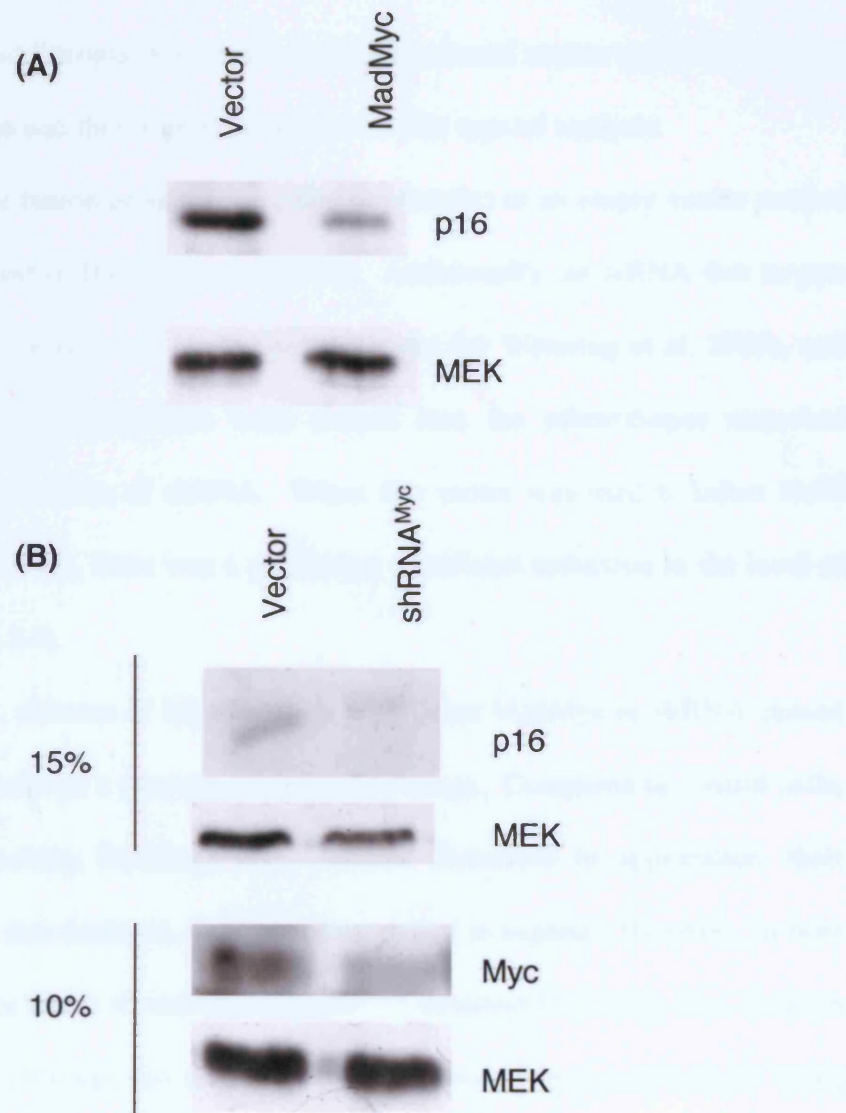


Figure 3.4 The contribution of Myc to the basal level of p16^{INK4a} in Hs68 fibroblasts nearing the end of their replicative lifespan

Hs68 cells nearing the end of their replicative lifespan were infected with an empty retrovirus control (pBabe^{bleo}, or pRetroSuper^{puro}) or with retrovirus expressing either a MadMyc fusion protein (A) or an shRNA targeting Myc (B). Pools of cells were recovered by selection in the appropriate drug.

(A) Samples (16 μ g) of total protein were fractionated by SDS-PAGE in an 15% gel, transferred to membrane and the immunoblot was developed with antibodies against the indicated proteins followed by ECL

(B) Samples (25 μ g) of total protein were fractionated by SDS-PAGE in 10% and 15% gels, transferred to membrane and the immunoblots were developed with antibodies against the indicated proteins followed by ECL.

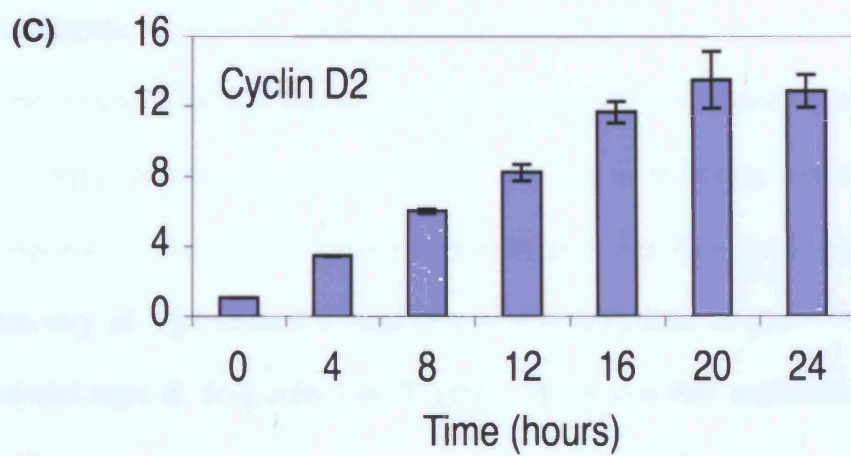
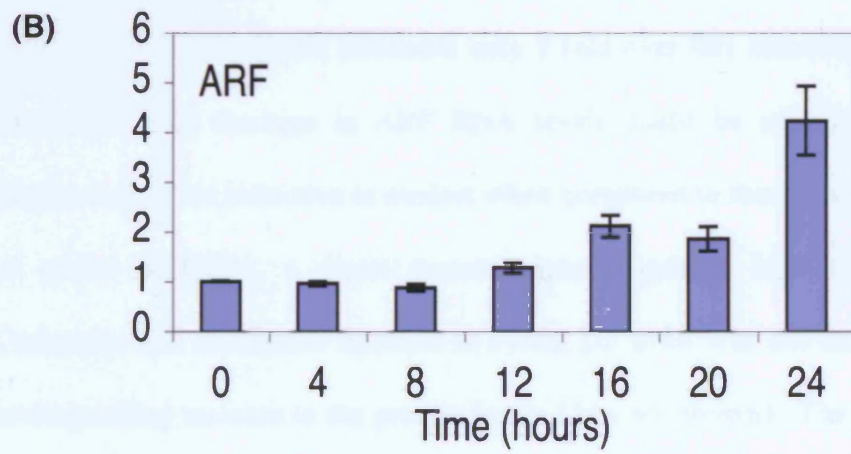
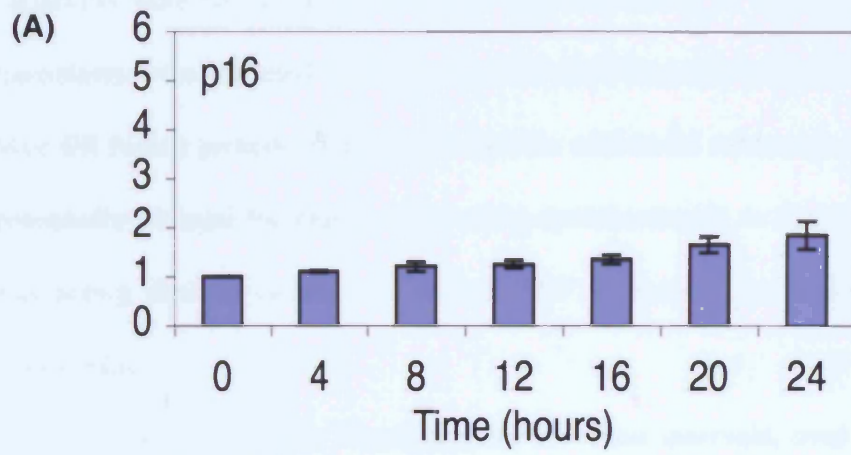
heterogeneous, with individual cells in the culture undergoing senescence at different times (Brookes et al. 2004), we decided to use the Hs68 strain of human diploid fibroblasts as embryonic and neonatal strains appear to be more homogeneous and therefore more suited for this type of analysis.

The MadMyc fusion protein (described previously) or an empty vector control were expressed in Hs68 cells at (PD46). Additionally, an siRNA that targets human c-Myc was found in the literature (van der Wetering et al. 2003), and appropriate oligonucleotides were cloned into the pRetroSuper retroviral vector for production of shRNA. When this vector was used to infect Hs68 fibroblasts (PD42), there was a partial but significant reduction in the level of Myc (Figure 3.4).

Interestingly, ablation of Myc function with either MadMyc or shRNA caused the cells to undergo a dramatic phenotypic change. Compared to control cells, fibroblasts lacking functional Myc became distressed in appearance, their proliferation rate declined, and the culture failed to expand. However, in both circumstances levels of endogenous p16^{INK4a} declined following Myc ablation (Figure 3.4), although this reduction was only modest in the experiment using shRNA targeting Myc. While these experiments cannot preclude an indirect effect of impaired cell growth on the endogenous levels of p16^{INK4a}, these experiments strongly suggest that Myc contributes to the basal level of p16^{INK4a} in HDFs.

3.5 Is the *CDKN2a* locus co-ordinately regulated in response to Myc?

As Myc is known to activate *ARF*, it was interesting to consider whether Myc targets separate elements in the *INK4a* and *ARF* promoters or has a more



global effect on expression from the entire locus. To try to minimise the variability inherent in the use of retroviral expression of Myc, normal Hs68 fibroblasts were infected with a retrovirus encoding the tamoxifen regulated Myc-ER fusion protein. This system had the additional advantage that it could potentially be used for experiments using cycloheximide to determine if Myc was acting directly on the *INK4a* and *ARF* promoters, or indirectly via an intermediate.

RNA and protein samples were prepared at 4 hour intervals, over a period of 24 hours following the addition of 4OH-tamoxifen. As judged by quantitative PCR, p16^{INK4a} RNA levels increased only 2-fold over this timecourse, while a maximal 4-fold increase in *ARF* RNA levels could be seen by 24 hours (Figure 3.5). This induction is modest when compared to the 14-fold induction of cyclin D2 RNA, a direct transcriptional target of Myc (Figure 3.5). Curiously, this substantial increase in cyclin D2 RNA was not mirrored by a corresponding increase in the protein levels (data not shown). The reasons are unclear but may reflect some control of cyclin D2 at the level of mRNA translation.

The relatively weak induction of *INK4a* and *ARF* compared to that of cyclin D2, suggested that the *CDKN2a* locus may not be behaving conventionally in response to Myc. It also contrasted with previous indications that retroviral delivery of Myc caused a relatively robust induction of p16^{INK4a} albeit after several days of drug selection (Figure 3.1). A possible explanation for these differences would be that the effects of Myc on the *CDKN2a* locus are indirect or require long-term alterations to chromatin structure. Alternatively, we noted that the levels of Myc expressed following retroviral infection continued

to rise for several days or even weeks after drug selection (data not shown). The reasons are presently unclear, but similar effects have been observed with Ras. Thus, in theory, the induction of p16^{INK4a} could simply parallel the accumulation of Myc.

To distinguish between these two possibilities we decided to conduct a longterm timecourse using the Myc-ER tamoxifen regulated system in the TIG3 strain of fibroblasts. The TIG3 strain of foetal fibroblasts were considered ideal for these experiments as they have been shown to undergo a relatively synchronous and robust induction of p16^{INK4a} at senescence. However, upon addition of 4-OH tamoxifen, to activate the Myc-ER construct, there was a significant degree of apoptosis that persisted until day 7. By day 11, the culture had started to expand at an increased rate, suggesting selection for cells that had overcome apoptosis or cell cycle arrest in response to Myc.

Despite these complications, cyclin D2 RNA levels were significantly increased by day 2 following addition of tamoxifen and continued to rise up to day 11, where induction was almost 20-fold. By comparison, the changes in *INK4a* and *ARF* RNA levels were relatively modest (2 to 4-fold) and rather erratic (Figure 3.6). As there was also some variability in the control cells that had not received tamoxifen, it is difficult to interpret these effects in terms of timescale of induction.

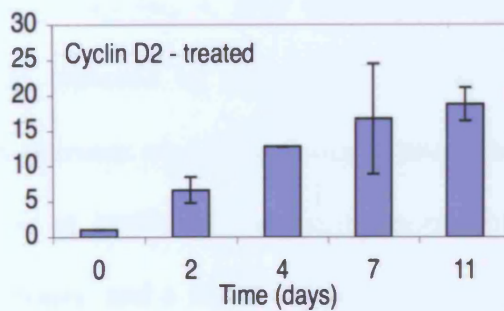
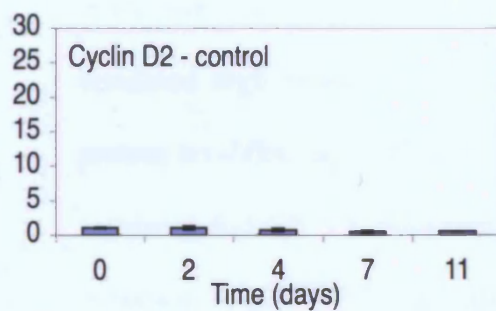
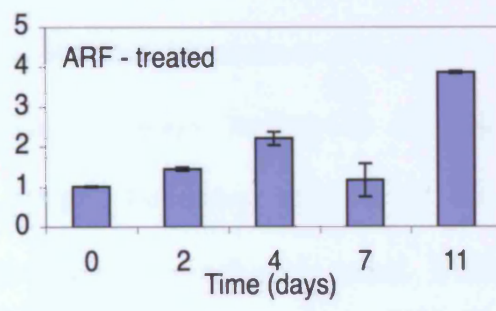
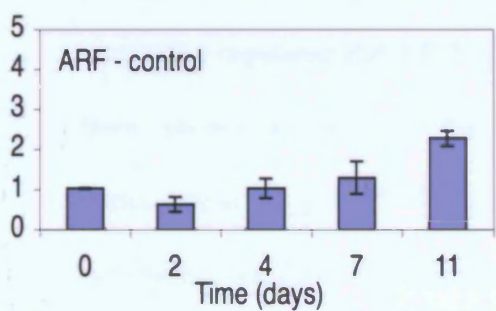
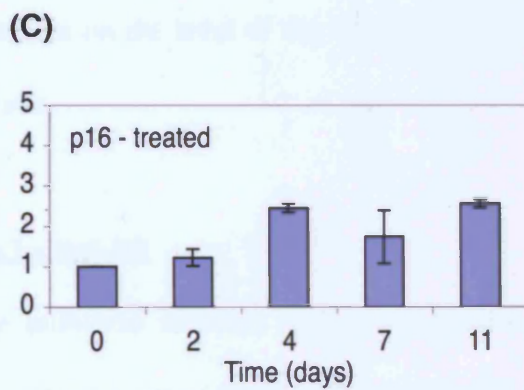
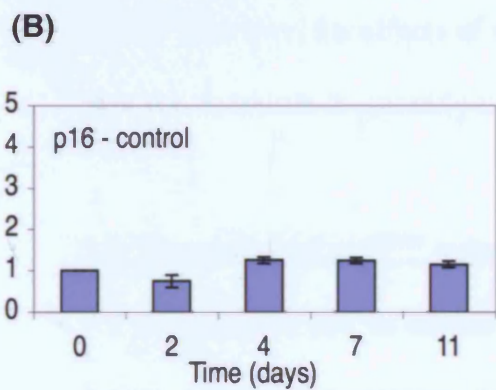
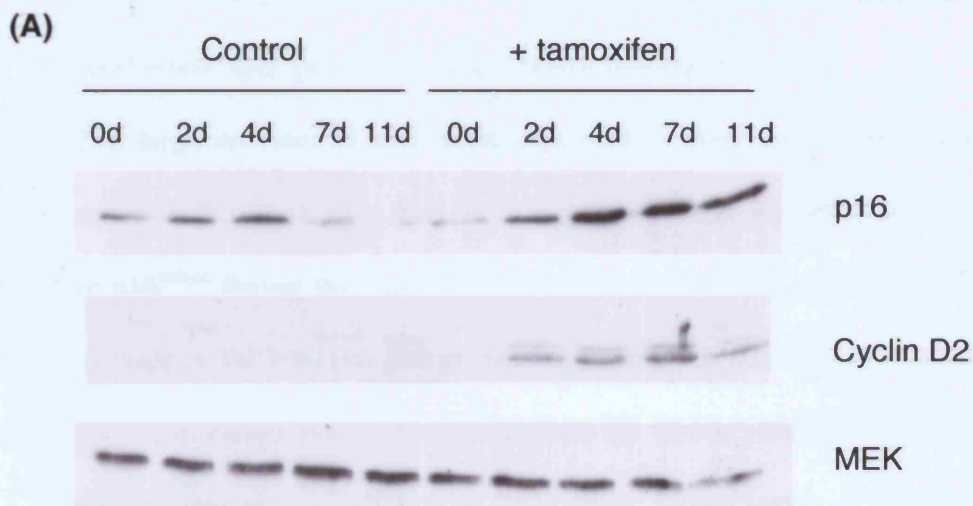
On the contrary, there was a clear increase in p16^{INK4a} protein levels by day 2 post-induction reaching a maximum after 4 days (Figure 3.6). Cyclin D2 protein levels also increased in response to the induction of Myc (Figure 3.5A), but as previously noted (Figure 3.5), the increase in cyclin D2 protein

Figure 3.6 The response of HDFs to the induction of Myc-ER over a timecourse of 11 days

TIG3 cells expressing Myc-ER were treated with 4OH-tamoxifen at day 0, or kept untreated as control cells. Cultures were passaged if they reached confluency.

(A) Samples (30µg) of total protein were fractionated by SDS-PAGE in a 15% gel, transferred to membrane, and the immunoblot was developed with antibodies against the indicated proteins followed by ECL.

(B) and **(C)** Samples of RNA (3µg) RNA were reverse transcribed into cDNA which was then used as a template for Quantitative PCR. The data were normalised to Beta-Actin. The Quantitative PCR was repeated three times, and the average value for each timepoint is shown. The error bar corresponds to the standard deviation between these three separate repeats. Cyclin D2 was used as an example of a gene which is directly induced by Myc at the RNA level.



was not as large as might have been expected from the induction at the RNA level while ARF protein remained below detectable levels.

The large amounts of cell death observed in these experiments give rise to concerns that there may have been a selection for cells expressing high levels of p16^{INK4a} during the course of the experiment, which would have caused an increase in the levels of p16 expression during this timecourse. Concerns have also been raised that levels of the Myc-ER fusion protein could vary during the timecourse experiments, as an increase in the levels of other ER-fusion proteins has been observed in response to addition of tamoxifen (Vance et al. 2004). However, the effects of tamoxifen on the level of the Myc-ER protein over this timescale is currently unknown.

3.6 Timecourse of p16^{INK4a} induction by Raf-ER

For comparison, and to expose any problems inherent in the experimental design, a parallel experiment was conducted using TIG3 cells expressing a tamoxifen regulated Raf-ER YY protein. Raf acts downstream of Ras and has been shown to activate the signalling pathways leading to increased transcription of p16^{INK4a} (Zhu et al. 1998). Following addition of 4OH-tamoxifen, the TIG3 Raf-ER fibroblasts underwent a cell cycle arrest. *INK4a* RNA levels did not increase significantly until day 4, after which point they remained high (Figure 3.7). This was mirrored by an increase in p16^{INK4a} protein levels by day 4 (Figure 3.7). A previous report also using a tamoxifen-regulated Raf-ER YY construct (Zhu et al. 1998) demonstrated a noticeable induction of p16^{INK4a} protein after 16 hours, and a further increase was seen after 32-48 hours. However, a marked increase in p16^{INK4a} was not observed

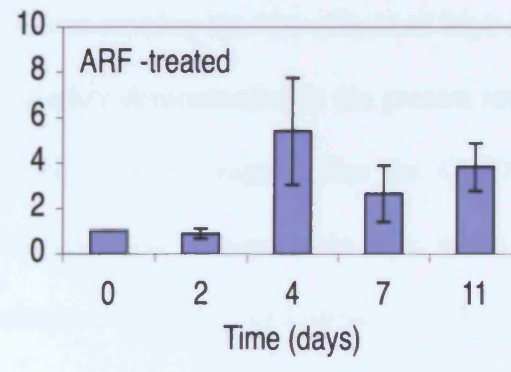
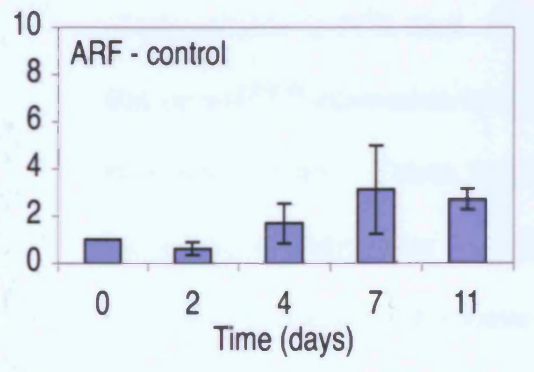
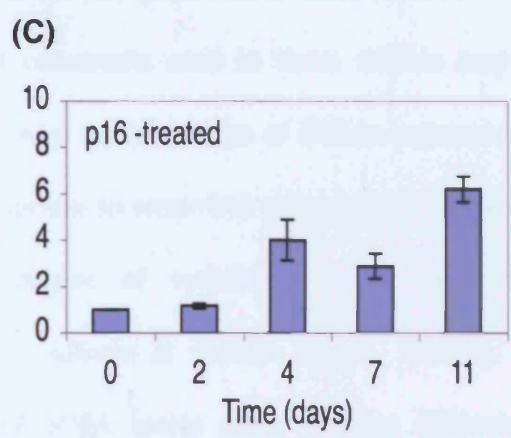
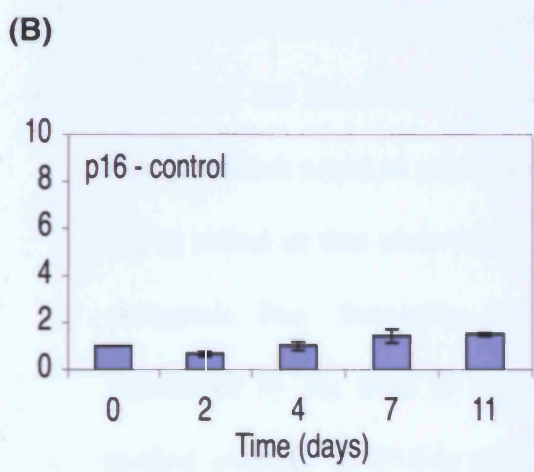
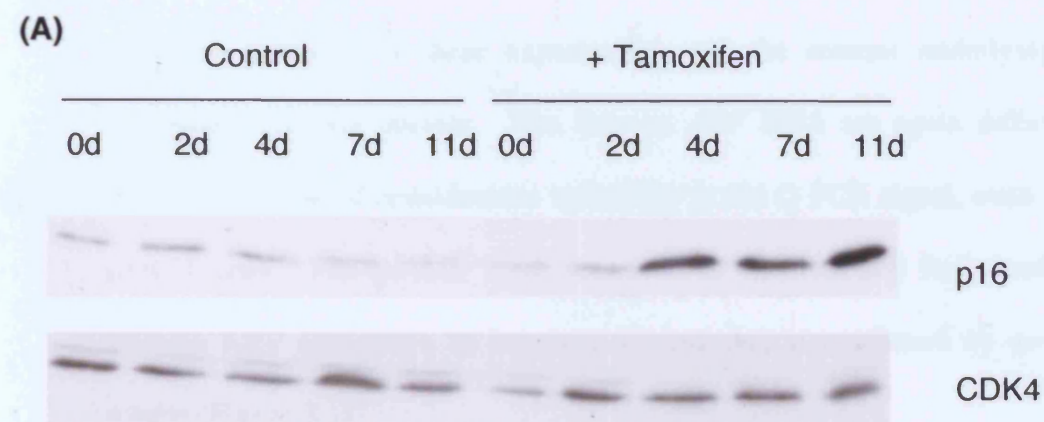


Figure 3.7 The effects of Raf-ER induction on *INK4a* and *ARF* RNA levels over a timecourse of 11 days

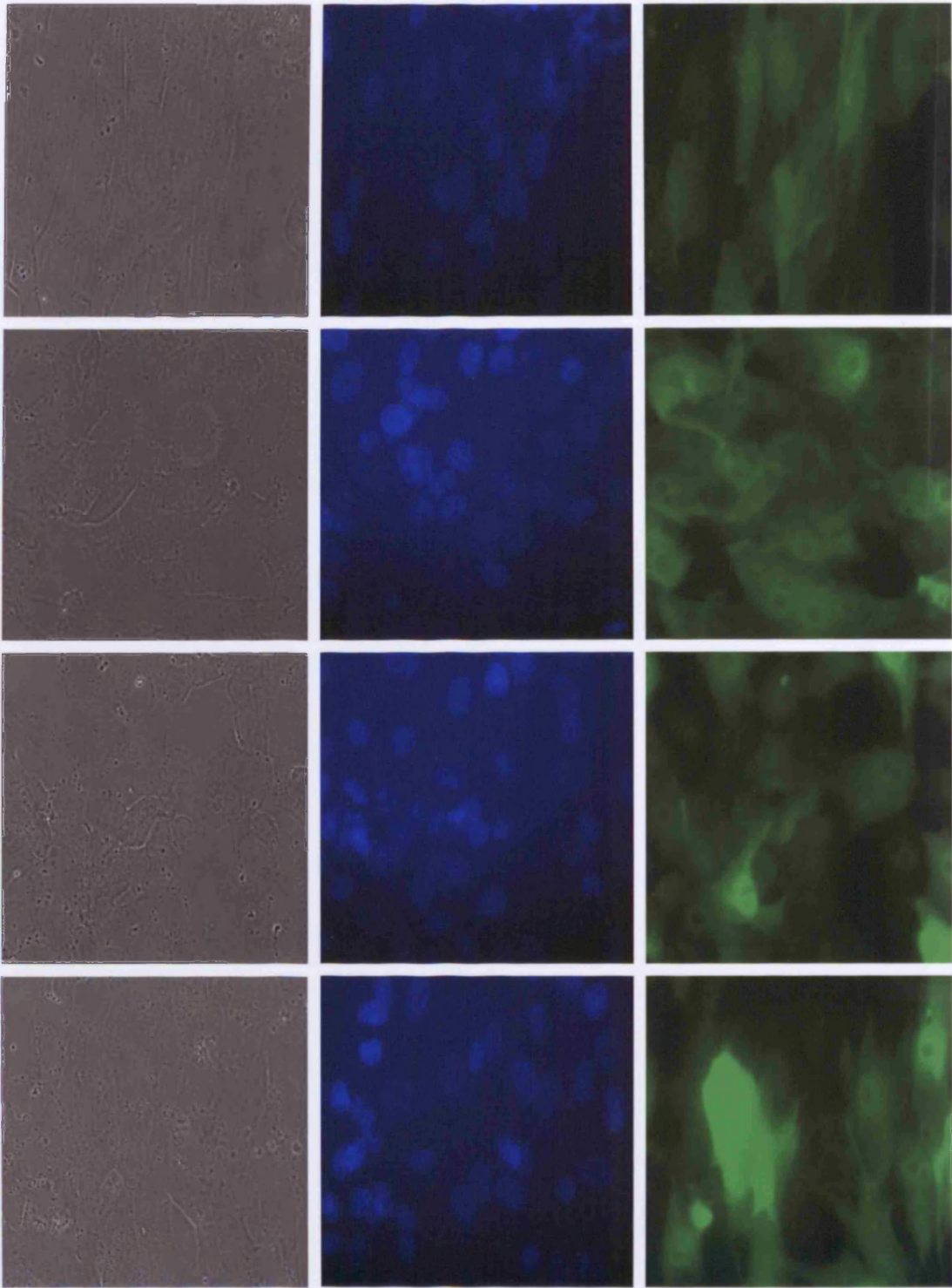
TIG3 cells expressing Raf-ER YY were treated with 4OH-tamoxifen at Day 0, or kept untreated as control cells. Cultures were passaged if they reached confluency. **(A)** Samples (30µg) of total protein were fractionated by SDS-PAGE in an 15% gel, transferred to membrane and the immunoblot was developed with antibodies against the indicated proteins followed by ECL. **(B)** and **(C)** Samples of RNA (3µg) RNA were reverse transcribed into cDNA which was then used as a template for Quantitative PCR. The data were normalised to Beta-Actin. The Quantitative PCR was repeated three times, and the average value for each timepoint is shown. The error bar corresponds to the standard deviation between these three separate repeats.

over this timescale in these experiments, and the reasons underlying this discrepancy remain unclear. The data on *ARF* RNA are again difficult to interpret because of considerable variability in the Q-PCR signal, even in the control cells. The general view, however, is that Ras and Raf should not activate ARF expression in human cells and this is confirmed by previous results (Figure 3.1).

There are several areas of concern in the interpretation of these results. In the first place the tamoxifen-regulated constructs used in these studies may be 'leaky', which could in part explain why the activation of *INK4a* expression is not as robust as that observed in response to retroviral expression of Myc and oncogenic Ras. Secondly, some degree of variability might have been introduced by the need to split cell cultures at various stages. Finally, the modest changes in *INK4a* and *ARF* RNA levels make it more difficult to obtain reliable Q-PCR data. It is however striking that the effects of Myc and Ras on p16^{INK4a} expression are more readily demonstrated at the protein rather than RNA levels. Taken together, these results suggest that the *CDKN2a* locus may be undergoing co-ordinate regulation in response to Myc, while the two genes encoded by this locus undergo differential regulation in response to Ras.

3.7 Increase in p16^{INK4a} protein levels in response to Myc and Raf at an individual cell level

Previous experiments followed the average induction of p16^{INK4a} and ARF at the RNA and protein levels across a pool of cells. However, within a culture, individual cells may respond heterogeneously to the overexpression of Myc,



Phase

DAPI

p16

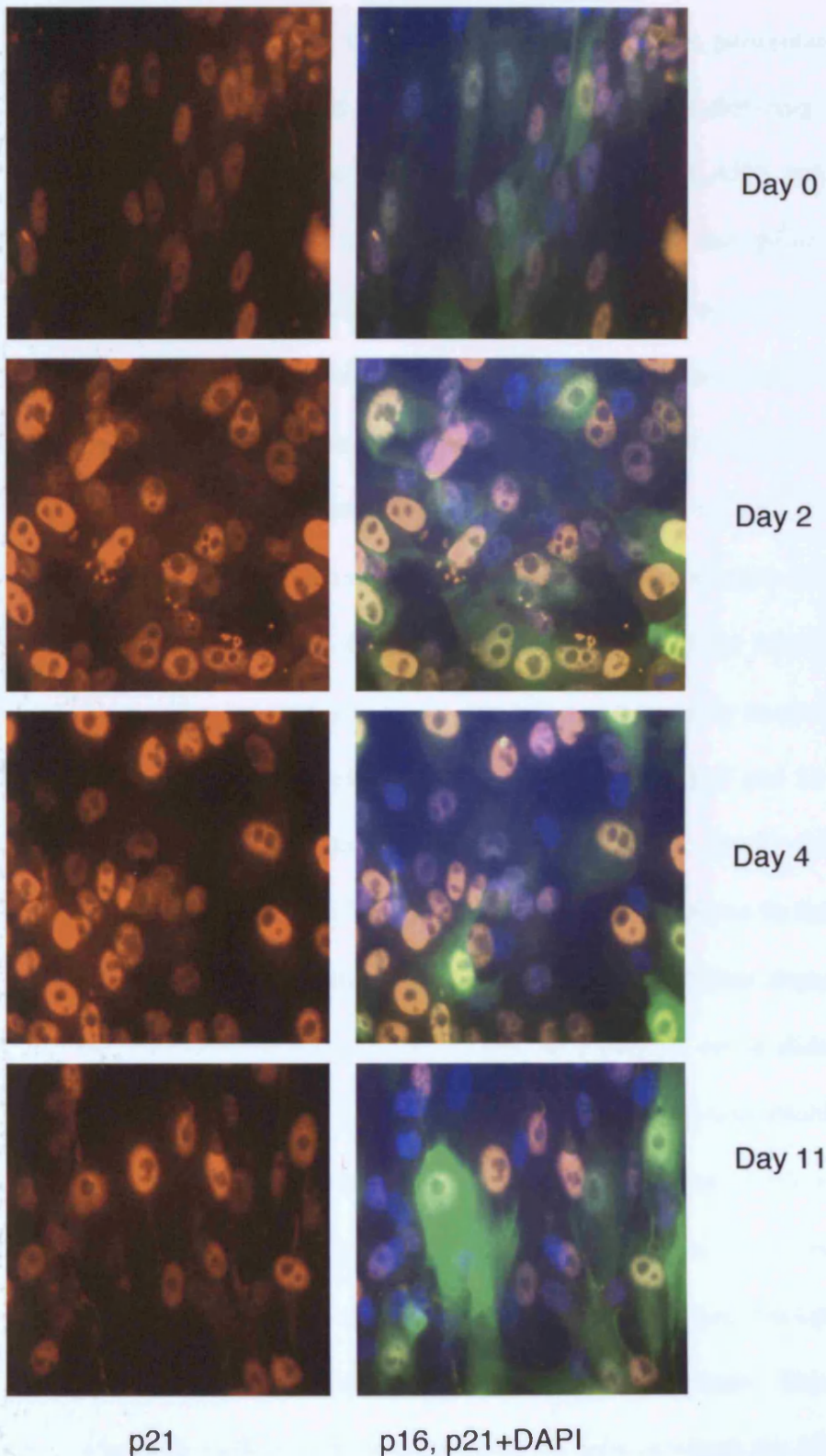


Figure 3.8 Induction of p16^{INK4a} in response to Myc-ER at the individual cell level over a timecourse of 11 days

TIG3 cells expressing Myc-ER were treated with 4OH-tamoxifen at Day 0, and were fixed after the indicated number of days. Cells were stained using immunofluorescence against p16^{INK4a} and p21^{CIP1}. Cell nuclei were visualised using a DAPI stain. Pictures were taken at 40x magnification.

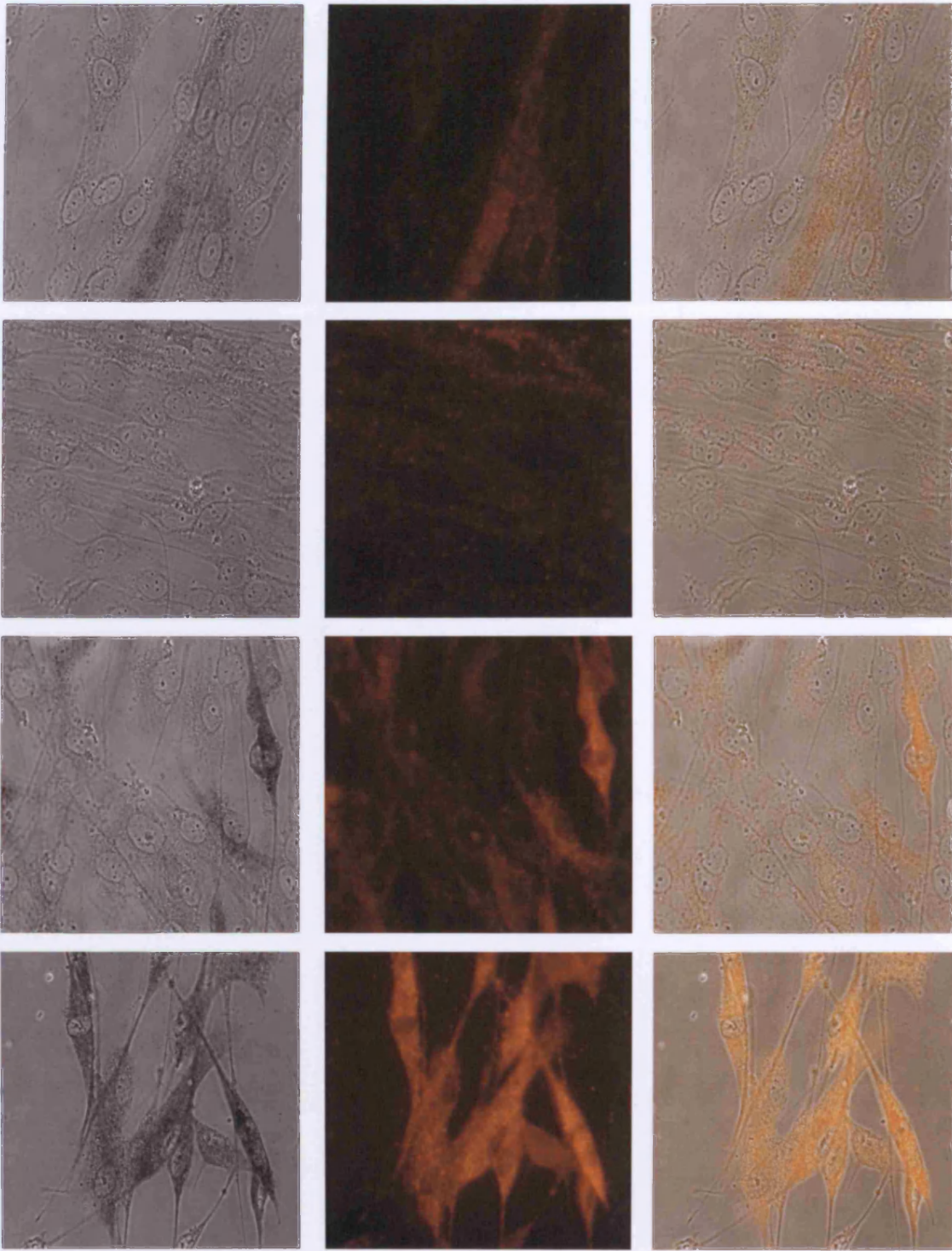
or to induction of the Ras signalling pathway. Cells, particularly those derived from surface exposed sites may have undergone differing levels of stress which may affect the basal levels of p16^{INK4a} and ARF and their ability to activate transcription of these genes in response to oncogenic insults (Benanti and Galloway 2004; Brookes et al. 2004). The possibility should also be considered that the induction of p16^{INK4a} may be binary, i.e. either off or on within a single cell, and would show “digital” rather than “analogue” kinetics. To try to address these issues, we elected to use immunohistochemical and fluorescent stains to monitor increased p16^{INK4a} expression in individual TIG3 cells expressing Myc-ER or Raf-ER. TIG3 fibroblasts were used as they are from a foetal source and should respond homogeneously to an oncogenic insult. Fibroblasts were plated out on glass slides and at 2, 4 and 11 days following addition of 4OH-tamoxifen, the cells were fixed and stained for immunofluorescence. The Raf-ER protein was found to be fused to GFP, and the secondary antibody used to detect p16^{INK4a} in these experiments emitted light at the same wavelength as GFP, so a parallel set of slides of TIG3 Raf-ER cells were used to visualise p16^{INK4a} induction by immunohistochemistry. In response to increased levels of Myc, cells underwent a morphological change becoming smaller and more transformed in appearance (Figure 3.8). At the beginning of the timecourse, some cells had background levels of p16^{INK4a} that could be visualised by immunofluorescence. This may have been a genuine background, or these could be cells in which the Myc-ER construct was ‘leaky’, as some background apoptosis was observed in uninduced cultures of TIG3 Myc-ER. During the timecourse, the intensity of p16^{INK4a} staining in individual cells increased, as did the proportion of cells staining

positive for p16^{INK4a}. However, even after 11 days, some cells did not have increased levels of p21^{CIP1} or p16^{INK4a}, as DAPI stained nuclei could be seen which were in cells that were negative for either p21^{CIP1} or p16^{INK4a}. Some cells stained positive for a single CDK inhibitor, and double positive cells could also be observed (Figure 3.8).

In response to activation of the Raf pathway, cells underwent a distinct morphological change becoming elongated and more “spindly” in appearance (Figure 3.9). It was also observed that by day 11, DAPI foci could be observed in the nuclei of cells in which Raf-ER had been induced (Figure 3.9), although these were not detected in cells expressing Myc-ER. The presence of these foci may suggest that the cells had undergone a senescence programme and formed SAHF, as described in other settings (Narita et al. 2003). Excepting the presence of DAPI foci, the pattern of p16^{INK4a} induction in response to Raf-ER, was reminiscent of that seen in response to Myc-ER. In the control cultures, some cells could be seen with low levels of p16^{INK4a} but the number of cells expressing p16^{INK4a} and the level of expression increased throughout the timecourse. However, unlike the Myc-ER cells, all the Raf-ER cells expressed high levels of p16^{INK4a} by day 11.

These observations supported the idea that induction of p16^{INK4a} may be “binary”, an idea which has been previously proposed (Brookes et al. 2004). However, fluorescence detection methods may have threshold levels which make analogue variations in p16^{INK4a} levels appear digital. These results are consistent with the idea that the response of individual cells to overexpressed Myc is heterogeneous and some cells do not induce p16^{INK4a}. Perhaps other factors can affect the expression of p16^{INK4a} in response to Myc, and some

(A)



Phase

p16

Merge

(B)

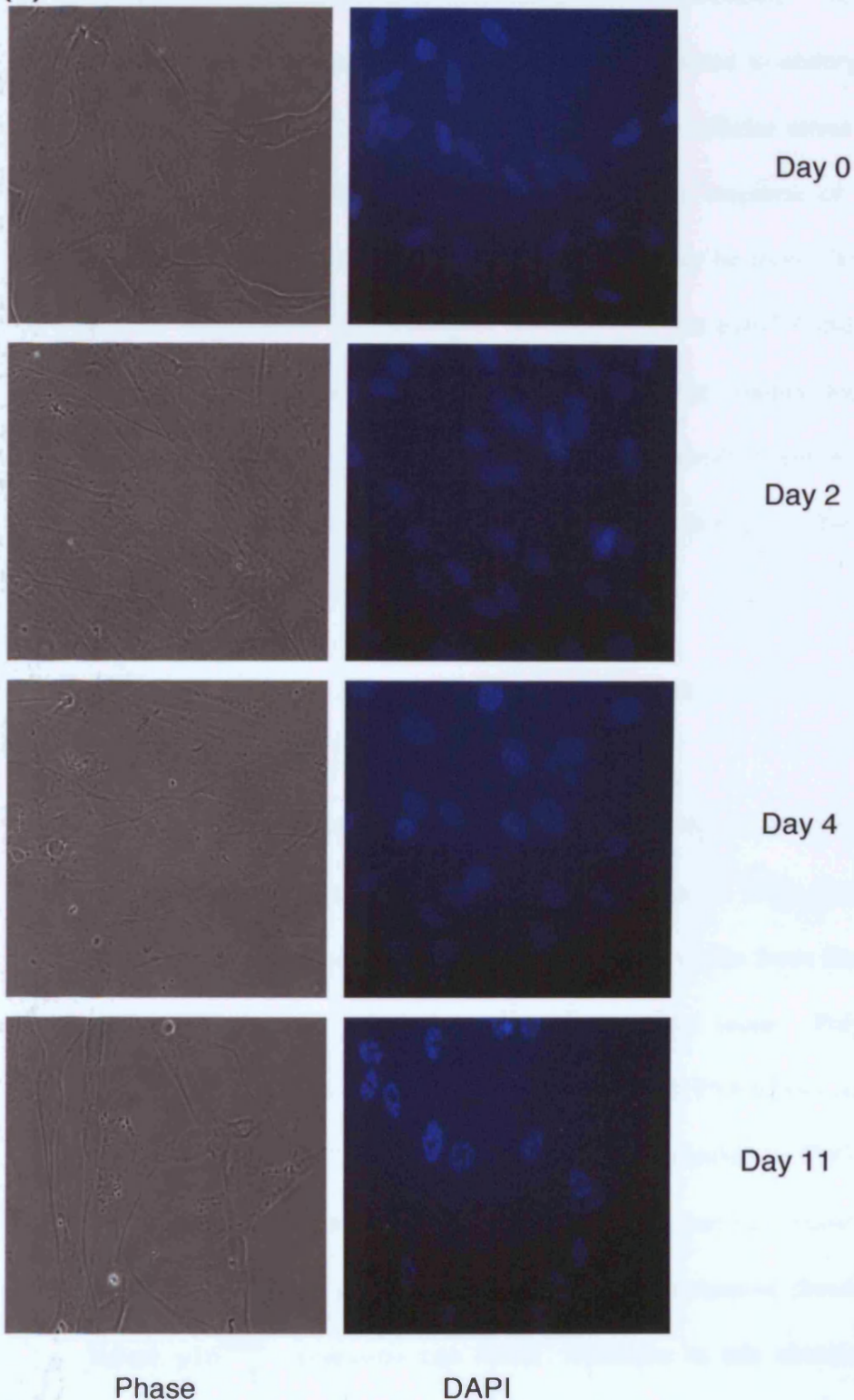


Figure 3.9 Induction of p16^{INK4a} at the single cell level in response to induction of Raf-ER

TIG3 cells expressing Raf-ER YY were treated with 4OH-tamoxifen at Day 0. Cells were fixed after the indicated number of days. p16^{INK4a} was visualised using immunohistochemistry (A), and cell nuclei were visualised using a DAPI stain (B). Pictures were taken at 40x magnification using phase contrast, and fluorescence to visualise p16^{INK4a}.

cells may be predisposed to activate p16^{INK4a} expression. A report in the literature suggests that fibroblasts become predisposed to undergo a cell cycle arrest in response to Ras as a result of previous cellular stress (Benanti and Galloway 2004). This may be analogous to the response of fibroblasts to Myc, and cells that have sustained more stress may be more likely to activate p16^{INK4a} expression. Interestingly, we observed that p16^{INK4a} did not appear to be present in the cell nuclei but appeared to be mainly localised in the cytoplasm of the cells. This is at odds with the involvement of p16^{INK4a} in the cell cycle, but has been previously reported (Nilsson and Landberg 2005).

3.8 Is cell division necessary for the induction of *INK4a* expression in response to Myc?

We were interested in finding an explanation for the slow kinetics of p16^{INK4a} induction, and the reasons that this induction appears to be binary. There is considerable evidence in the literature that transcription from the *INK4a* locus can be affected by chromatin remodelling of the locus. Polycomb group proteins are known to repress transcription of both *INK4a* and *ARF* (Jacobs et al. 1999a; Gil et al. 2004), and the locus is susceptible to CpG methylation. This led us to consider the intriguing hypothesis that fibroblasts may need to replicate their DNA and undergo cell division to remove chromatin imprints before p16^{INK4a} expression can occur. Attempts to use chemical inhibitors, such as aphidicolin, to block cell division proved unsatisfactory because it exacerbated the apoptosis observed following induction of the Myc-ER construct. Serum starvation was equally problematic and as an alternative strategy, Hs68 cells expressing the Myc-ER fusion protein were grown to

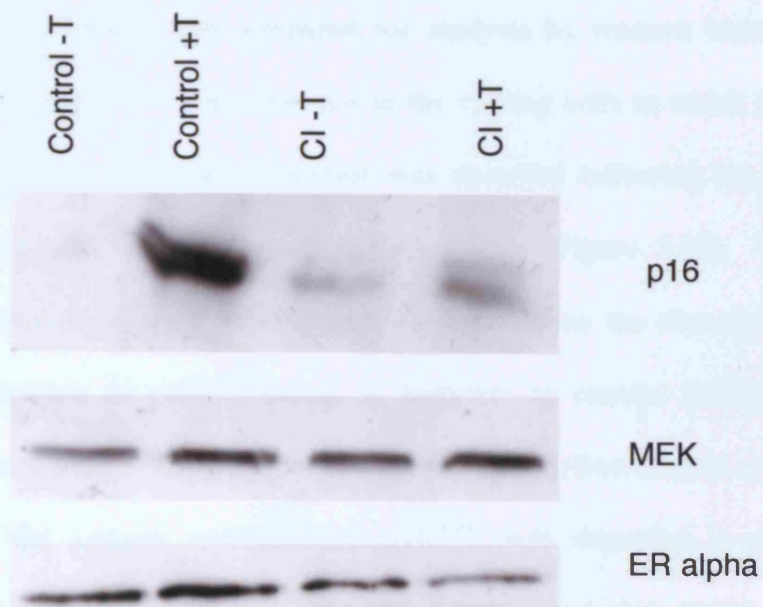


Figure 3.10 The effects of contact inhibition on the induction of p16^{INK4a} in response to Myc-ER

Hs68 cells expressing Myc-ER were treated for 5 days with 4OH tamoxifen or cold ethanol as a control. Samples (25µg) of total protein were fractionated by SDS-PAGE in an 15% gel, transferred to membrane and the immunoblot was developed with antibodies against the indicated proteins followed by ECL.

CI = contact inhibited T = 4-OH tamoxifen

confluency, and kept in this state for several weeks to ensure that all the cells were quiescent. Some of the Hs68s were replated at sub-confluent levels and re-entered the cell cycle, while other cells were kept contact inhibited. Myc-ER was induced by the addition of 4-OH tamoxifen, and 5 days post induction, lysates were prepared for analysis by western blotting. A large increase in p16^{INK4a} was observed in the cycling cells in which Myc had been induced, but a far smaller increase was observed following the addition of 4-OH tamoxifen to the contact inhibited cells (Figure 3.10). However, the interpretation of these results were confounded by the observation that there was increase in p16^{INK4a} levels in response to contact inhibition. This is consistent with a recent report in the literature (Ben-Saadon et al. 2004), in which the authors reported that p16^{INK4a} was degraded in a cell density dependent manner by the ubiquitin system, and that sparse cell cultures expressed less p16^{INK4a} than dense cell cultures.

From these crude initial experiments, it is difficult to conclude that cell division is indeed required for expression of p16^{INK4a} in response to Myc, as there is likely to be a general decrease in protein synthesis in the density arrested cells.

3.9 The effects of 5-azacytidine on p16^{INK4a} induction

It is known that p16^{INK4a} expression increases upon the treatment of cells with 5-azacytidine to remove methylation imprints, and methylation is a known mechanism by which p16^{INK4a} expression is silenced during cancer (Herman et al. 1995; Merlo et al. 1995; Otterson et al. 1995; Costello et al. 1996; Lo et al. 1996). As an alternative approach we considered the possibility that cell

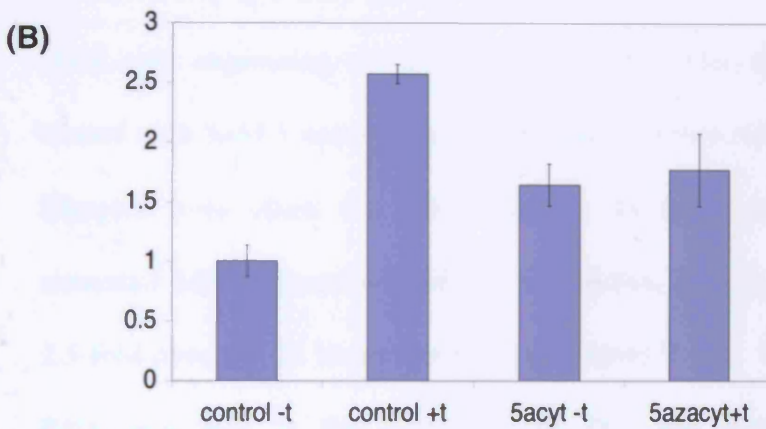
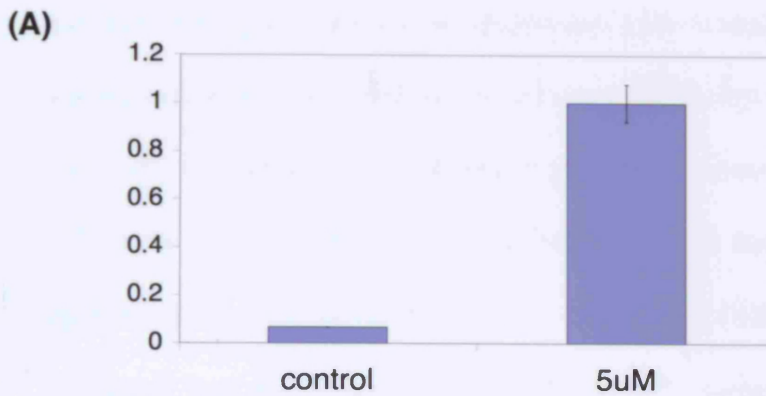


Figure 3.11 The effects of treatment with 5-azacytidine on the induction of p16^{INK4a} by Myc-ER

(A) U2OS cells were treated with 5 μ M 5-Azacytidine for 48h.

(B) Hs68 Myc-ER cells were treated with 5 μ M 5-Azacytidine for 64 hours before being additionally treated with 4OH tamoxifen for a further 24 hours.

Samples of RNA (3 μ g) RNA were reverse transcribed into cDNA which was then used as a template for Quantitative PCR. The data were normalised to Beta-Actin.

division and replication of the cellular DNA may be erasing a methylation imprint, thereby allowing the subsequent transcription of *INK4a* RNA. If this was true, then pre-treatment of fibroblasts with 5-azacytidine to remove any methylation would facilitate the induction of *INK4a* by Myc-ER.

To verify the effectiveness of the 5-azacytidine concentration used, U2OS cells were treated with 5 μ M 5-azacytidine for 48 hours, and samples were taken for RNA analysis by quantitative PCR. The *INK4a* locus is methylated in this cell line, and using this protocol, p16^{INK4a} expression was reactivated as determined by quantitative PCR (Figure 3.11).

Hs68 cells expressing the tamoxifen inducible Myc-ER construct were pre-treated with 5 μ M 5-azacytidine for 64 hours, before induction with tamoxifen. Samples were taken for RNA analysis 24 hours post-induction. In the untreated cells induced with 4-OH tamoxifen, *INK4a* RNA levels increased 2.5-fold over the 24 hours timecourse (Figure 3.11). No induction of *INK4a* RNA was seen in the induced cells that had been pre-treated with 5-azacytidine. However, the pre-treated cells had an increased basal level of *INK4a* RNA relative to the untreated controls (Figure 3.11) suggesting that there may be some methylation of this locus in normal human diploid fibroblasts.

3.10 Discussion

Overexpression of Myc is generally viewed as promoting growth and proliferation, and it does this by altering the level of many cellular proteins. Among the reported Myc target genes are proteins such as CDK4, cdc25, cyclin D1 and cyclin D2 (Galaktionov et al. 1996; Bouchard et al. 1999; Perez-Roger et al. 1999; Collier et al. 2000; Hermeking et al. 2000), and increased levels of these proteins helps to drive the cell cycle. Myc also down-regulates, or overrides the effects of, a number of cell cycle inhibitors such as p21^{CIP1}, p27^{KIP1}, and p15^{INK4b} (Bouchard et al. 1999; Perez-Roger et al. 1999; Claasen and Hann 2000; Collier et al. 2000; Hermeking et al. 2000; O'Hagan et al. 2000; Staller et al. 2001; Herold et al. 2002; Seoane et al. 2002).

In contrast to its effects on cell division and growth, Myc also engages anti-proliferative mechanisms such as apoptosis. Although it has generally been assumed that the activation of ARF in response to Myc is pro-apoptotic, overexpression of ARF in HDFs causes a cell-cycle arrest. Myc has also been reported to arrest HDFs in a p53-dependent manner via the upregulation of p21^{CIP1} (Felsher et al. 2000). This suggests that Myc may cause a cell-cycle arrest and in our system, Myc activates p16^{INK4a} and ARF (Drayton et al. 2003)(Figures 3.1 and 3.6), and can arrest HDFs in a p16^{INK4a}-dependent fashion (Figure 3.2). This resembles the response of HDFs to overexpression of oncogenic Ras, and reinforces the idea that cells may trigger a cell-cycle arrest if they sense aberrant oncogenic signalling. However, the ability of Myc to arrest cells remains controversial, and the outcome of Myc overexpression is likely to depend on the balance of pro- and anti-proliferative

factors induced in an individual cell. The effects of Myc may even be dose-dependent, with the level of Myc expressed by an individual cell determining its fate.

Overexpression of Myc has been reported to activate expression of hTERT, by inducing transcription of the gene directly (Wang et al. 1998; Greenberg et al. 1999; Wu et al. 1999; Cerezo et al. 2002; McMurray and McCance 2003; Veldman et al. 2003). Although this would be expected to facilitate immortality, only one report suggests that expression of Myc alone can immortalise cells (Gil et al. 2005). Even the ability of Myc to activate hTERT remains controversial, and some reports suggest that activation of hTERT expression by Myc may be insufficient to increase telomerase activity (Gewin and Galloway 2001; Oh et al. 2001; Cerezo et al. 2002). It has also been reported that expression of exogenous hTERT can activate Myc (Wang et al. 2000). Work in this laboratory has shown that expression of Myc does not automatically activate hTERT (S Drayton, unpublished observations), but may increase the probability of hTERT activation or increase the levels of hTERT in cells in which the gene is already active.

Microarray and ChIP analyses suggest that in addition to the target genes already discussed, Myc has multiple target genes and exerts both positive and negative effects on their expression (Coller et al. 2000; Eisenman 2001; Fernandez et al. 2003; Haggerty et al. 2003). Indeed, it seems possible that Myc is involved in the general facilitation of transcription, as a large number of Myc target genes are induced only weakly by Myc alone (Fernandez et al. 2003). It is also becoming apparent that Myc modulates the expression of genes by influencing the chromatin structure at the locus working in

combination with a variety of co-factors including GCN5, TIP60, TIP58, TIP59 (McMahon et al. 1998; Cheng et al. 1999b; Wood et al. 2000; Betz et al. 2002; Frank et al. 2003; Liu et al. 2003; Oruetebarria et al. 2004; Vries et al. 2005). Another Myc co-factor is Snf5, which has been shown to reactivate p16^{INK4a} expression upon its reintroduction into Snf5-null tumour cells (Cheng et al. 1999b; Betz et al. 2002; Oruetebarria et al. 2004; Vries et al. 2005). However, we have been unable to demonstrate induction of p16^{INK4a} in HDFs in which Snf5 expression is intact (R Jones, unpublished observations), reinforcing the point that expression of a gene depends upon a balance of factors, only one of which may be rate-limiting within a certain system.

There has been little insight into the nature of Myc binding domains beyond the canonical E-box and variations thereof (Blackwell et al. 1993). A scan of the *INK4a/ARF* human genomic locus revealed multiple potential binding sites, but attempts to detect Myc at these sites using ChIP (in collaboration with Bernard Luscher, Aachen, Germany), proved unrewarding, and it still remains unclear whether p16^{INK4a} is a direct transcriptional target of Myc. In support of this hypothesis, it has been demonstrated that *INK4a* RNA levels increase in response to overexpressed Myc. Also, the induction of p16^{INK4a} in response to Myc can be reduced by co-expression of the MadMyc fusion protein, demonstrating that the mechanism by which Myc affects p16^{INK4a} levels involves the DNA binding activities of Myc. However, the induction of *INK4a* in response to Myc is very slow when compared to that of the well-documented Myc target gene cyclin D2. The effects of Myc on p16^{INK4a} expression at the RNA level are reproducibly modest, and a greater induction of p16^{INK4a} is seen at the protein level suggesting that Myc may affect p16^{INK4a}

levels by mechanisms other than transcription. Attempts to address these doubts using protein synthesis inhibitors are confounded by the timescale of the response, reporter assays using Myc are notoriously susceptible to the balance of proteins such as Myc and Mad.

In summary, while efforts to uncover the mechanism by which Myc activates p16^{INK4a} were confounded by the heterogeneity of the response of individual cells and different fibroblast strains, it remains clear that Myc is able to activate both p16^{INK4a} and ARF reinforcing the role of these proteins as important tumour suppressors in the response to oncogenic challenges within the cell.

Chapter 4

Characterisation of the Milan fibroblast strain

The R24P variant of p16^{INK4a} has been described in multiple melanoma families (Ruas and Peters 1998; Della Torre et al. 2001). While arginine 24 is not conserved between the four different members of the human INK4 family of CDK inhibitors, it lies on the edge of a conserved alpha-helix region (Ruas and Peters 1998). Binding experiments using *in vitro* translated products have suggested that this variant of p16^{INK4a} retains some ability to associate with CDK6, but is incapable of binding to CDK4 (Harland et al. 1997) (Figure 4.1). This implies that it should be possible use the R24P variant to distinguish between the two functions of p16^{INK4a}, inhibition of CDK4 and CDK6.

While analysing the transmission of the R24P mutation in a family showing inherited predisposition to melanoma, our collaborators Gabriella Della Torre and Domenico Delia (Istituto Nazionale Tumori, Milan) identified an individual who is homozygous for the R24P variant of p16^{INK4a} (Figure 4.2). We obtained primary skin fibroblasts from a biopsy conducted on this patient, and designated this strain as “Milan”. As well as providing information on the relative importance of CDK4 and CDK6 in senescence and transformation, it was anticipated that the Milan cells would enable us to consolidate and extend our observations with other strains of p16^{INK4a}-deficient fibroblasts.



Figure 4.1 Binding of the R24P variant of p16^{INK4a} to CDK4 and CDK6

CDK4, CDK6, wild-type p16^{INK4a}, and the p16^{INK4a} variants R24P, and M52I (a non-binding mutant), were translated from pBluescript and radio-labelled with methionine. The p16^{INK4a} variants were then incubated with the CDK4 and CDK6 proteins for 30 minutes at 30°C. The mixture was then incubated with 5µl DPAR12 antibody raised against p16^{INK4a}, and 25µl protein A beads in high salt buffer containing 3% BSA and protease inhibitors. Proteins bound to the beads were separated by SDS-PAGE in a 12% gel, and transferred to membrane which was then incubated with film.

Figure provided courtesy of Sharon Brookes



Figure 4.2 Pedigree of the family from which the homozygous carrier of R24P was identified

Allelic status of *INK4a* is indicated in red where known, and the presence of a black quarter indicates that the patient has suffered from cancer. MM indicates that the patient has suffered from metastatic melanoma, while the number indicates the age at which this was discovered. The homozygous patient (identified by *) is the patient who presented with metastatic melanoma at the age of 45.

(Figure provided by Gabriella della Torre, Istituto Nazionale Tumori, Milan, Italy)

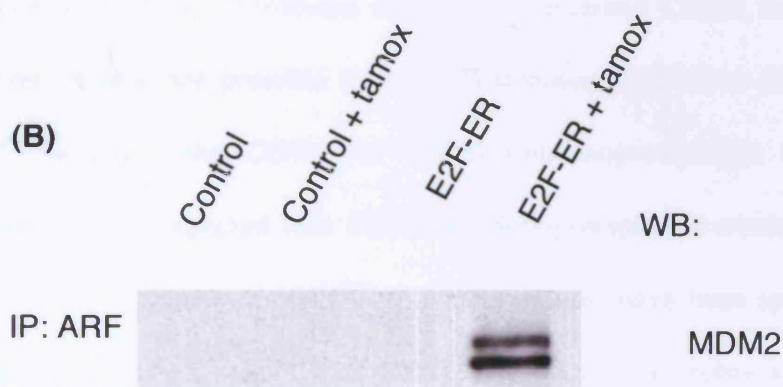
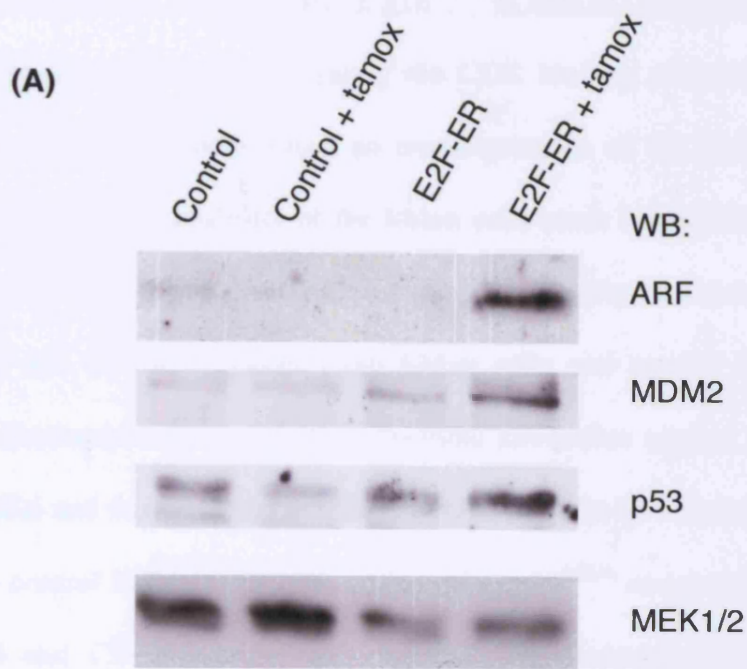


Figure 4.3 ARF function in Milan fibroblasts

Milan cells expressing the E2F-ER fusion protein, or an empty vector control (pBabe^{puro}) were treated with 4-OH tamoxifen for 24 hours before samples were taken.

(A) Samples (25 μ g) of total protein were fractionated by SDS-PAGE in a 15% gel, transferred to membrane, and the immunoblot was developed with antibodies against the indicated proteins followed by ECL.

(B) Samples of total protein (1mg) were incubated with 20 μ l protein A beads and 5 μ l rabbit polyclonal anti-ARF antibody. Proteins bound to the beads were separated by SDS-PAGE in a 10% gel, transferred to membrane, and the immunoblot was developed with an antibody against MDM2 followed by ECL.

4.2 Ability of the R24P variant of p16^{INK4a} to bind to CDK4 and CDK6

Previous experiments investigating the CDK binding properties of the R24P variant of p16^{INK4a} have relied on overexpression of the protein, or *in vitro* translation. The availability of the Milan cells made it possible to ask whether the endogenous R24P protein also showed a capacity to discriminate between CDK4 and CDK6. Lysates from Milan cells and normal Hs68 fibroblasts were immunoprecipitated with polyclonal antibodies against p16^{INK4a}, CDK4 or CDK6 and the immune complexes were analysed by immunoblotting.

In the control Hs68 fibroblasts, endogenous p16^{INK4a} co-precipitated with both CDK4 and CDK6 and in the reciprocal immunoprecipitation, CDK4 and CDK6 co-precipitated with endogenous p16^{INK4a} (Figure 4.4). In contrast in Milan cells, the p16^{INK4a} immune complexes contained CDK6, but not CDK4. However, it was not possible to detect immunoprecipitation of endogenous p16^{INK4a} in either the CDK4 or CDK6 immunoprecipitates (Figure 4.4). Although it was expected that CDK4 immunoprecipitates would not contain p16^{INK4a}, some binding of p16^{INK4a} to CDK6 should have been apparent in the CDK6 immunoprecipitate. The likely explanation is technical in that the R24P variant is not recognised by the JC8 monoclonal antibody used routinely for immunoblotting of p16^{INK4a}. Other monoclonal antibodies give much weaker signals when used for immunoblotting and in the panel shown in Figure 4.4, the R24P was detected with a rabbit polyclonal antibody. However, Milan fibroblasts also contain relatively low levels of CDK6, compared to Hs68 cells compounding the difficulty in detecting this binding.

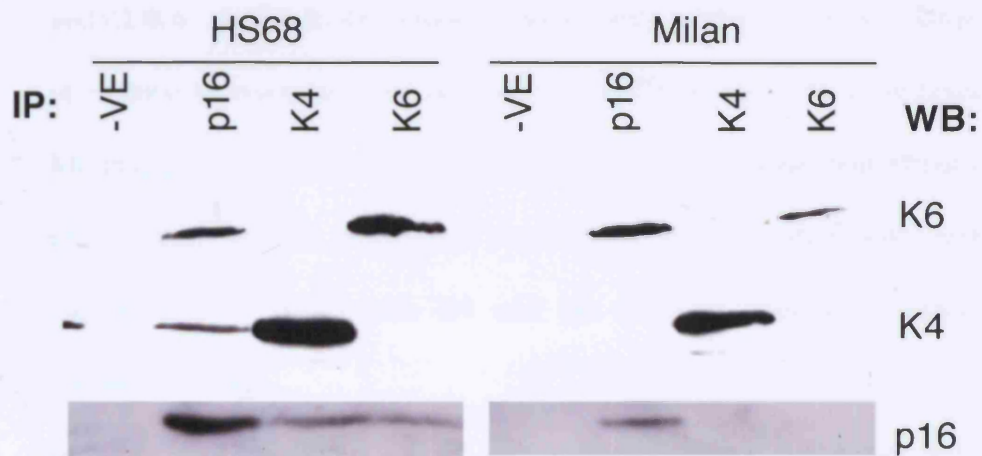


Figure 4.4 Binding properties of the R24P variant of p16^{INK4a}

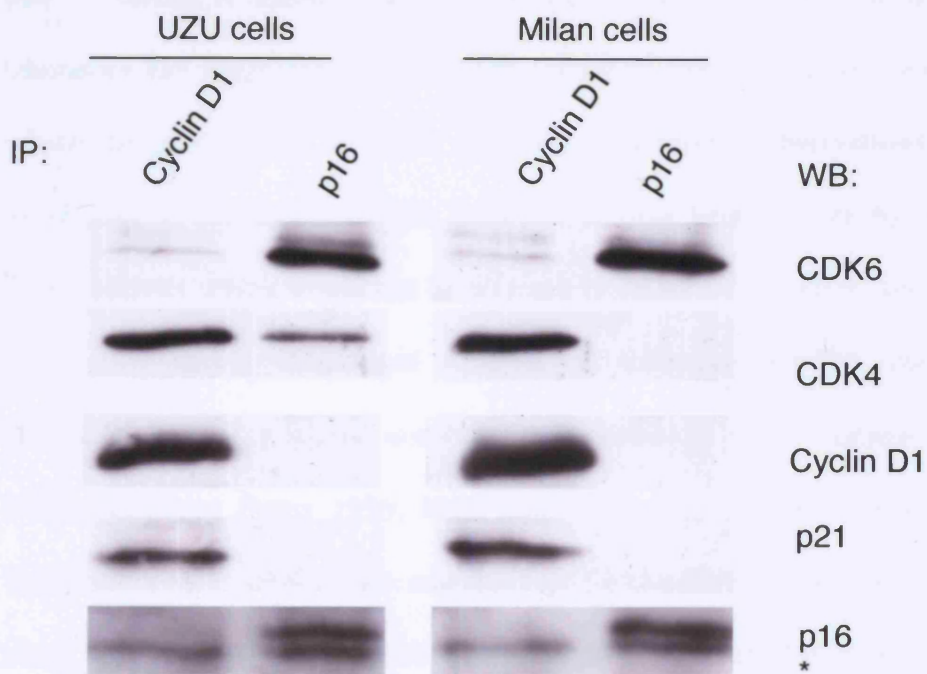
Samples of Milan cells (PD23) and wild-type Hs68 cells (PD41) were prepared. Samples of total protein (500µg) were incubated with 20µl protein A beads and 5µl rabbit polyclonal antibodies against the indicated proteins. Proteins bound to the beads were separated by SDS-PAGE in a 12% gel, transferred to membrane, and the immunoblot was developed with antibodies against the indicated proteins followed by ECL. While the wild-type p16^{INK4a} expressed in Hs68 cells could be detected using the monoclonal antibody JC8, the R24P variant of p16^{INK4a} cannot be detected by this antibody so it was visualised using the rabbit polyclonal antibody SC468. (-ve denotes negative control)

4.3 Composition of p16^{INK4a} and cyclin D1 complexes in senescent Milan cells

It is generally assumed that the accumulation of p16^{INK4a} that occurs in senescent cells contributes to the proliferative arrest via inhibition of CDK4 and CDK6. As the R24P variant is presumably unable to inhibit CDK4, it was of interest to consider what happens to the Cyclin D-CDK complexes when Milan cells reach senescence. Lysates prepared from senescent Milan (PD48) and normal control fibroblasts were immunoprecipitated with antibodies against p16^{INK4a} and cyclin D1 and the immune complexes analysed by western blotting.

In the control fibroblasts, CDK4 was mainly present in a complex with cyclin D1 and p21^{CIP1}, while CDK6 was predominantly bound to p16^{INK4a} (Figure 4.5). In the senescent Milan fibroblasts, none of the CDK4 was bound to p16^{INK4a}, confirming the results from previous experiments, but there was little discernible difference in the distribution of CDK6 between cyclin D1 and p16^{INK4a} relative to the control.

These observations suggest that senescence in both control and Milan fibroblasts is accompanied by a loss of cyclin D1/CDK6 complexes, while cyclin D1/CDK4 complexes are still present. While these observations are consistent with previous data (F Gregory, unpublished observations)(Stein et al. 1999), they also raise further questions about the composition of the cyclin D1/CDK4 complexes at senescence and their possible activity. Evidence exists that these complexes are inactive at senescence, and their activity is probably inhibited by the presence of high levels of p21^{CIP1} at senescence (F Gregory and E Sanij, unpublished observations), although the presence of p21^{CIP1} in these complexes in Milan cells is unconfirmed.



* Denotes background band

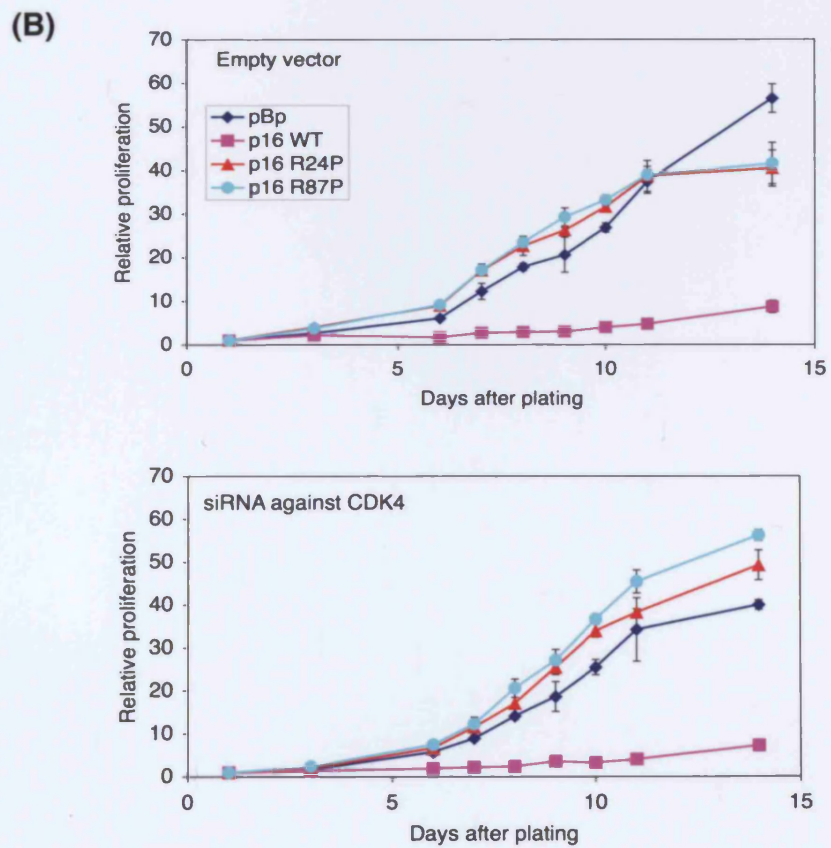
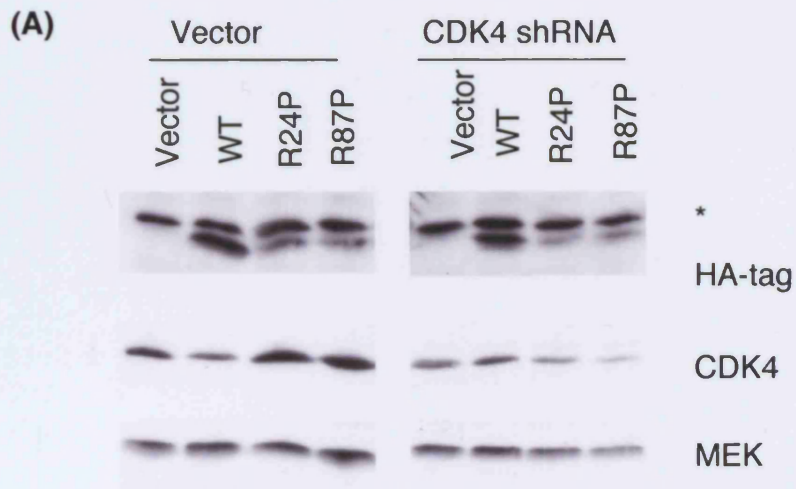
Figure 4.5 Composition of Cyclin D1 and p16^{INK4a} complexes in senescent Milan and UZU fibroblasts

Samples of Milan cells (PD48) and control infant skin fibroblasts, UZU cells (PD58) were prepared. Samples of total protein (350µg) were incubated with 50µl protein A beads and 5µl rabbit polyclonal antibodies against the indicated proteins. Proteins bound to the beads were separated by SDS-PAGE in a 12% gel, transferred to membrane and the immunoblot was developed with antibodies against the indicated proteins followed by ECL. The R24P variant of p16^{INK4a} was visualised using the SC468 rabbit polyclonal antibody.

4.4 Analysis of the function of the R24P variant of p16^{INK4a}

Overexpression of wild-type p16^{INK4a} in normal human diploid fibroblasts causes a cell cycle arrest. In contrast, overexpression of a non-functional p16^{INK4a} variant is unable to halt the growth of HDFs. Previous work in the laboratory had suggested that the R24P variant of p16^{INK4a} was also unable to inhibit the proliferation of HDFs (M Ruas, unpublished observations). The assumption at the time was that proliferation was being driven by residual CDK4 activity which would not be affected by R24P. To confirm and extend these observations, HA-tagged versions of wild-type p16^{INK4a}, the R24P variant, and R87P, a proven non-functional mutant of p16^{INK4a} (Ranade et al. 1995; Parry and Peters 1996; Ruas and Peters 1998; Walker et al. 1999; Yarborough et al. 1999), were expressed in TIG3 cells by retroviral infection along with an empty vector control. In a parallel set of experiments, the same viruses were introduced into TIG3 cells in which CDK4 expression was knocked down with shRNA constructs targeting CDK4. After selection, lysates were analysed by immunoblotting to confirm expression of the exogenous proteins, and the proliferation of the different cell types was monitored using a proliferation assay based on the crystal violet stain.

Expression of the different p16^{INK4a} constructs was confirmed by immunoblotting with an HA antibody (Figure 4.6). As shown in the right hand panel, only a partial knockdown of CDK4 was achieved in the cells expressing shRNA constructs targeting CDK4, possibly because of the use of the same drug selectable marker in all the retroviral vectors used (Figure 4.6). It was also observed that during these experiments, wild-type p16^{INK4a} was expressed at higher levels than the R24P and R87P variants.



Within the limits of this experiment, neither R24P nor R87P was able to block the proliferation of TIG3 cells, irrespective of the levels of CDK4. In contrast, wild-type p16^{INK4a} caused a profound arrest under both conditions (Figure 4.6). This suggests that although the R24P variant retains some binding to CDK6, the effects of this binding are insufficient to inhibit the proliferation of the TIG3 cells. Either the R24P variant of p16^{INK4a} is unable to bind to and inhibit a significant fraction of the CDK6 present within these cells, or the R24P may be unable to inhibit the function of the CDK6 that it is bound to.

4.5 Effects of pRb and p53 ablation on the lifespan of Milan fibroblasts

Primary human fibroblasts undergo a define number of divisions before undergoing an irreversible cell cycle arrest known as senescence, or M1. This is accompanied by phenotypic changes in the cell, with the cell become larger and flatter, and the nucleolus becoming more prominent. Historical analyses of the mechanisms that implement M1 have revealed contributions from both pRb and p53. Overcoming both these pathways allows the fibroblasts to continue growing until they reach a second stage termed M2, or crisis. At this stage there is no net increase in the number of cells present in the culture. Cells attempt to undergo division but this is unsuccessful and results in cell death. Disabling one or other of these pathways results in a partial bypass of M1, with cells arresting at an intermediate stage between M1 or M2 termed M^{Int} or M1.5. For example, overcoming the p53 pathway in wild-type fibroblasts using the viral oncoprotein HPV E6 allows the fibroblasts to undergo an extended number of population doublings before undergoing an

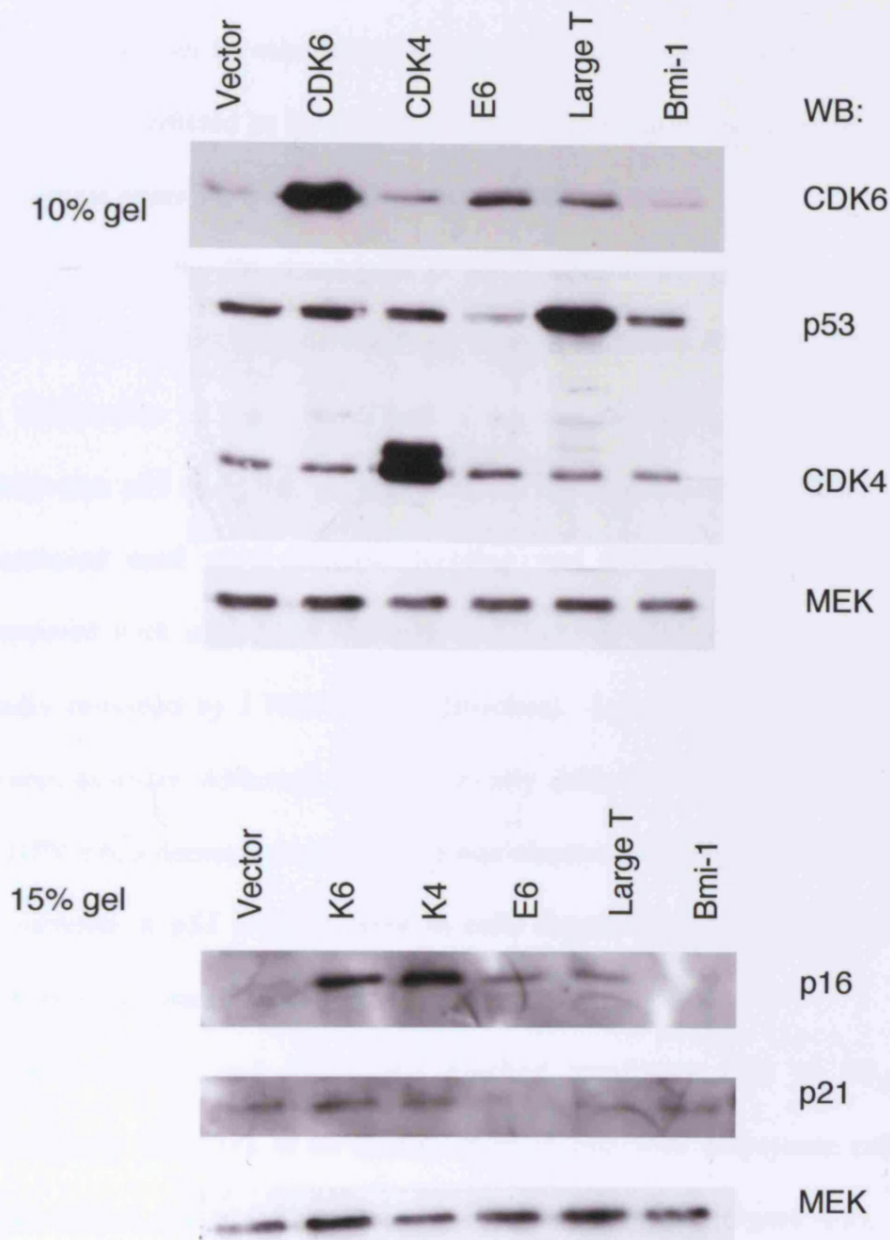


Figure 4.7 Immunoblot analysis of the expression of exogenous proteins in Milan cells

Milan cells were infected with retrovirus encoding CDK6, CDK4, HPV16 E6, SV40 Large T antigen, Bmi-1 and an empty vector control (pBabe^{puro}). Pools of cells were recovered by selection in the appropriate drug. Samples (15 μ g) of total protein were fractionated by SDS-PAGE in an 10% and 15% gels, transferred to membranes, and the immunoblots were developed with antibodies against the indicated proteins followed by ECL.

M1.5 arrest which phenotypically resembles M1 (Bond et al. 1999). Based on precedents set by other fibroblast strains with compromised p16^{INK4a}, Milan cells were predicted to have an extended lifespan culminating at M1.5, with a phenotype resembling that seen at senescence.

To assess whether the senescence of Milan fibroblasts reflects an M1 or M1.5 stage, recombinant retroviruses were used to introduce HPV E6, which results in destruction of p53, or SV40 T-Ag which binds to and functionally inactivates p53 and pRb. After selection, the proliferation of Milan cells was monitored until they stopped dividing and the maximum PDs achieved compared with analogous findings with Leiden, Q34 and control cells (data kindly provided by J Rowe and S Brookes). Lysates were also prepared for protein analysis. Although it is technically difficult to confirm the expression of HPV E6, a decrease in p53 levels was observed in E6 expressing cells while an increase in p53 levels is seen in cells expressing Large T antigen in line with expectations (Figure 4.7).

Whereas Leiden and Q34 cells reached maximum PDs of 60 and 88 respectively (Brookes et al. 2004), more in line with embryonic rather than adult origins, Milan cells senesced after only 39 PDs (Figure 4.8). This is typical of the normal range for adult fibroblasts, and the rate of proliferation of Milan cells resembles that of other adult fibroblasts strains. These results should be interpreted with the caveat that as with all such measurements, there is some uncertainty about the exact number of PDs required to reach confluence before the first passage. It is also worth noting that the measurement for lifespan in Milan fibroblasts was made using cells expressing

Figure 4.8 The effects of the viral oncoproteins E6 and Large T on the behaviour of Milan cells at senescence

Fibroblasts were infected with retrovirus encoding SV40 Large T antigen, HPV16 E6, or an empty vector control (pBabe^{puro}). After the recovery of pools of cells by selection in the appropriate drug, growth of the culture was monitored. Upon reaching confluence, cultures were split 1 to 4, equivalent to 2 population doublings.

904, Leiden and Q34 data is shown courtesy of Janice Rowe and Sharon Brookes.

an empty antibiotic resistance vector, compared with the values for Leiden and Q34 fibroblasts which were achieved with cells which were uninfected.

In normal human diploid fibroblasts, such as the 904 strain of adult skin fibroblasts, SV40 T-Ag enables the cells to continue growing until they reach M2 or crisis. In contrast, HPV16 E6, which only ablates the p53 pathway causes them to arrest at M1.5 (Figure 4.8). Expression of either Large T antigen or E6 in Milan fibroblasts allowed them to continue growing until they reach M2, and this is the same trend which is observed in Leiden and Q34 cells (Figure 4.8). This suggests that only the p53 pathway needs to be disabled for cells with non-functional p16^{INK4a} to reach crisis, and supports the hypothesis that p16^{INK4a}-compromised fibroblasts arrest at an intermediate stage between senescence and crisis, presumably because the pRb pathway is disabled by the absence of functional p16^{INK4a}. Thus despite the unusual properties of the R24P variant Milan cells are similar to the Q34 and Leiden strains in terms of the implementation of senescence.

4.6 The effects of Bmi-1 on the lifespan of Milan cells

As further confirmation that they have a partially disabled senescence response, Milan fibroblasts were infected with retrovirus encoding the Bmi-1 protein or empty vector control. Bmi-1 is a polycomb group protein which represses transcription from the *INK4a/ARF* locus, and extends the lifespan of cultures of normal HDFs (Jacobs et al. 1999a; Itahana et al. 2003b). After selection in puromycin, cell proliferation was followed and lysates were prepared to determine the relative protein concentrations by western blotting. The basal level of p16^{INK4a} in the Milan cells is already low, but this was



Figure 4.9 The effects of Bmi-1 on the lifespan of Milan fibroblasts

Fibroblasts were infected with retroviruses encoding Bmi-1 and an empty vector control (pBabe^{puro}). After the recovery of pools of cells by selection in the appropriate drug, growth of the culture was monitored. Upon reaching confluence, cultures were split 1 to 4, equivalent to 2 population doublings.

(904 and Leiden data is shown courtesy of Sharon Brookes)

decreased further upon expression of Bmi-1 (Figure 4.7), suggesting that Bmi-1 had been successfully expressed in these cells. The lifespan of Milan cells was not extended upon expression of Bmi-1 (Figure 4.9), and in this respect Milan cells are behaving like fibroblasts which are completely deficient in functional p16^{INK4a} (Brookes et al. 2004).

4.7 The effects of expression of exogenous CDK4 and CDK6 on the lifespan of Milan fibroblasts

It has become relatively common practice to try to phenocopy p16^{INK4a}-deficiency by overexpression of CDK4 or a mutant version (R24C) that is unable to bind to and is therefore insensitive to INK4 proteins (Hahn et al. 2002; Wei et al. 2003b). Indeed expression of exogenous CDK4 or CDK6 has been shown to extend the lifespan of human diploid fibroblasts (Morris et al. 2002)(S Brookes and M Ruas, unpublished observations). However, CDK4 and CDK6 were also found to extend the lifespan of Q34 and Leiden cells which do not have functional p16^{INK4a}, and mutants of CDK4 and CDK6 that do not bind to p16^{INK4a} can also extend the lifespan of HDFs (S Brookes and M Ruas, unpublished observations). This suggests a more complex mechanism, and that in addition to titrating p16^{INK4a}, the excess CDK4 and CDK6 may act as a sink for p21^{CIP1} and p27^{KIP1} and relieve inhibition of CDK2. In view of the unusual properties of the R24P variant it was interesting to investigate whether CDK4 and CDK6 could extend the lifespan of Milan fibroblasts.

Retroviruses encoding CDK4, CDK6 and an empty vector control were used to infect Milan cells and, after selection in puromycin, cells were kept in

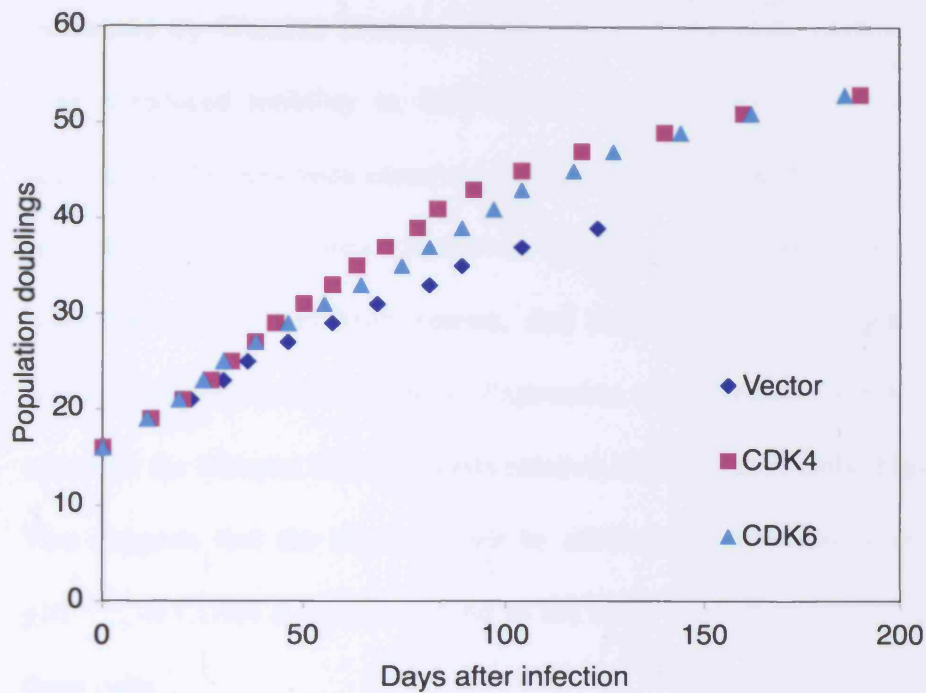


Figure 4.10 The effect of exogenous CDK4 and CDK6 on the lifespan of Milan fibroblasts

Milan cells were infected with retrovirus encoding CDK4, CDK6, or an empty vector control (pBabe^{puro}). After recovery of pools of cells by selection in the appropriate drug, growth of the culture was monitored. Upon reaching confluence, cultures were split 1 to 4, equivalent to 2 population doublings.

continuous culture until they reached senescence. Samples were taken for protein analysis and the expression of exogenous CDK4 and CDK6 was confirmed by Western Blotting (Figure 4.7). Exogenous CDK4 appears to have a reduced mobility in SDS-PAGE gels compared to the endogenous protein and this has been observed in other experiments (S Brookes, M Ruas unpublished observations). However, the plasmid has been fully sequenced and compared to GenBank entries, and contains the full-length wild-type cDNA (R Jones, data not shown). Expression of exogenous CDK4 and CDK6 extended the lifespan of Milan cells relative to the control cells (Figure 4.10). This suggests that the effect cannot be attributed to titration of endogenous p16^{INK4a}, as CDK4 is unable to bind to the R24P variant of p16^{INK4a} present in these cells.

4.8 The ability of kinase dead CDK4 and CDK6 to extend the lifespan of HDFs

To further investigate the underlying mechanism, we investigated whether the kinase activity of CDK4 and CDK6 was necessary for lifespan extension, rather than their ability to sequester p21^{CIP1} and p27^{KIP1}. A kinase dead mutant of CDK4 (CDK4 KD) in which residue 157 in the ATP-binding site is changed from a Asp to an Asn, and a corresponding Asp163Asn mutant of CDK6 (CDK6 KD) were cloned into the pBabe^{puro} or pBabe^{bleo} retroviral vectors respectively.

Wild-type TIG3 fibroblasts were then infected with retroviruses encoding CDK4, CDK4 KD, CDK6, CDK6 KD and empty vector controls. CDK4 KD, CDK6 and CDK6 KD also have a carboxy-terminal HA tag. After selection,

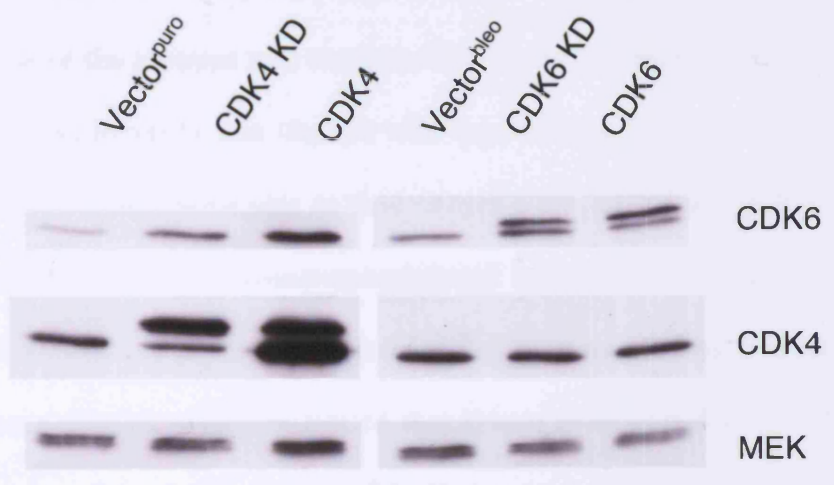
Figure 4.11 The affinity of kinase dead CDK4 and CDK6 for Cyclin D1, p21^{CIP1} and p16^{INK4a}

TIG3 cells were infected with retrovirus encoding CDK4, CDK4 KD, CDK6, CDK6 KD, and empty bleomycin and puromycin vectors (pBabe). Pools of cells were recovered by selection in the appropriate drug.

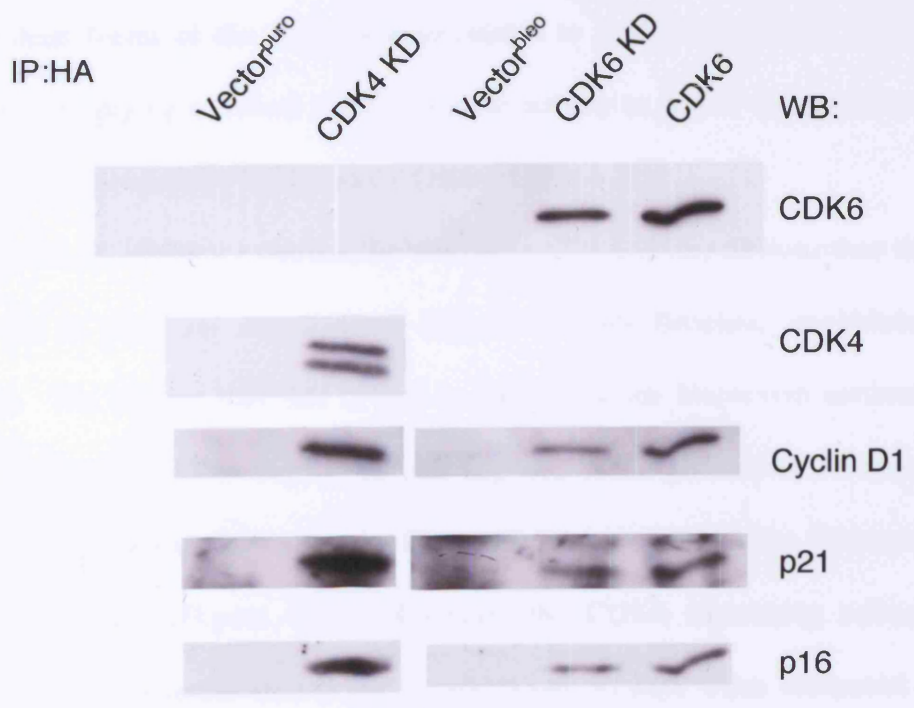
(A) Samples (25µg) of total protein were fractionated by SDS-PAGE in an 12% gel, transferred to membrane, and the immunoblot was developed with antibodies against the indicated proteins followed by ECL.

(B) Samples of total protein (500µg) were incubated with 20µl protein G beads and 2µl of anti-HA monoclonal antibody. Proteins bound to the beads were separated by SDS-PAGE in a 12% gel, transferred to membrane, and the immunoblot was developed with antibodies against the indicated proteins followed by ECL. (Cyclin D1 shows as a background band in the CDK4 blot, as the membrane had previously been probed for Cyclin D1.)

(A)



(B)



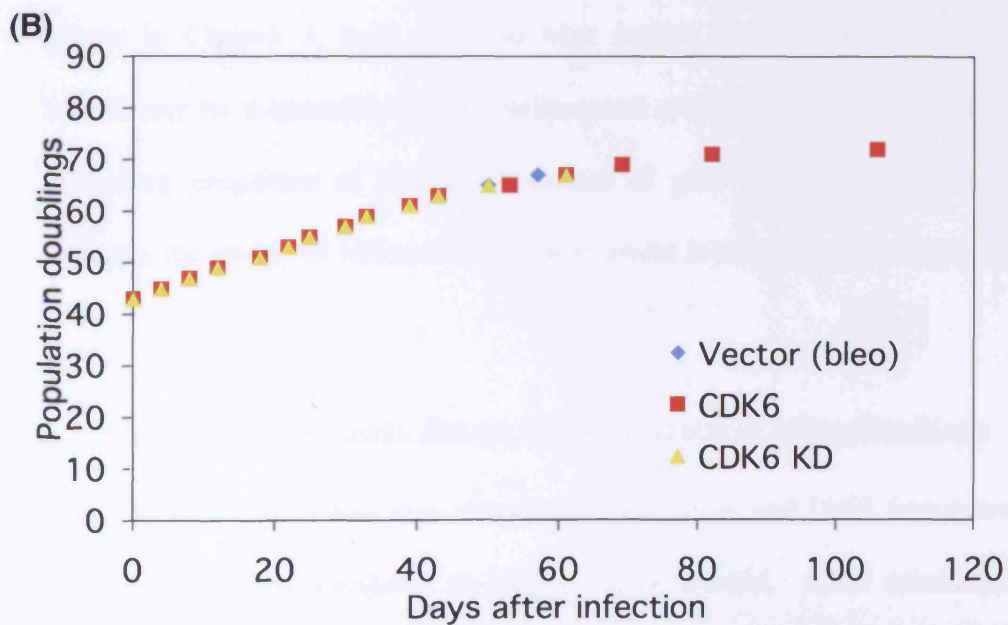
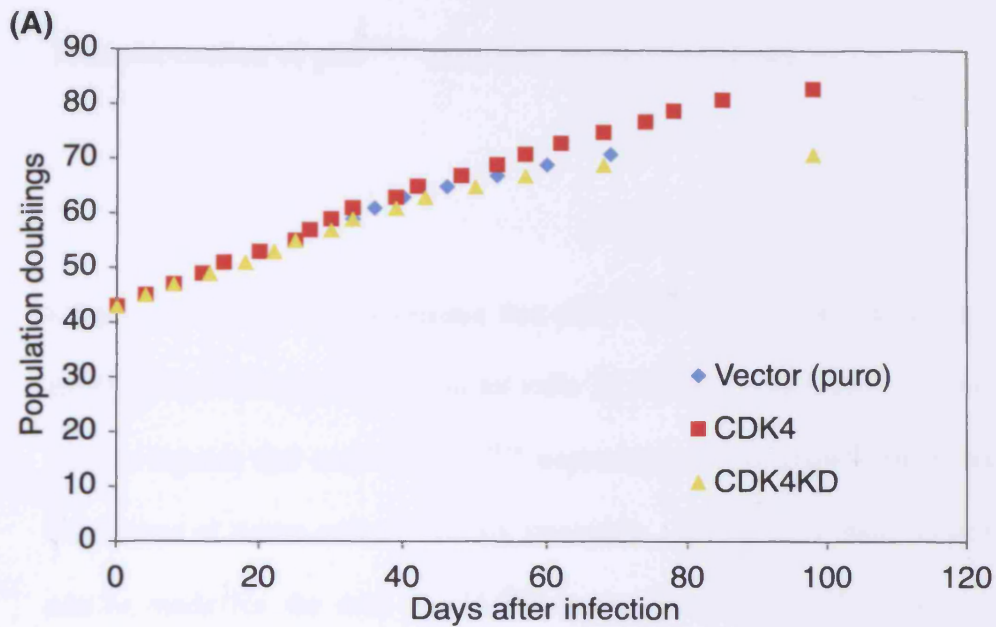


Figure 4.12 The role of the kinase activity of CDK4 and CDK6 in lifespan extension caused by exogenous expression of the kinases

TIG3 cells were infected with (A) CDK4, CDK4 KD and empty puromycin vector (pBabe), or (B) CDK6, CDK6 KD, and empty bleomycin resistance vector (pBabe). After recovery of pools of cells by selection in the appropriate drug, growth of the culture was monitored. Upon reaching confluence, cultures were split 1 to 4, equivalent to 2 population doublings.

Chapter 5

Transformation of p16^{INK4a}-deficient Milan fibroblasts

Despite the unequivocal evidence that p16^{INK4a} accumulation contributes to the spontaneous senescence of human cells in culture, it is clearly not essential and the signals that activate p16^{INK4a} expression during growth under standard conditions of tissue culture remain uncertain. However, a more cogent case can be made for the role of p16^{INK4a} in oncogene-mediated senescence. As shown in Chapter 3, both Ras and Myc induce the expression of p16^{INK4a}, which may be responsible for the subsequent arrest of HDFs. In view of the intriguing properties of the R24P variant of p16^{INK4a}, it was interesting to examine the ability of Milan fibroblasts to arrest in response to oncogenic Ras.

5.1 The effect of oncogenic Ras on the proliferation of Milan fibroblasts

The V12 allele of H-Ras was introduced into Milan and Hs68 fibroblasts by retroviral infection alongside an empty vector control. After selection, cell lysates were prepared to confirm Ras expression by western blotting (Figure 5.1). As expected, overexpression of Ras resulted in an upregulation of p16^{INK4a} in the Hs68 cells, although only a negligible induction of p16^{INK4a} was observed in the Milan cells. Proliferation was monitored by growing cells in the presence of BrdU labelling medium for 19 hours, followed by fixation and staining to determine the percentage of cells that had incorporated BrdU.

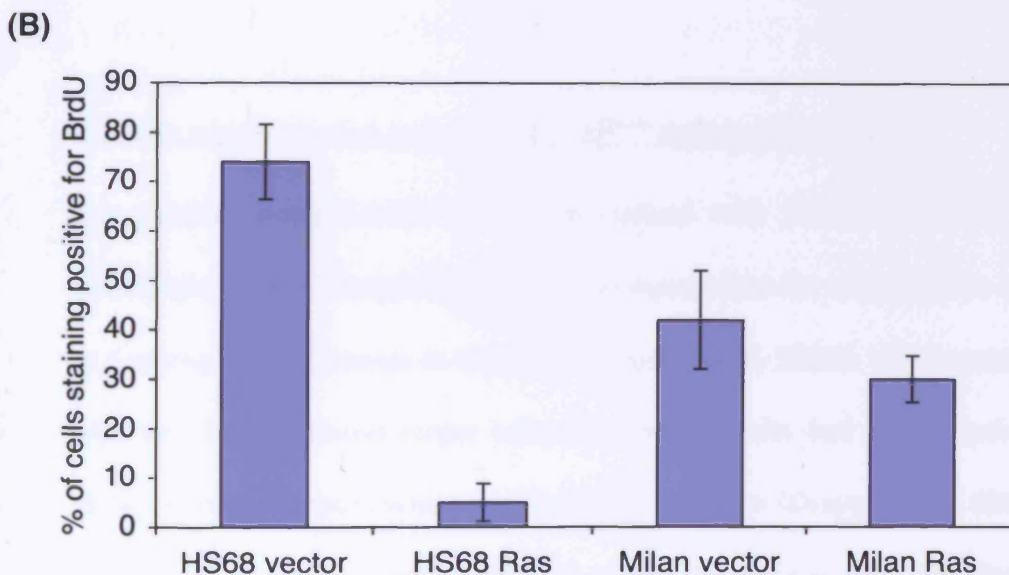


Figure 5.1 The response of Milan fibroblasts to the overexpression of oncogenic Ras

Milan fibroblasts and control Hs68 cells were infected with retrovirus encoding Ras, or an empty vector control (pBabe^{puro}). Pools of cells were recovered by selection in the appropriate drug.

(A) Samples (30µg) of total protein were fractionated by SDS-PAGE in 10% and 15% gels, transferred to membranes, and the immunoblots were developed with antibodies against the indicated proteins followed by ECL. The p16 variants were detected using the SC468 rabbit polyclonal antibody.

(B) Cells were cultured in BrdU labelling medium for 19 hours before staining for BrdU incorporation. The proportion of stained versus unstained cells was determined by counting at least 300 cells of each type. The average of these counts is plotted, and the standard deviation between counts is shown as the error bar.

Hs68 fibroblasts showed a significant decrease in BrdU labelling in response to oncogenic Ras (Figure 5.1), while Milan cells showed a relatively slight decrease in proliferation. Previous work in the laboratory has indicated that the p16^{INK4a}-deficient Leiden and Q34 fibroblast strains undergo a transient period of slower growth in response to Ras overexpression (Brookes et al. 2002; Huot et al. 2002), and a similar phenomenon is likely to occur in Milan cells. This adaptation period is unlikely to reflect the outgrowth of mutant clones as it occurs over a fairly short timescale and the cultures do not show visible signs of colony formation.

5.2 The transformation potential of p16^{INK4a} deficient fibroblasts

Experiments using Leiden cells immortalised with telomerase showed that upon expression of exogenous Myc or oncogenic Ras the cells became capable of forming small colonies in soft agar (Drayton et al. 2003). Co-expression of Myc and Ras produced larger colonies, and the cells had now acquired the ability to form tumours when injected into nude mice (Drayton et al. 2003).

Interestingly, the tumours generated using the Leiden cells fell into two distinct categories. In the first experiment, tumours arose at low frequency (5/16), and after a long latency that indicates probable selection for an additional event. Cytogenetic analyses suggested that these tumours comprised mono- or oligoclonal outgrowths of three dominant clones, one of which had clearly shut down expression of ARF. However, all 5 tumours had wild-type p53 and expressed very high levels of Ras (Drayton et al. 2003). In the second experiment, tumours arose at 8/8 injection sites and all of them were found to have the same biallelic mutations in p53 suggesting a

monoclonal origin (S Brookes and H Rodway, unpublished observations). Curiously, these tumours expressed much lower levels of oncogenic Ras than the first group.

To address doubts that the Leiden cells may be particularly sensitive to transformation, we were keen to validate these observations in a different cell background in which p16^{INK4a} function was compromised. Because of restrictions on the use of the Q34 cells strain in animal experiments, the Milan cells provided an ideal opportunity to repeat and extend the previous work. In particular, we wanted to determine whether the efficiency of tumorigenesis could be increased by shRNA-mediated knockdown of p53 or ARF.

5.3 Generation of a panel of Milan Tert cells expressing combinations of Myc, Ras and shRNA targeting ARF

Milan cells were immortalised by infection with a retrovirus encoding hTERT (pBabe^{puro}-Tert) to form Milan Tert (MT) cells. After selection, the activity of telomerase in these cells was confirmed by TRAP assay (data not shown). The cells were then subjected to repeated rounds of retroviral infection and selection to build up a panel of MT cells expressing combinations of Myc, Ras and ARF shRNA (Figure 5.2). Unfortunately despite repeated attempts, it was not possible to recover blasticidin resistant cells using the empty control vector (pWZL^{blast}) used in parallel with the plasmid encoding Myc. In these circumstances, uninfected cells served as the control, but in all other instances each infection included an empty vector control.

These rounds of sequential infection and selection generated a panel of Milan Tert (MT) cells, expressing Ras (MTR cells), Myc (MTM cells), and a

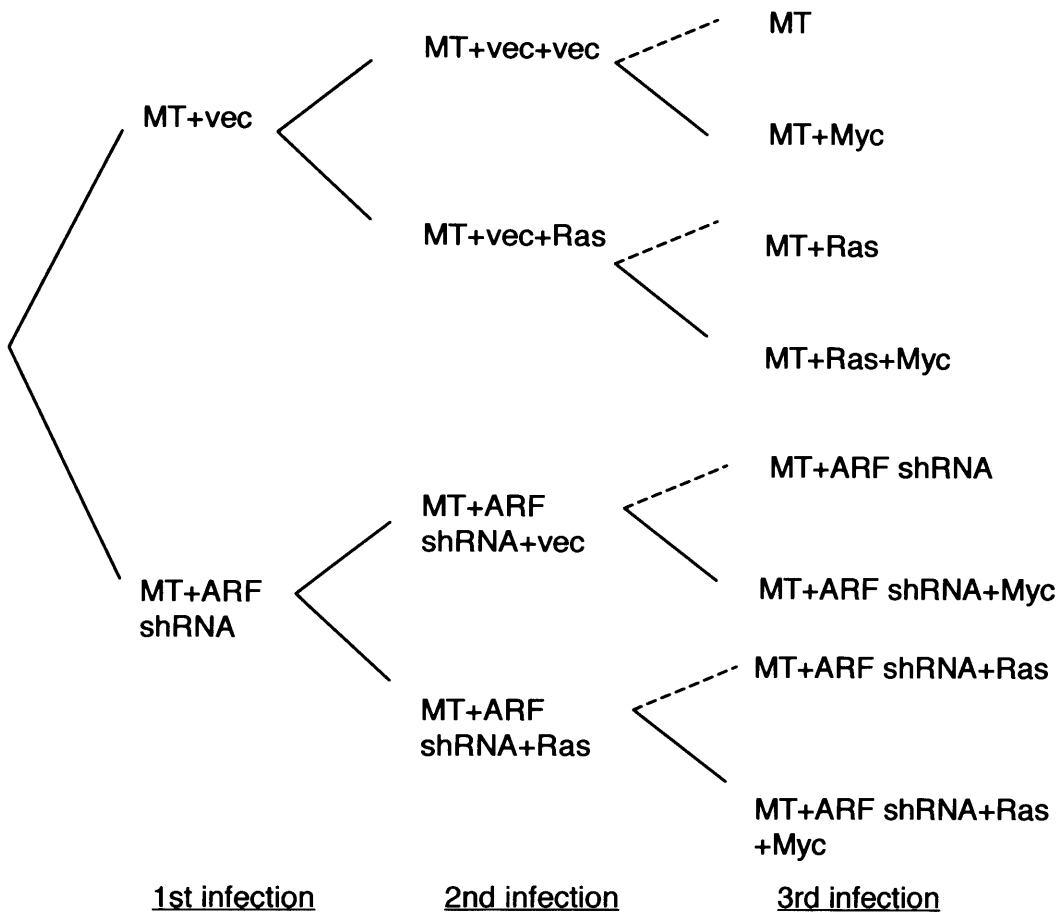


Figure 5.2 Generation of a panel of Milan cells expressing telomerase, Myc, Ras and shRNA against ARF

Milan cells expressing telomerase (from the pBabe^{puro} vector) were infected with retrovirus encoding an shRNA targeting ARF, or an empty vector control (pRetroSuper^{hygro}). After the recovery of a pool of cells by selection in hygromycin, cells were subjected to an additional round of infection with retrovirus encoding H-Ras, or empty vector control, which was produced using the GP+E system. Cells were subsequently selected in zeocin, and either infected with retrovirus encoding c-Myc (pWZL^{blast}), or left uninfected as control cells. This generated a panel of Milan tert cells expressing combinations of Arf shRNA, H-Ras and c-Myc.



Figure 5.3 Immunoblot analysis of Milan tert cells expressing combinations of Myc, Ras and ARF shRNA

Extracts were prepared from the pools of Milan tert cells whose generation was described in section 5.3. Samples (25 μ g) of total protein were fractionated by SDS-PAGE in an 12% gel, transferred to membrane, and the immunoblot was developed with antibodies against the indicated proteins followed by ECL.

combination of Ras and Myc (MTRM cells), together with a parallel series containing shRNA against ARF (MT \bar{a} , MT \bar{a} R, MT \bar{a} M, and MT \bar{a} RM cells). Cell extracts were analysed to confirm the expression of Ras and Myc and the effects of ARF knockdown (Figure 5.3). The immunoblot showed that exogenous Ras was being expressed at relatively low levels in the appropriate cells, and appeared as a band of reduced mobility compared to endogenous Ras. A similar effect has previously been observed by others in the laboratory, but the molecular basis is unclear (S Brookes, unpublished data). The knockdown of ARF could not be confirmed by western blot due to the difficulty of visualising ARF with the available antibodies, and there was an inconsistent effect on p53 levels.

5.4 Generation of a panel of Milan Tert cells expressing combinations of Myc, Ras and shRNA targeting p53

As one of the intentions was to compare the effects of ARF knockdown versus p53 knockdown an analogous panel of cells was generated, designated 2MT, 2MTR, 2MTM, 2MTRM cells both with and without p53 shRNA. In this instance, hTERT was in pBabe^{hygro} vector and p53 shRNA in pRetroSuper^{puro}. The expression of the relevant proteins was assessed by immunoblotting (Figure 5.4). Expression of Ras was observed in the correct cell lines, and the presence of shRNA targeting p53 coincided with ablation of the p53 protein, showing that an efficient knockdown of p53 had been achieved. Myc was expressed in the expected cell lines, but only a low level of expression was observed.

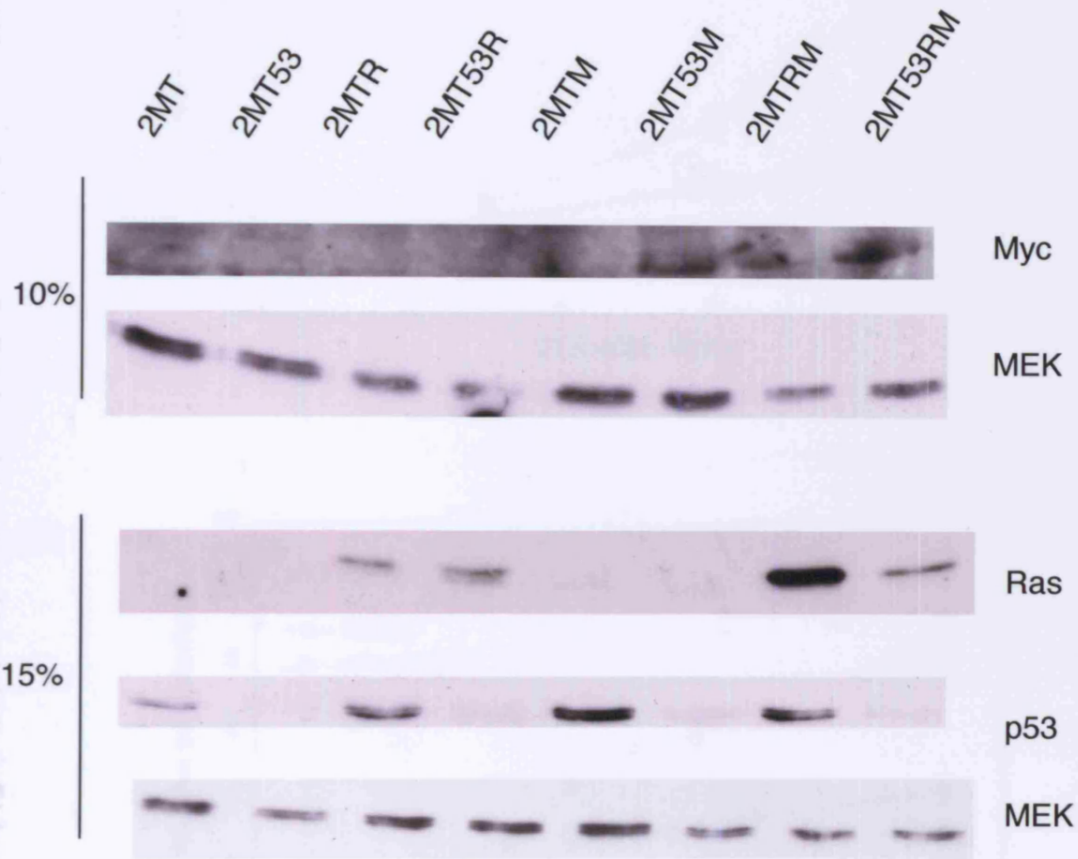
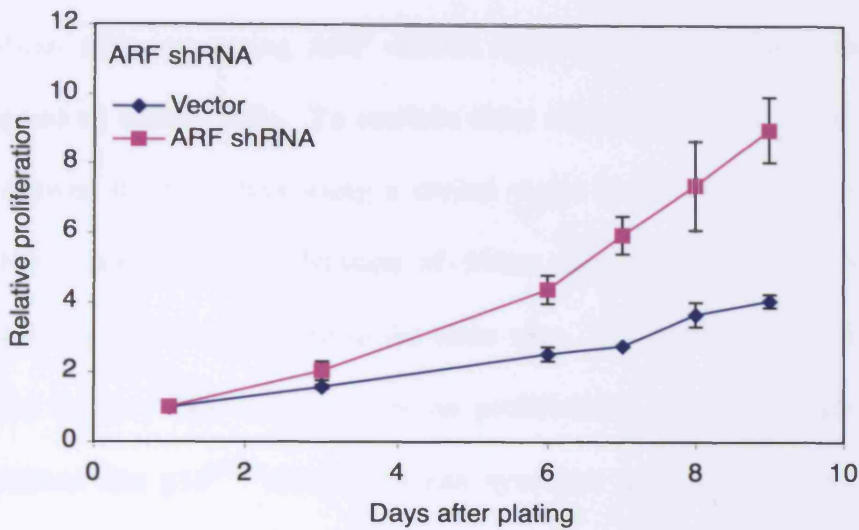


Figure 5.4 Immunoblot analysis of MT cells expressing combinations of Myc, Ras and p53 shRNA

Extracts were prepared from the pools of Milan tert cells whose generation was described in section 5.4. Samples (16 μ g) of total protein were fractionated by SDS-PAGE in 10% and 15% gels, transferred to membranes and the immunoblots were developed with antibodies against the indicated proteins followed by ECL.

(A)



(B)

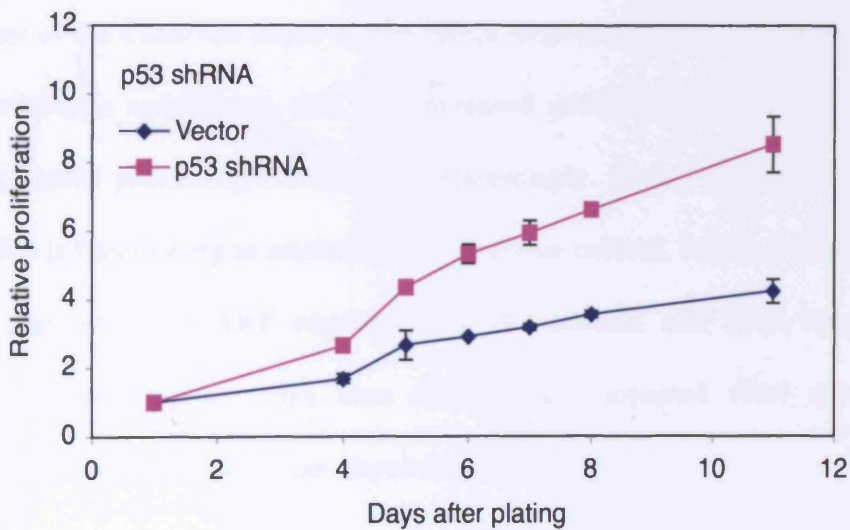


Figure 5.5 Effects of ARF or p53 knockdown on Milan cell proliferation

(A) Milan cells expressing an shRNA targeting ARF, or empty vector control (pRetroSuper^{hygro}), and (B) Milan cells expressing a pool of 3 shRNAs targeting p53, or empty vector control (pRetroSuper^{puro}) were plated out in 24 well plates with 1×10^4 cells per well, and triplicate wells of each cell type. Proliferation was monitored by following the uptake of crystal violet stain by the different cell types. The average value across the triplicates is plotted, and the standard deviation between the triplicates is shown as the error bar.

5.5 The effect of ARF knockdown on the proliferation of Milan fibroblasts

The Milan cells expressing ARF shRNA appeared to grow faster than the corresponding control cells. To confirm these observations, cell proliferation was followed for nine days using a crystal violet proliferation assay (Figure 5.5). For comparison, proliferation of Milan tert cells expressing shRNA against p53 was also monitored in the same way. The ARF and p53 shRNAs appeared to have equivalent effects on proliferation, confirming published observations that p16^{INK4a}-deficiency can synergise with a deficiency in the p53 pathway leading to an increase in proliferation rate (Voorhoeve and Agami 2003). These observations suggest that cells which have silenced both products of the *CDKN2a* locus would gain a large proliferative advantage over their wild-type neighbours, and this increased proliferation may give rise to further cancer promoting mutations. Interestingly, these results also suggest that ARF is functioning in normal HDFs in tissue culture, which is unexpected given that levels of ARF expression at the protein and RNA levels are virtually undetectable. This also counters the accepted view that ARF responds to aberrant rather than physiological stimuli.

5.6 Requirement for anchorage independent growth of Milan fibroblasts

Three weeks after the final infection with retrovirus expressing Myc, the panel of MT cells described above were plated out in 0.2% soft agar. After five weeks in soft agar, the percentage of cells forming multicellular colonies was calculated by microscopic visualisation of at least 500 cells. The cell pools were also scored for the formation of at least one macroscopically visible colony (Table 5.1).

Cell Type	Experiment 1: % colony forming cells	Macroscopically visible?	Experiment 2: % colony forming cells	Macroscopically visible?
MT	1	No	0	No
MT+Ras	2	No	1	No
MT+Myc	11	Yes	5	Yes
MT+Ras+Myc	2	No	1	Yes
MT+ARF shRNA	17	Yes	11	No
MT+ARF shRNA+Ras	36	Yes	31	Yes
MT+ARF shRNA+Myc	11	Yes	4	Yes
MT+ARF shRNA+Ras+Myc	20	Yes	38	Yes

Table 5.1 Anchorage independent growth of Milan Tert cells expressing combinations of ARF shRNA, Myc and Ras

The panel of MT cells were plated out in 0.2% agarose three weeks after the final infection. After five weeks, counts were made of the percentage of cells forming colonies (Experiment 1). The cells had been frozen down, but were subsequently recovered (except MTa and MTR which were continuously growing in culture), and grown on for several weeks before replating in 0.2% agarose (Experiment 2). 23 days after plating colony formation was scored. At least 500 cells of each type were counted, and the presence of macroscopic colonies was also noted.

Although MTM cells formed a significant number of anchorage independent colonies, at least some of which were visible macroscopically, the MTR and MTRM cells had an unexpectedly low frequency of colony formation. Based on previous observations with Leiden cells, this may be because the cells had not had sufficient time to adapt to the increased levels of Myc and Ras. To address this possibility, cells that had been frozen down were recovered and grown on for several weeks before replating in soft agar. Despite this increased period of adaptation, fewer colonies were formed in the second experiment (Table 5.1). However, for technical reasons colony formation was scored after a shorter time, which may have affected the number of colonies formed. The frequency with which MTR, MTM and MTRM cells formed anchorage independent colonies was still lower than observed during the analogous experiment with Leiden cells (Table 5.1) (Drayton et al. 2003).

5.7 The effects of ARF knockdown on the anchorage independent growth of Milan fibroblasts

In both experiments, it was obvious that in all the cells pools except the MTM cells, the presence of shRNA against ARF allowed Milan cells to form anchorage independent colonies with an increased frequency. Photographs of representative colonies from experiment 1 were taken using a light microscope (Figure 5.6). These clearly show that the presence of ARF shRNA also allows the colonies formed to reach a larger size, probably due to the proliferative advantage conferred on Milan cells when ARF is ablated using shRNA.

Surprisingly, MT cells expressing ARF shRNA alone (MT \bar{a}) showed a substantial frequency of colony formation. This suggested that perhaps the

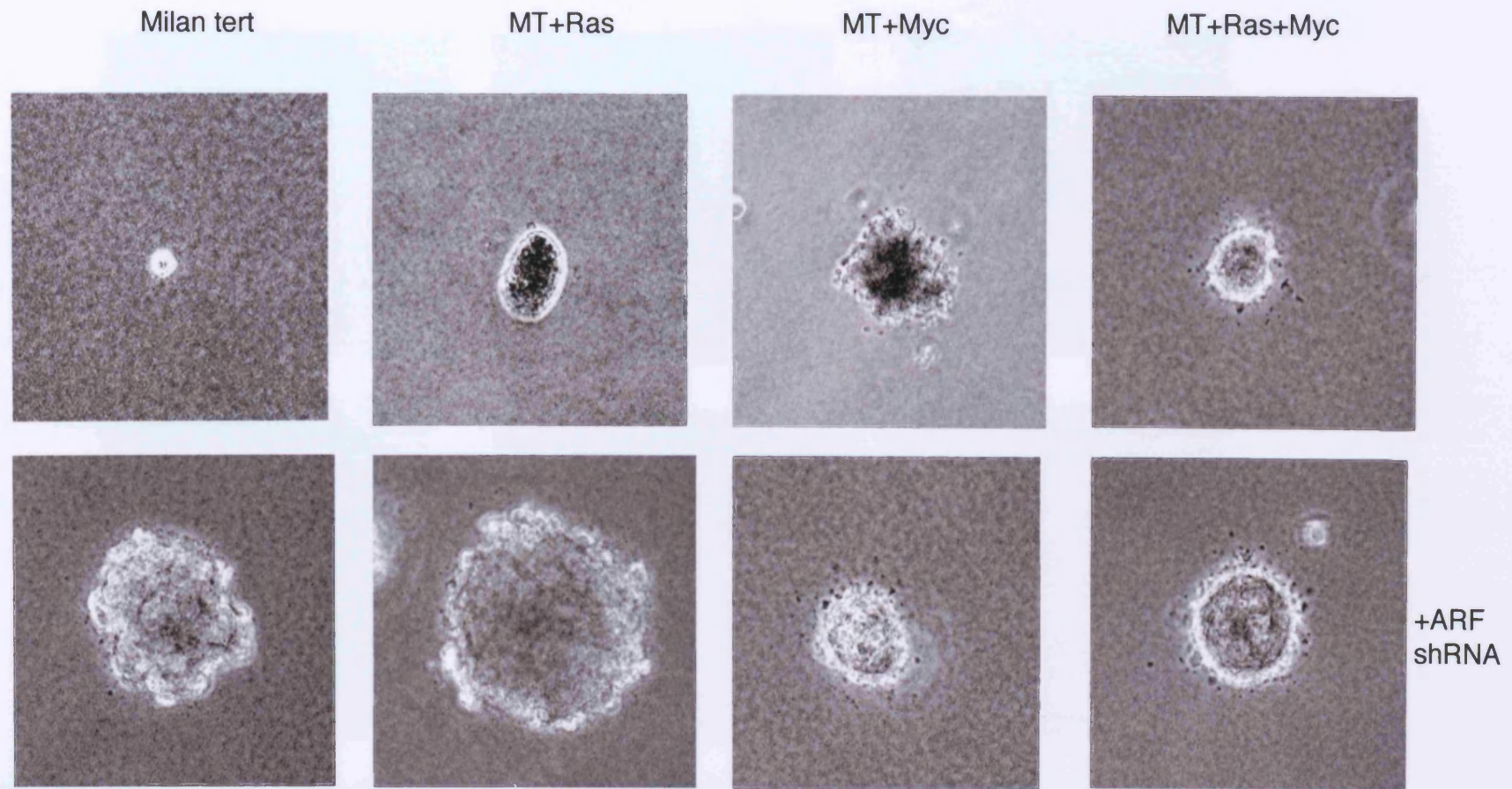


Figure 5.6 Effects of ARF knockdown on the size of anchorage independent colonies formed by Milan Tert cells
Pictures were taken of the colonies described in Table 5.1 using phase contrast and a 10x objective

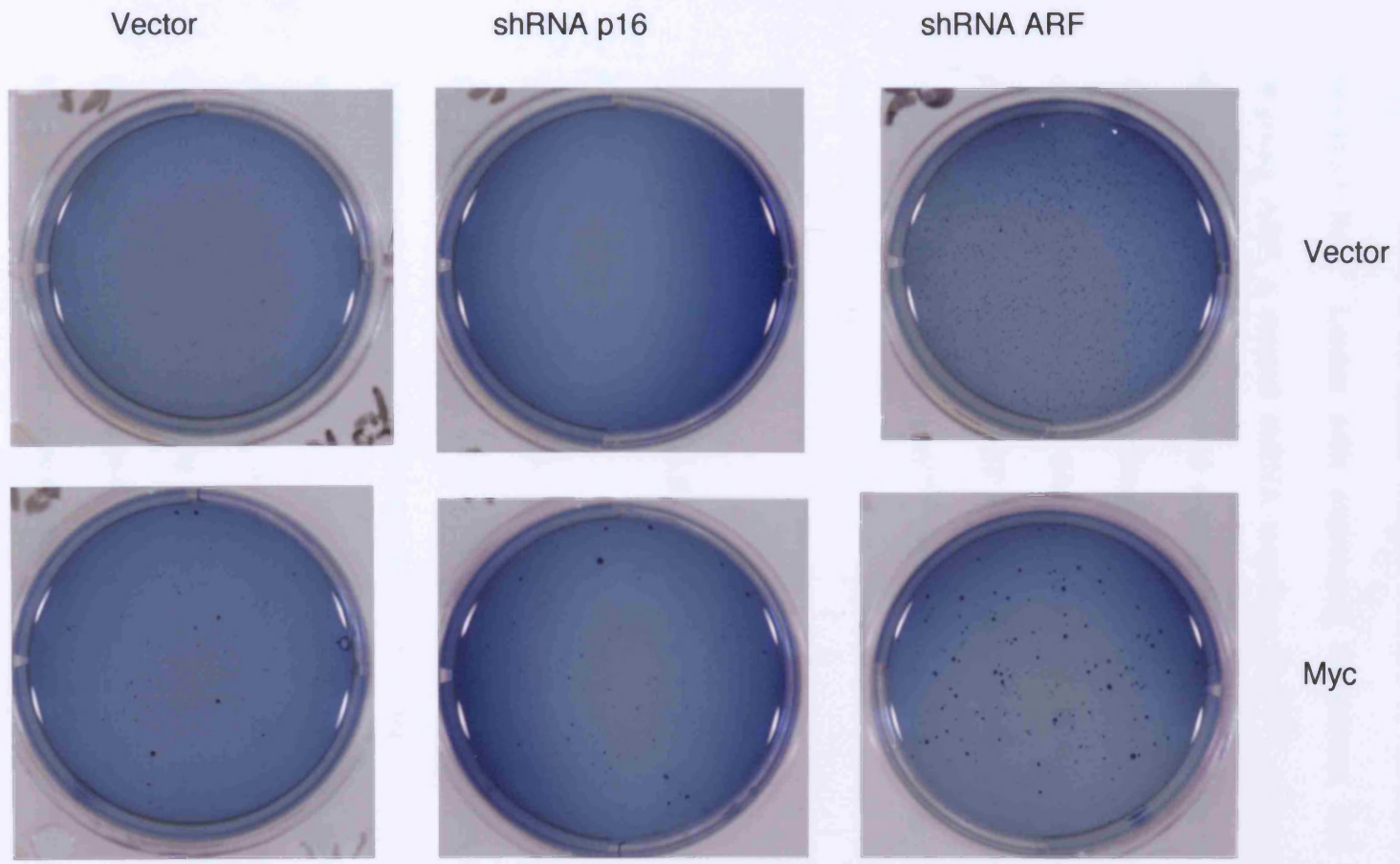


Figure 5.7 Effects of ARF knockdown on the anchorage independent growth of Leiden Tert cells

Leiden cells expressing telomerase were infected with a retrovirus encoding an shRNA targeting ARF, and an empty vector control (pRetroSuper^{hygro}). After selection in the appropriate drug, cells were subjected to a second round of retroviral infection with retrovirus encoding c-Myc or an empty vector control (pBabe^{puro}). After selection in the appropriate drug, cells were plated out in 0.2% agarose.. Twenty days after plating, colonies were stained with Giemsa, and photographed.

Milan cells were predisposed to form colonies upon loss of ARF. To check that these effects of ARF shRNA were not an artefact associated with Milan cells, we looked at the effects of ARF ablation in another p16^{INK4a}-deficient fibroblast line. Leiden cells expressing telomerase, and either shRNA targeting ARF, a control shRNA targeting p16^{INK4a}, or empty vector were further infected with retrovirus expressing Myc or an empty vector control. After selection, cells were plated out in soft agar. 20 days after plating, colonies were stained using Giemsa stain and photographed. From these photographs, it is clear that ARF shRNA also increases the frequency and size of colonies formed by p16^{INK4a}-deficient Leiden cells, confirming the observations in Milan cells.

5.8 Effects of shRNA against p53 on the anchorage independent growth of Milan cells

To investigate whether the effects of ARF knockdown were comparable to those achieved by ablation of p53 by shRNA, a similar series of anchorage independence assays was performed on the 2MT panel. Surprisingly, 2MTM cells did not form a significant number of colonies in soft agar (Table 5.2) in contrast with the MTM cells, whereas 10% of 2MTR cells were capable of forming anchorage independent colonies which were macroscopically visible upon careful examination, again contrasting with the result observed using MTR cells. These observations correlated with the expression levels of the oncogenes in the different panels of Milan cells, suggesting that a high level of expression of the activating protein needs to be achieved to allow the cells to

Cell Type	% colony forming cells	Macroscopically visible?
2MT	0	No
2MT+Ra s	10	?
2MT+Myc	0.004	No
2MT+Ras+Myc	11	No
2MT+p53 shRNA	1	No
2MT+p53 shRNA +Ra s	17	Yes
2MT+p53 shRNA+Myc	15	Yes
2MT+p53 shRNA+Ras+Myc	30	Yes

Table 5.2 Anchorage independent growth of Milan Tert cells expressing combinations of p53 shRNA, Myc and Ras

Approximately five weeks after the final infection, the panel of 2MT cells were plated out in 0.2% soft agarose and fed weekly. After 26 days, the percentage of cells forming colonies was determined.

become capable of anchorage independent growth. This also highlights the different levels of expression achieved in different retroviral infections.

However, reduction of p53 in combination with over-expression of Myc allowed 15% of the cells to undergo anchorage independent growth, and some of the colonies formed were macroscopically visible. Upon shRNA mediated knockdown of p53 in the MTR background, 17% of cells became capable of growth in soft agar and these colonies were easily visible by eye. 2MTRM cells could form small colonies, but the presence of p53 shRNA in these cells trebled the number of cells forming colonies and increased the size of the colonies which were easily visible by eye. It was noted that a reduction in functional p53 usually allowed a larger proportion of colony formation. Photographs were taken of the colonies to illustrate that the presence of shRNA against p53 allowed the colonies to grow to an increased size (Figure 5.8). While the knockdown of p53 alone did not allow 2MT cells to form anchorage independent colonies, this is inconsistent with observations in Leiden cells (E Sanij, unpublished results), and the results using MT \bar{a} cells where knockdown of ARF attenuated the p53 pathway.

These results suggest that compromised p16^{INK4a} function predisposes fibroblasts to anchorage independent growth, and the effect can be enhanced by the knockdown of ARF or p53. To follow up on these observation testing is being undertaken to determine whether the panels of MT and 2MT cells are capable of tumour formation in nude mice.

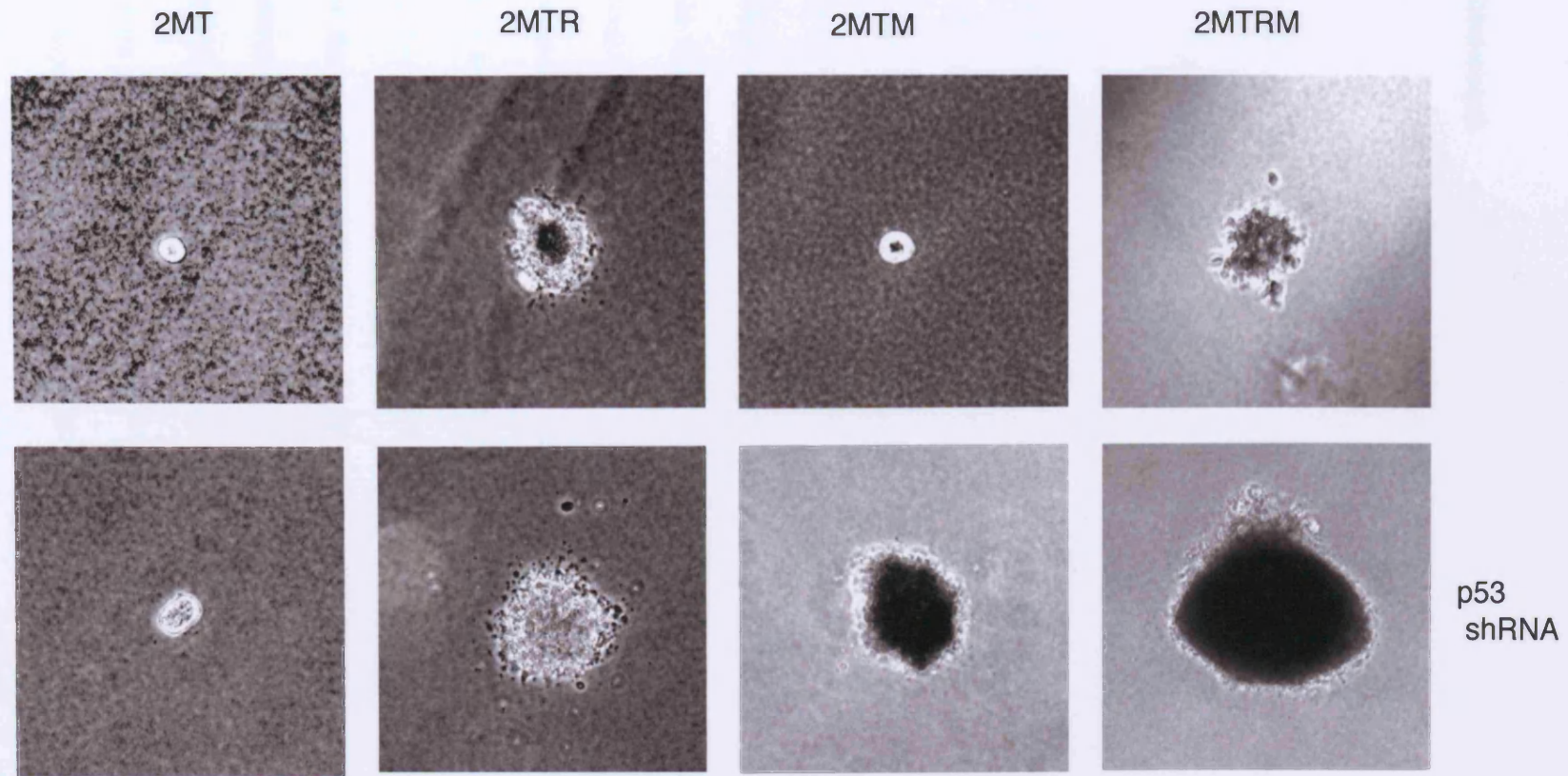


Figure 5.8 Effects of p53 shRNA on the size of anchorage independent colonies formed by Milan Tert cells

After 27 days in soft agar, photographs were taken of the colonies described in Table 5.2 using phase contrast and a 10x objective.

2MT and 2MTM are shown as single cells because no colonies were formed by these cells.

Chapter 6

Discussion

6.1 The significance of the R24P variant of p16^{INK4a}

The germline mutation responsible for the R24P variant of p16^{INK4a} has been described in a number of melanoma kindreds, and in a melanoma patient with no familial history of the disease (Holland et al. 1995; Harland et al. 1997; Della Torre et al. 2001; Monzon et al. 2004). While some reports suggest that this variant of p16^{INK4a} is able to bind to CDK4 but is defective in causing a cell cycle arrest (Becker et al. 2001; Monzon et al. 2004), others indicate that the R24P variant is unable to bind to CDK4 and inhibit its kinase activity, but retains binding to CDK6 (Harland et al. 1997; Nishiwaki et al. 2000). These inconsistencies probably reflect technical variations and reliance on over-expression or *in vitro* assays. The availability of a strain of fibroblasts that are homozygous for the R24P mutation has allowed a more definitive assessment of the properties of the endogenous protein. Data presented in this thesis show unequivocally that in Milan cells, the R24P variant of p16^{INK4a} is able to bind CDK6 but is unable to bind CDK4, and this has been confirmed by others using Milan cells expressing SV40 Large T antigen to enhance p16^{INK4a} expression (J Rowe, unpublished observations). Interestingly, the R24P variant of p16^{INK4a} has also been shown to be deficient in inhibiting CDK7 kinase activity. Although this function of p16^{INK4a} could contribute to its

ability to cause a cell-cycle arrest, its relevance remains uncertain as the observation has not been developed in further publications (Nishiwaki et al. 2000).

The observations from the Milan cells are consistent with a more prominent role for CDK4 than CDK6 in melanoma, which is also suggested by the discovery of melanoma families in which the mutation causes expression of the R24C variant of CDK4 which is impaired in its binding to p16^{INK4a} (Wolfel et al. 1995; Zuo et al. 1996; Soufir et al. 1998). Residue 24 of p16^{INK4a} is in the first ankyrin repeat in a region which lies between helix-1 and helix-2. The crystal structure of p16^{INK4a} bound to CDK6 (Russo et al. 1998) implies that this residue is adjacent to residues involved in the interaction with CDK6, but is not itself directly implicated in the interaction. At this point, it is difficult to judge whether this residue is directly involved in binding to CDK4, as no crystal structure of CDK4 bound to p16^{INK4a} is available. Interestingly, the introduction of the neighbouring R22P mutation in p16^{INK4a} abolishes binding to both CDK4 and CDK6 (S Brookes, unpublished data). As a number of studies suggest that INK4 proteins bind more avidly to CDK6 than to CDK4 (Guan et al. 1994; Hannon and Beach 1994; Quelle et al. 1995a; Guan et al. 1996; Palmero et al. 1997), a possible explanation for the retention of CDK6 binding and loss of CDK4 binding by R24P is that this variant simply has reduced CDK binding, but due to the avidity of binding to CDK6, some residual CDK6 binding is still present. However, it seems unlikely as fibroblasts express much less CDK6 than CDK4, and the binding of R24P to CDK6 but not to CDK4 is very clear cut, and has been reproduced by *in vitro* binding assays.

This is an important issue, as various pieces of data imply that R24P is as functionally impaired as other p16^{INK4a} mutants which cannot bind to either CDK4 or CDK6. For example, the R24P variant of p16^{INK4a} is unable to cause a cell cycle arrest (Figure 4.6) (Nishiwaki et al. 2000; Becker et al. 2001). Also, Milan cells behave as if they are p16^{INK4a}-deficient, both in terms of their replicative lifespan, and in their ability to arrest in response to oncogenic Ras (Figures 4.8, 4.9 and 5.1). However, it is still not resolved whether CDK4 and CDK6 are functionally redundant.

It is also necessary to consider the function of the R24P variant of p16^{INK4a} in the context of the two different modes of action of the cyclin D-CDK complexes. The classical mode of action of these complexes is “kinase-dependent” and depends upon the phosphorylation of specific substrates. In this mode of action, it remains plausible that CDK4 and CDK6 are not redundant, and indeed the kinases have been shown to phosphorylate different sites within pRb (Takaki et al. 2005). The alternative mode of action of the complexes is “kinase-independent”, and relates to the ability of cyclin D-CDK complexes to act as a buffer for p21^{CIP1} and p27^{KIP1}. It remains a matter of debate whether p21^{CIP1} and p27^{KIP1} act as essential assembly factors for cyclin D/CDK complexes (LaBaer et al. 1997; Hengst et al. 1998; Cheng et al. 1999a; Sherr and Roberts 1999), and whether cyclin D-CDK-CIP complexes are active, although convincing evidence exists that this is unlikely to be true (LaBaer et al. 1997; Hengst et al. 1998; Cheng et al. 1999a; Sherr and Roberts 1999; Bagui et al. 2000; Bagui et al. 2003; Olashaw et al. 2004).

However, evidence exists that the cell cycle arrest induced by p16^{INK4a} in HDFs involves the redistribution of p21^{CIP1} from cyclin D/CDK/CIP

complexes onto cyclin E/CDK2 complexes (McConnell et al. 1998). This mechanism depends on the total levels of cyclin D-CDK complexes present in the cell, and the effectiveness of p16^{INK4a} is dependent on its ability to disrupt these cyclin D/CDK/CIP complexes. In HDFs a greater proportion of the p21^{CIP1} present in the cell will be bound to cyclin D/CDK4 than to cyclin D/CDK6. Consequently, R24P will only be able to cause the redistribution of a minor fraction of p21^{CIP1} onto cyclin E/CDK2 complexes, and this will not cause a noticeable inhibition of CDK2 function. However, under circumstances in which the proportion of p21^{CIP1} bound to cyclin D/CDK6 is increased, for example when CDK6 is overexpressed, an increased proportion of p21^{CIP1} will be redistributed upon overexpression of R24P. Consistent with this, it has been observed that expression of the R24P variant of p16^{INK4a} in HDFs in which CDK6 is overexpressed, and in U2OS cells which express higher levels of CDK6 than CDK4 causes an inhibition of cells proliferation (M Ruas and F Gregory, unpublished observations). This mechanism provides an explanation of the apparent paradox of the R24P variant on p16^{INK4a} retaining binding to CDK6 whilst appearing to be non-functional in many assays.

6.2 The role of CDK4 and CDK6 inhibition at senescence

The observation that p21^{CIP1} and p16^{INK4a} levels increase at senescence (Alcorta et al. 1996; Hara et al. 1996) has generally been assumed to mean that CDK4 and CDK6 kinases are inhibited. Consistent with this view, overexpression of CDK4 and CDK6 can extend the lifespan of HDFs causing them to arrest at M1.5, an intermediate stage between senescence and crisis (Morris et al.

2002)(M Ruas and S Brookes, unpublished observations). The accepted interpretation has been that excess CDK4/6 will evade inhibition by p16^{INK4a} and reduce the availability of p21^{CIP1} by promoting the formation of stable cyclin D/CDK complexes. However, new evidence presented in Chapter 4, in combination with other work in our laboratory suggests that the situation is more complicated. Thus, not only do versions of CDK4 and CDK6 that cannot bind p16^{INK4a} have similar effects on HDFs, but they also extend the lifespan of p16^{INK4a}-deficient HDFs such as Q34 and Leiden cells (S Brookes, unpublished observations). This observation is not easy to reconcile with the sequestration model, although there would be effects on the distribution of p21^{CIP1}. Importantly, we find that kinase dead versions of CDK4 and CDK6 are unable to extend the lifespan of HDFs (Figure 4.12). Thus, the mechanism by which CDK4 and CDK6 cause lifespan extension involves phosphorylation of a substrate, although it remains unclear which substrate of CDK4 and CDK6 is responsible for the lifespan extension. While pRb is the acknowledged substrate of both CDK4 and CDK6, other substrates such as Smad3 which is known to be phosphorylated by CDK4 (Matsuura et al. 2004), could be responsible for the lifespan extension. However, ectopic expression of both kinases fails to cause a greater lifespan extension than that of either kinase alone.

6.3 The importance of p16^{INK4a} and ARF in the cellular defences against transformation

The Milan strain of fibroblasts is an attractive subject for study, as the R24P mutation carried by these cells does not affect the coding capacity of the *ARF*

gene. This is in contrast to the Leiden cells, which have been used as a model of p16^{INK4a}-deficient cells, as Leiden cells express an ARF/p16^{INK4a} fusion protein (Brookes et al. 2002). Initially, it was thought that the fusion protein could be functionally impaired, despite performing normally in functional assays. However, it was subsequently proposed that in fact the ARF/p16^{INK4a} fusion protein could be hyperactive, perhaps because of the enhanced stability of the fusion protein relative to wild-type ARF, which may have resulted in attenuation of some aspects of the p53 pathway (Wei et al. 2003b). These challenges were raised in response to several studies which attempted to delineate the minimum requirements for the transformation of HDFs to allow them to form tumours in nude mice. Other groups reported the need to incapacitate p53, while results obtained in Leiden cells suggested that it was not essential (Hahn et al. 1999; Hahn et al. 2002; Drayton et al. 2003; Voorhoeve and Agami 2003; Wei et al. 2003b).

pRb checkpoint	p53 checkpoint	Telomere checkpoint	Oncogenes	Reference
SV40 T-Ag	SV40 T-Ag	hTERT	H-Ras + SV40 t-Ag	Hahn et al., 1999
HPV E7	HPV E6	hTERT	H-Ras + SV40 t-Ag	Hahn et al., 2002
Cyclin D1 + K4 ^{R24C}	DN p53	hTERT	H-Ras + SV40 t-Ag	Hahn et al., 2002
pRb siRNA	p53 siRNA	hTERT	H-Ras + SV40 t-Ag	Voorhoeve and Agami, 2003
p16 ^{INK4a} siRNA	p53 siRNA	hTERT	H-Ras + SV40 t-Ag	Voorhoeve and Agami, 2003
E1A	MDM2		H-Ras	Seger, et al., 2002
p16 ^{INK4a} – deficiency		hTERT	H-Ras + Myc	Drayton et al., 2003

Table 6.1 Published protocols for the neoplastic transformation of primary human fibroblasts

As summarised in the table above, most successful transformation protocols involve the provision of telomerase, (although one report suggests that this is not essential (Seger et al. 2002)). However, it is becoming obvious that overexpression of TERT may have additional functions beyond the maintenance of telomere length. A mouse model in which TERT was overexpressed in basal keratinocytes, suggested that this could promote tumour formation in cells which already had sufficiently long telomeres (Gonzalez-Suarez et al. 2001). ALT is an alternative method to maintain

telomere length where telomeres are extended by a mechanism similar to homologous recombination. A mouse model of tumour development suggested that ALT could not substitute for TERT, especially during metastasis (Chang et al. 2003), while a more direct comparison of ALT and telomerase-mediated telomere maintenance during tumorigenicity concluded that the mechanisms were not equivalent (Stewart et al. 2002), and that TERT has other tumour-promoting roles. These experiments were extended, and the authors were able to demonstrate that a variant of TERT that was unable to mediate telomere extension, was still capable of promoting tumour formation. Different protocols to transform human fibroblasts employ alternative ways of inactivating the pRb and p53 pathways, such as DNA virus proteins (SV40 Large T Ag or adenovirus E1A), or siRNA targeting p53 in combination with siRNA against either pRb or p16^{INK4a}. Some studies have also employed a cyclin D1-CDK4 fusion protein which is insensitive to p16^{INK4a}, reasoning that the presence of this protein should over-ride the effects of p16^{INK4a}. However, data presented in this thesis suggests that the situation may be more complicated as expression of exogenous CDK4 causes an increase in the levels of p16^{INK4a} expressed by the cell (Figure 4.7), but also the kinase activity of CDK4 is likely to have additional effects within the cell. There are also reports in the literature that p16^{INK4a} may have other targets than just cyclin D-CDK complexes, and can inhibit CDK7 and phosphorylation of c-Jun by JNKs (Nishiwaki et al. 2000; Choi et al. 2005). As a result, it seems probable that expression of exogenous CDK4 is not synonymous with p16^{INK4a}-deficiency. Most protocols also provide two co-operating oncogenes, usually H-Ras in combination with SV40 small t antigen. The only documented

function of the small t antigen is to bind to and inactivate some isoforms of PP2A, and it has been suggested that this results in the stabilisation of Myc, and that a mutated version of Myc which is more stable is able to substitute for small t in transformation (Chen et al. 2004b; Yeh et al. 2004). The importance of Myc in transformation was demonstrated in a similar experiment investigating the neoplastic transformation of HMECs, where up-regulation of endogenous Myc was observed in the tumours (Elenbaas et al. 2001).

Work in our laboratory used the p16^{INK4a}-deficient Leiden cell system to generate two distinct sets of tumours which expressed hTERT, H-Ras and c-Myc. The first set of tumours were formed from three different clones which were present in the parental cell population which was injected into mice, and the tumours were found to express wild-type p53 (Drayton et al. 2003). One of these clones had silenced expression of ARF, and it seems possible that the other tumours has sustained alteration in other components of the p53 pathway, and attempts are underway to identify these possible changes using gene expression arrays. The second set of tumours were also formed from Leiden cells expressing hTERT, H-Ras and Myc, but were found to have resulted from the expansion of a single clone which expressed mutant p53. Therefore, there is remarkable consistency that five alterations enable a normal human cell to form a tumour, and there is agreement over the five major pathways which need to be altered in these cells; Ras, Myc, p53, pRb and hTERT.

The results obtained in Milan cells support this contention. The impetus for studying these cells was to reinforce the results observed using Leiden cells in a system where ARF is unequivocally wild-type, and to address the relative

contributions of *INK4a* and *ARF* to tumour suppression in human cells. Evidence presented within this thesis demonstrates that the knockdown of ARF provides a proliferative advantage and facilitates anchorage independence. Thus far, data has only been obtained using the agar colony formation assay, but the tumorigenesis experiments using the panels of Milan cells whose generation was described in the thesis, are ongoing. It will be very interesting to discover if loss of ARF is able to substitute for loss of p53 in our model of tumour formation. If this is not the case, then it will be interesting to analyse the tumours formed to identify mutations may have substituted for loss of p53. It would also be interesting to extend this work, and to assess whether the tumours formed by Milan and Leiden cells demonstrate changes in similar cellular functions. This may suggest genes and pathways whose alteration promotes the formation of cancer regardless of the underlying genetic background. Another future direction would be to look for other oncogenes that can substitute for Myc and/or Ras in our assay, perhaps using a screening approach. This may provide information about the critical functions which are being provided by these oncogenes during the transformation of HDFs. This approach could also be extended to screen for genes which can be altered and can substitute for loss of p53, to gain insights into the p53 pathways which are important in the tumour suppressive role of the protein.

The observed effect of ARF knockdown on cell proliferation is in line with a published report which found that ARF knockdown conferred a growth advantage on HDFs which was dependent on p53 (Voorhoeve and Agami 2003). However, in contrast to our results from the anchorage independence

assay, which suggested that loss of ARF and loss of p53 were equivalent in our system, the authors of this report suggested that loss of ARF could not substitute for loss of p53 in their system (Voorhoeve and Agami 2003). However, while we found that loss of p16^{INK4a} enabled Milan fibroblasts to bypass an arrest induced by oncogenic Ras (Figure 5.1), the authors of this paper found that in their system loss of p53 was sufficient to allow bypass of a Ras-induced arrest suggesting the existence of differences between the two systems used.

It is also necessary to consider the reasons for the inconsistencies between different reports. One of the major reasons underlying these discrepancies is likely to be that different fibroblast strains respond differently when challenged with oncogenic stress. For example, IMR90 cells are quite hard to transform, while in comparison, BJ fibroblasts are relatively easy to transform. (Akagi et al. 2003). It has also been shown that the response of HDFs to Ras can depend on how long the cells have been in culture and the level of stress to which they have been exposed, as freshly explanted fibroblasts were shown not to arrest in response to oncogenic Ras (Benanti and Galloway 2004). The ability of cells to resist transformation seems to correlate with the basal levels of p16^{INK4a} expressed by the different fibroblast strains, and may reflect the differing dependence on the p16^{INK4a} and p21^{CIP1} pathways of different fibroblast strains at senescence (Beausejour et al. 2003). An additional factor is that fibroblasts derived from adult skin are heterogenous and individual cells within a culture would respond differently when challenged with an oncogenic stress (Brookes et al. 2004). An extra level of complexity is added by the use of a retroviral infection system for the expression of exogenous

proteins. Differing levels of expression can be obtained depending on the integration site of the retrovirus and the vector used. During these studies, striking differences have been observed in the levels of expression and phenotypic outcome in different infections (e.g. between MT and 2MT panels), and different efficiencies of infection have been seen simply by changing the drug selection marker in the retroviral vector used. Similar effects have been observed by others in the laboratory (S Brookes and J Rowe), and have also been reported in the literature (Elenbaas et al. 2001). At a practical level, differences in expression levels may explain why some reports demonstrate upregulation of p53 in response to oncogenic Ras (Serrano et al. 1997; Lin et al. 1998; Ferbeyre et al. 2000; Ries et al. 2000; Wei et al. 2001; Wei et al. 2003b), while the same is not observed in other reports (Zhu et al. 1998; Ries et al. 2000; Brookes et al. 2002; Huot et al. 2002; Lazarov et al. 2002; Drayton et al. 2003; Voorhoeve and Agami 2003; Benanti and Galloway 2004; Drayton et al. 2004). These technical observations underline the need to be cautious when comparing results obtained using different infections, vectors, and fibroblast strains. It is also necessary to consider that in our system there has been chronic loss of p16^{INK4a}, as our cells carry germline mutations of the *INK4a* gene. This may have allowed some compensation to occur in these cells, potentially by changing the levels of CDK4, CDK6, or other CDK inhibitors present in these cells. This may mean that our p16^{INK4a}-deficient cell strains behave differently from cells which have undergone acute loss of p16^{INK4a}. Indeed differences have been reported between chronic and acute loss of pRb in mouse models. Acute loss of pRb allows senescence to be overcome (Sage et al. 2003), while

this does not occur in cells carrying a germline mutation of Rb as a result of compensation. The ability of p16^{INK4a} loss to overcome oncogene-induced premature senescence seems to be retained regardless of whether p16^{INK4a} loss was acute or chronic (Figure 3.2). However, it may be informative to generate tumours using HDFs expressing shRNA targeting p16^{INK4a}. This would provide an insight into whether the Leiden and Milan cells have undergone compensation which has affected their requirements for transformation.

There are also major differences between mouse and human cells that present difficulties when attempting to reconcile results obtained in the different species. Mouse cells can be transformed solely by the expression of two cooperating oncogenes such as Myc and Ras (Hahn and Weinberg 2002), and the p53/ARF pathway has been shown to be central to determining the resistance of these cells to oncogenic challenges (Kamijo et al. 1997). As well as the different sensitivity of mouse and human cells to oxidative stress (Sherr and DePinho 2000), it has been reported that different Ras effector pathways are implicated in the transformation of mouse and human cells (Akagi and Hanafusa 2004; Rangarajan et al. 2004).

Tumours contain widely differing cancer cells that exhibit different phenotypes. While investigating this heterogeneity, it was demonstrated that only a small minority of cells in a cancer were able to proliferate extensively. This suggested that cancers contain a subset of cells known as cancer stem cells, which could divide giving rise to phenotypically diverse progeny cells. If this theory was correct then these stem cells would be capable of self-renewal, in addition to producing differentiated cancer cells with more limited proliferative potential. The cancer stem cells could arise either from

mutations in a stem cell compartment allowing the cells to overcome barriers to continued proliferation, or when differentiated cells gained the characteristics of stem cells, perhaps by mutations in the pathways involved in maintaining stem cell characteristics. The presence of cancer stem cells was originally demonstrated in AML, but has recently been demonstrated in breast cancer and glioblastoma (Pardal et al. 2003). This has relevance to experimental approaches attempting to delineate the minimum requirements for tumorigenesis, and questions the validity of experiments performed in more differentiated cell types. It would be interesting to investigate the effects of the overexpression of oncogenes in stem cells, and whether the response of these cells is similar to that observed in other cell types. The stem cell nature of cancer should be considered when attempting to model the genesis of cancer, but technical difficulties may limit the work that can actually be performed using cancer stem cells.

6.4 Senescence as a tumour suppressive mechanism *in vivo*

The relevance of senescence as a tumour-suppressive mechanism *in vivo* has been the subject of intense debate. It has been argued that senescence in response to oncogenic stress may be an artefact caused by the expression of oncogenes in cells already subjected to stress due to their growth in tissue culture. There has also been intense debate about the validity of experiments which use the overexpression of oncogenes, such as activated Ras, at very high levels. Several mouse models (Guerra et al. 2003; Tuveson et al. 2004) using the knock-in of oncogenic K-Ras V12, have suggested that expression of activated Ras at physiological levels *in vivo* does not cause senescence. It

has also been suggested that the progression of tumours caused by overexpression of oncogenic Ras may differ from those caused by the activation of Ras at endogenous levels (Meuweissen et al. 2001). However, a similar mouse model expressing oncogenic Ras at endogenous levels has recently been used to demonstrate the presence of senescent cells in pre-malignant lesions (Collado et al. 2005), and the expression of oncogenic B-Raf at levels similar to endogenous in human cells can cause inhibition of proliferation and oncogene-induced senescence (Michaloglou et al. 2005). Recently, it has been ably demonstrated that senescence is acting as a tumour-suppressive mechanism in a variety of settings in both the mouse and human (Braig et al. 2005; Chen et al. 2005; Collado et al. 2005; Michaloglou et al. 2005). The presence of senescent cells in pre-malignant tumours was demonstrated in mouse models of Ras-induced lung and pancreatic cancer, in pre-malignant prostate tumours from humans, and in human benign tumours composed of melanocytes (naevi). Interestingly however, senescent cells were not present in melanomas or in malignant tumours formed in the mouse models, suggesting that the senescence was bypassed when the tumours progressed to malignancy. Two further mouse models where tumours were induced by loss of PTEN or the histone methyltransferase Suv39h1 (implicated in senescence-associated chromatin remodelling) also demonstrated that senescence is not an artefact, but an important mechanism by which tumour progression can be restrained. Interestingly these experiments also showed that p53 was not only important in invoking apoptosis as an anti-tumour mechanism but could also invoke senescence.

6.5 Concluding remarks

This thesis describes the use of cells from genetically compromised individuals to try to discern the relative roles of *INK4a* and *ARF*. The cells carrying a mutation responsible for the expression of the R24P variant of p16^{INK4a} are particularly interesting as the mutation leaves *ARF* unaffected, and disables only one of the known activities of p16^{INK4a}, inhibition of CDK4.

This *CDKN2a* locus provides an intriguing situation where the locus contains three genes *INK4b*, *ARF*, and *INK4a* which have been implicated in the response to oncogenic challenges and tumour suppression. However, most mutations in germline and sporadic tumours affect only *INK4a* (Ruas and Peters 1998; Sharpless and DePinho 1999). Deletions and methylation of the locus often affects all three genes, but cases have been described where selective loss of *INK4b* or *ARF* is observed. However, until we understand the regulation of the locus we cannot exclude indirect effects on the *INK4a* response to specific signals which could be influenced by deletions which appear to affect only *ARF*. We can also speculate that mutations may exist in the regulatory regions of the locus in families with a history of melanoma who show linkage of the disease-causing mutation to 9p21, but no alterations are observed in the coding domains of these genes. These mutations may also give us insights into the regulation of the locus.

However, the discovery of a cell strain genetically deficient only in *INK4a*, in combination with the advent of shRNA technology opens up the possibility of being able to definitively address some of these questions.

References

Akagi, T. and Hanafusa, H. 2004. Human diploid fibroblasts are refractory to oncogene-mediated transformation. *Cell Cycle* **3**(3): 257-258.

Akagi, T., Sasai, K., and Hanafusa, H. 2003. Refractory nature of normal human diploid fibroblasts with respect to oncogene-mediated transformation. *Proceedings of the National Academy of Science* **100**(23): 13567-13572.

Alani, R., Young, A., and Shifflett, C. 2001. Id1 regulation of cellular senescence through transcriptional repression of p16/Ink4a. *Proceedings of the National Academy of Science* **98**(14): 7812-7816.

Alcorta, D., Xiong, Y., Phelps, D., Hannon, G., Beach, D., and Barrett, C. 1996. Involvement of the cyclin-dependent kinase inhibitor p16 (INK4a) in replicative senescence of normal human fibroblasts. *Proceedings of the National Academy of Science* **93**: 13742-13747.

Ameyar-Zazoua, M., Wisniewska, M., Bakiri, L., Wagner, E., Yaniv, M., and Weitzman, J. 2005. AP-1 dimers regulate transcription of the *p14/p19^{ARF}* tumor suppressor gene. *Oncogene* **24**: 2298-2306.

Andrique, L., Ayrault, O., Larsen, C.-J., and Seite, P. 2005. *In vitro* and *in vivo* analysis of the interaction between 5.8S rRNA and ARF protein reveal a

new difference between murine p19ARF and human p14^{ARF}. *Oncogene* **24**: 2580-2584.

Aslanian, A., Iaquina, P., Verona, R., and Lees, J. 2004. Repression of the *Arf* tumor suppressor by E2F3 is required for normal cell cycle kinetics. *Genes and Development* **18**: 1413-1422.

Ayrault, O., Andrique, L., Larsen, C.-J., and Seite, P. 2004. Human *Arf* tumour suppressor specifically interacts with chromatin containing the promoter of rRNA genes. *Oncogene* **23**: 8097-8104.

Bagui, T., Jackson, R., Agrawal, D., and Pledger, W. 2000. Analysis of cyclin D3-cdk4 complexes in fibroblasts expressing and lacking p27^{KIP1} and p21^{CIP1}. *Molecular and Cellular Biology* **20**(23): 8748-8757.

Bagui, T., Mohapatra, S., Haura, E., and Pledger, W. 2003. p27^{KIP1} and p21^{CIP1} are not required for the formation of active D cyclin-cdk4 complexes. *Molecular and Cellular Biology* **23**(20): 7285-7290.

Bates, S., Philips, A., Clark, P., Stott, F., Peters, G., Ludwig, R., and Vousden, K. 1998. p14^{ARF} links the tumour suppressors RB and p53. *Nature* **395**: 124-125.

Beausejour, C., Krtolica, A., Galimi, F., Narita, M., Lowe, S., Yaswen, P., and Campisi, J. 2003. Reversal of human cellular senescence: roles of the p53 and p16 pathways. *EMBO Journal* **22**(16): 4212-4222.

Becker, T.M., Rizos, H., Kefford, R.F., and Mann, G.J. 2001. Functional impairment of melanoma-associated p16^{INK4a} mutants in melanoma cells despite retention of cyclin-dependent kinase 4 binding. *Clinical Cancer Research* **7**: 33282-33288.

Ben-Porath, I. and Weinberg, R. 2004. When cells get stressed: an integrative view of cellular senescence. *The Journal of Clinical Investigation* **113**(1): 8-13.

Ben-Saadon, R., Fajerman, I., Ziv, T., Hellman, U., Schwartz, A., and Ciechanover, A. 2004. The tumour suppressor protein p16^{INK4A} and the human papillomavirus oncoprotein-58 E7 are naturally occurring lysine-less proteins that are degraded by the ubiquitin system. *Journal of Biological Chemistry* **279**(40): 41414-41421.

Benanti, J. and Galloway, D. 2004. Normal human fibroblasts are resistant to ras-induced senescence. *Molecular and Cellular Biology* **24**: 2842-2852.

Berns, K., Hijmans, M., and Bernards, R. 1997. Repression of c-myc responsive genes in cycling cells causes G₁ arrest through reduction of cyclin E/CDK2 kinase activity. *Oncogene* **15**: 1347-1356.

Berthet, C., Aleem, E., Coppola, V., Tessarollo, L., and Kaldis, P. 2003. Cdk2 knockout mice are viable. *Current Biology* **13**: 1775-1785.

Betz, B., Strobeck, M., Reisman, D., Knudsen, E., and Weissman, B. 2002. Re-expression of hSNF5/INI1/BAF47 in paediatric tumour cells leads to G₁ arrest associated with induction of p16^{INK4A} and activation of RB. *Oncogene* **21**: 5193-5203.

Blackwell, T.K., Huang, J., Ma, A., Kretzner, L., Alt, F., Eisenman, R., and Weintraub, H. 1993. Binding of Myc proteins to canonical and non-canonical DNA sequences. *Molecular and Cellular Biology* **13**(9): 5216-5224.

Bodnar, A., Ouellette, M., Frolkis, M., Holt, S., Chiu, C.-P., Morin, G., Harley, C., Shay, J., Lichtsteiner, S., and Wright, W. 1998. Extension of life-span by introduction of telomerase into normal human cells. *Science* **279**: 349-352.

Bond, J., Haughton, M., Rowson, J., Smith, P., Gire, V., Wynford-Thomas, D., and Wyllie, F. 1999. Control of replicative life span in human cells: barriers to clonal expansion intermediate between M1 senescence and M2 crisis. *Molecular and Cellular Biology* **19**(4): 3103-3114.

Bond, J., Jones, C., Haughton, M., DeMicco, C., Kipling, D., and Wynford-Thomas, D. 2003. Direct evidence from siRNA-directed "knockdown" that p16^{INK4A} is required for human fibroblast senescence and for limiting ras-

induced epithelial cell proliferation. *Experimental Cell Research* **292**: 151-156.

Bouchard, C., Thieke, K., Maier, A., Saffrich, R., Ansorge, W., Reed, S., Sicinski, P., Bartek, J., and Eilers, M. 1999. Direct induction of cyclin D2 by Myc contributes to cell cycle progression and sequestration of p27. *The EMBO Journal* **18**(19): 5321-5333.

Braig, M., Lee, S., Loddenkemper, C., Rudolph, C., Peters, A., Schlegelberger, B., Stein, H., Dorken, B., Jenuwin, T., and Schmitt, C. 2005. Oncogene-induced senescence as an initial barrier in lymphoma development. *Nature* **436**: 660-665.

Brenner, A., Stampfer, M., and Aldaz, M. 1998. Increased p16 expression with first senescence arrest in human mammary epithelial cells and extended growth capacity with p16 inactivation. *Oncogene* **17**: 199-205.

Brookes, S., Rowe, J., Gutierrez del Arroyo, A., Bond, J., and Peters, G. 2004. Contribution of p16^{INK4a} to replicative senescence of human fibroblasts. *Experimental Cell Research* **298**: 549-559.

Brookes, S., Rowe, J., Ruas, M., Llanos, S., Clark, P.A., Lomax, M., James, M., Vatcheva, R., Bates, S., Vousden, K.H., Parry, D., Gruis, N., Smit, N., Bergman, W., and Peters, G. 2002. INK4a-deficient human diploid fibroblasts

are resistant to RAS-induced senescence. *The EMBO Journal* **21**(12): 2936-2945.

Brooks, C. and Gu, W. 2004. Dynamics in the p53-Mdm2 ubiquitination pathway. *Cell Cycle* **3**(7): 895-899.

Brummelkamp, T., Bernards, R., and Agami, R. 2002a. Stable suppression of tumorigenicity by virus-mediated RNA interference. *Cancer Cell* **2**: 243-247.
-. 2002b. A system for stable expression of short interfering RNAs in mammalian cells. *Science* **296**: 550-553.

Campisi, J. 2001. Cellular senescence as a tumor-suppressor mechanism. *Trends in Cell Biology* **11**(11): S27-S31.

Carnero, A., Hudson, J., Price, C., and Beach, D. 2000. p16^{INK4A} and p19^{ARF} act in overlapping pathways in cellular immortalisation. *Nature Cell Biology* **2**: 148-155.

Cerezo, A., Kalthoff, H., Schuermann, M., Schafer, B., and Boukamp, P. 2002. Dual regulation of telomerase activity through c-Myc-dependent inhibition and alternative splicing of hTERT. *Journal of Cell Science* **115**: 1305-1312.

Chang, S., Khoo, C., Naylor, M., Maser, R., and DePinho, R. 2003. Telomere-based crisis: functional differences between telomerase activation and ALT in tumour progression. *Genes and Development* **17**: 88-100.

Chen, J.-H., Stoeber, K., Kingsbury, S., Ozanne, S., Williams, G., and Hales, N. 2004a. Loss of proliferative capacity and induction of senescence in oxidatively stressed human fibroblasts. *Journal of Biological Chemistry* **279**(47): 49439-49446.

Chen, Q., Prowse, K., Tu, V., Purdom, S., and Linsken, M. 2001. Uncoupling the senescent phenotype from telomere shortening in hydrogen peroxide-treated fibroblasts. *Experimental Cell Research* **265**: 294-303.

Chen, W., Possemato, R., Campbell, K., Plattner, C., Pallas, D., and Hahn, W. 2004b. Identification of specific PP2A complexes involved in human cell transformation. *Cancer Cell* **5**(2): 127-136.

Chen, Z., Trotman, L., Shaffer, D., Lin, H.-K., Dotan, Z., Niki, M., Koutcher, J., Scher, H., Ludwig, T., Gerald, W., Cordon-Cardo, C., and Pandolfi, P.P. 2005. Crucial role of p53-dependent cellular senescence in suppression of Pten-deficient tumorigenesis. *Nature* **436**: 725-730.

Cheng, M., Olivier, P., Diehl, J.A., Fero, M., Roussel, M., Roberts, J., and Sherr, C. 1999a. The p21^{CIP1} and p27^{KIP1} CDK 'inhibitors' are essential

activators of cyclin D-dependent kinases in murine fibroblasts. *The EMBO Journal* **18**(6): 1571-1583.

Cheng, S.-W., Davies, K., Yung, E., Beltran, R., Yu, J., and Kalpana, G. 1999b. c-MYC interacts with INI/hSNF5 and requires the SWI/SNF complex for transactivation function. *Nature Genetics* **22**: 102-105.

Choi, B.Y., Choi, H.S., Ko, K., Cho, Y.-Y., Zhu, F., Kang, B.S., Ermakova, S., Ma, W.-Y., Bode, A., and Dong, Z. 2005. The tumour suppressor p16 inhibits cell transformation through inhibition of c-Jun phosphorylation and AP-1 activity. *Nature Structural and Molecular Biology* **12**(8): 699-707.

Claasen, G. and Hann, S. 2000. A role for transcriptional repression of p21^{CIP1} by c-Myc in overcoming transforming growth factor β -induced cell-cycle arrest. *Proceedings of the National Academy of Science* **97**(17): 9498-9503.

Collado, M., Gil, J., Efeyan, A., Guerra, C., Schuhmacher, A., Barradas, M., Benguria, A., Zaballos, A., Flores, J., Barbacid, M., Beach, D., and Serrano, M. 2005. Senescence in premalignant tumours. *Nature* **436**: 642.

Coller, H., Grandori, C., Tamayo, P., Colbert, T., Lander, E., Eisenman, R., and Golub, T. 2000. Expression analysis with oligonucleotide microarrays reveals that Myc regulates genes involved in growth, cell cycle, signaling, and adhesion. *Proceedings of the National Academy of Science* **97**(7): 3260-3265.

Costello, J., Berger, M., Huang, S., and Cavenee, W. 1996. Silencing of *p16/CDK2* expression in human gliomas by methylation and chromatin condensation. *Cancer Research* **56**(2405-2410).

d'Adda di Fagagna, F., Reaper, P., Clay-Farrace, L., Fiegler, H., Carr, P., von Zglinicki, T., Saretzki, G., Carter, N., and Jackson, S. 2003. A DNA damage checkpoint response in telomere-initiated senescence. *Nature* **426**: 194-198.

Damalas, A., Kahan, S., Shtutman, M., Ben-Ze'ev, A., and Oren, M. 2001. Deregulated β -catenin induces a p53- and ARF-dependent growth arrest and cooperate with Ras in transformation. *The EMBO Journal* **20**(17): 4912-4922.

Datta, A., Nag, A., and Raychaudhuri, P. 2002. Differential regulation of E2F1, DP1, and the E2F1/DP1 complex by ARF. *Molecular and Cellular Biology* **22**(24): 8398-8408.

de Lange, T. 2002. Protection of mammalian telomeres. *Oncogene* **21**: 532-540.

de Stanchina, E., McCurrach, M., Zindy, F., Shieh, S.-Y., Ferbeyre, G., Samuelson, A., Prives, C., Roussel, M., Sherr, C., and Lowe, S. 1998. E1A signalling to p53 involves the p19^{ARF} tumor suppressor. *Genes and Development* **12**: 2434-2442.

Della Torre, G., Pasini, B., Frigerio, S., Donghi, R., Rovini, D., Delia, D., Peters, G., Huot, T., Bianchi-Scarra, G., Lantieri, F., Rodolfo, M., Parmiani, G., and Pierotti, M. 2001. *CDKN2A* and *CDK4* mutation analysis in Italian melanoma-prone families: functional characterization and of a novel *CDKN2A* germ line mutation. *British Journal of Cancer* **85**(6): 836-844.

Dellambra, E., Golisano, O., Bondanza, S., Siverio, E., Lacal, P., Molinari, M., D'Arti, S., and De Luca, M. 2000. Downregulation of 14-3-3 σ prevents clonal evolution and leads to immortalisation of primary human keratinocytes. *Journal of Cell Biology* **149**(5): 1117-1129.

Deng, Q., Liao, R., Wu, B.-L., and Sun, P. 2004. High intensity Ras signalling induces premature senescence by activating p38 pathway in primary human fibroblasts. *Journal of Biological Chemistry* **279**(2): 1050-1059.

Dimri, G., Itahana, K., Acosta, M., and Campisi, J. 2000. Regulation of a senescence checkpoint response by the E2F1 transcription factor and p14^{ARF} tumor suppressor. *Molecular and Cellular Biology* **20**(1): 273-285.

Drayton, S., Brookes, S., Rowe, J., and Peters, G. 2004. The significance of p16^{INK4a} in cell defences against transformation. *Cell Cycle* **3**(5): 611-615.

Drayton, S. and Peters, G. 2002. Immortalisation and transformation revisited. *Current opinion in genetics and development* **12**: 98-104.

Drayton, S., Rowe, J., Jones, R., Vatcheva, R., Cuthbert-Heavens, D., Marshall, J., Fried, M., and Peters, G. 2003. Tumour suppressor p16^{INK4A} determines the sensitivity of human cells to transformation by cooperating cellular oncogenes. *Cancer Cell* **4**: 301-310.

Eisenman, R. 2001. Deconstructing Myc. *Genes and Development* **15**: 2023-2030.

Elenbaas, B., Spirio, L., Koerner, F., Fleming, M.D., Zimonjic, D.B., Donaher, J.L., Popescu, N.C., Hahn, W.C., and Weinberg, R.A. 2001. Human breast cancer cells generated by oncogenic transformation of primary mammary epithelial cells. *Genes and Development* **15**: 50-65.

Eymin, B., Karayan, L., Seite, P., Brambille, C., Brambilla, E., Larsen, C.-J., and Gazzeri, S. 2001. Human ARF binds E2F1 and inhibits its transcriptional activity. *Oncogene* **20**: 1033-1041.

Fatyor, K. and Szalay, A. 2001. The p14^{ARF} tumor suppressor protein facilitates nucleolar sequestration of Hypoxia-inducible factor-1 α (HIF-1 α) and inhibits HIF-1-mediated transcription. *Journal of Biological Chemistry* **276**(30): 28421-28429.

Felsher, D., Zetterberg, A., Zhu, J., Tlsty, T., and Bishop, J.M. 2000. Overexpression of *MYC* causes p53-dependent G₂ arrest of normal fibroblasts. *Proceedings of the National Academy of Science* **97**(19): 10544-10548.

Ferbeyre, G., de Stanchina, E., Querido, E., Baptiste, N., Prives, C., and Lowe, S. 2000. PML is induced by oncogenic ras and promotes premature senescence. *Genes and Development* **14**(16): 2015-2027.

Fernandez, P., Frank, S., Wang, L., Schroeder, M., Liu, S., Greene, J., Cocito, A., and Amati, B. 2003. Genomic targets of the c-Myc protein. *Genes and Development* **17**: 1115-1129.

Foster, S., Wong, D., Barrett, M., and Galloway, D. 1998. Inactivation of p16 in human mammary epithelial cells by CpG island methylation. *Molecular and Cellular Biology* **18**(4): 1793-1801.

Frank, S., Parisi, T., Taubert, S., Fernandez, P., Fuchs, M., Charr, H.-M., Livingston, D., and Amati, B. 2003. MYC recruits TIP60 histone acetyltransferase complex to chromatin. *EMBO Reports* **4**(6): 575-580.

Galaktionov, K., Chen, X., and Beach, D. 1996. Cdc25 cell-cycle phosphatase as a target of c-myc. *Nature* **382**: 511-517.

Gewin, L. and Galloway, D. 2001. E box-dependent activation of telomerase by human papillomavirus type 16 E6 does not require activation of c-myc. *Journal of Virology* **75**(15): 7198-7201.

Gil, J., Bernard, D., Martinez, D., and Beach, D. 2004. Polycomb CBX7 has a unifying role in cellular lifespan. *Nature Cell Biology* **6**(1): 67-72.

Gil, J., Kerai, P., Leonart, M., Bernard, D., Cigudosa, J., Peters, G., Carnero, A., and Beach, D. 2005. Immortalization of primary human prostate epithelial cells by c-Myc. *Cancer Research* **65**(6): 2179-2185.

Gire, V., Roux, P., Wynford-Thomas, D., Brondello, J.-M., and Dulic, V. 2004. DNA damage checkpoint kinase Chk2 triggers replicative senescence. *The EMBO Journal* **23**(13): 2554-2563.

Gonzalez-Suarez, E., Samper, E., Ramirez, A., Flores, J., Martin-Caballero, J., Jorcano, J., and Blasco, M. 2001. Increased epidermal tumors and increased skin wound healing in transgenic mice overexpressing the catalytic subunit of telomerase, mTERT, in basal keratinocytes. *The EMBO Journal* **20**(11): 2619-2630.

Greenberg, R., O'Hagan, R., Deng, H., Xiao, Q., Hann, S., Adams, R., Lichtsteiner, S., Chin, L., Morin, G., and DePinho, R. 1999. Telomerase reverse transcriptase gene is a direct target of c-Myc but is not functionally equivalent in cellular transformation. *Oncogene* **18**: 1219-1226.

Guan, K.-L., Jenkins, C., Li, Y., Nichols, M., Wu, X., O'Keefe, C., Matera, A., and Xiong, Y. 1994. Growth suppression by p18, a p16INK4/MTS1- and p14INK4B/MTS2-related CDK6 inhibitor, correlates with wild-type pRb function. *Genes and Development* **8**(24): 2939-2952.

Guan, K.-L., Jenkins, C., Li, Y., O'Keefe, C., Noh, S., Wu, X., Zariwala, M., Matera, A., and Xiong, Y. 1996. Isolation and characterization of p19INK4d, a p16-related inhibitor specific to CDK6 and CDK4. *Molecular Biology of the Cell* **7**(1): 57-70.

Guerra, C., Mijimolle, N., Dhawahir, A., Dubus, P., Barradas, M., Serrano, M., Campuzano, V., and Barbacid, M. 2003. Tumor induction by an endogenous *K-ras* oncogene is highly dependent on cellular context. *Cancer Cell* **4**: 111-120.

Gump, J., Stokoe, D., and McCormick, F. 2003. Phosphorylation of p16^{INK4A} correlates with CDK4 association. *Journal of Biological Chemistry* **278**(9): 6619-6622.

Haggerty, T., Zeller, K., Osthus, R., Wonsey, D., and Dang, C. 2003. A strategy for identifying transcription factor binding sites reveals two classes of genomic c-Myc target sites. *Proceedings of the National Academy of Science* **100**(9): 5313-5318.

Hahn, W., Counter, C., Lundberg, A., Beijersbergen, R., Brooks, M., and Weinberg, R. 1999. Creation of human tumour cells with defined genetic elements. *Nature* **400**: 464-468.

Hahn, W., Dessain, S., Brooks, M., King, J., Elenbaas, B., Sabatini, D., DeCaprio, J., and Weinberg, R. 2002. Enumeration of the Simian Virus 40

early region elements necessary for human cell transformation. *Molecular and Cellular Biology* **22**(7): 2111-2123.

Hahn, W. and Weinberg, R. 2002. Rules for making human tumor cells. *New England Journal of Medicine* **347**(20): 1593-1603.

Hanahan, D. and Weinberg, R. 2000. The hallmarks of cancer. *Cell* **100**: 57-70.

Hannon, G. and Beach, D. 1994. p15^{INK4B} is a potential effector of TGF-beta-induced cell cycle arrest. *Nature* **371**(6494): 257-261.

Hansson, A., Manetopoulos, C., Jonsson, J.-I., and Axelson, H. 2003. The basic helix-loop-helix transcription factor TAL1/SCL inhibits the expression of the p16^{INK4A} and pT α genes. *Biochemical and Biophysical Research Communications* **312**: 1073-1081.

Hara, E., Smith, R., Parry, D., Tahara, H., Stone, S., and Peters, G. 1996. Regulation of p16^{CDKN2} expression and its implications for cell immortalization and senescence. *Molecular and Cellular Biology* **16**(3): 859-867.

Harland, M., Melani, R., Gruis, N., Pinney, E., Brookes, S., Spurr, N., Frischauf, A.-M., Bataille, V., Peters, G., Cuzick, J., Selby, P., Bishop, T., and Newton Bishop, J. 1997. Germline mutations of the CDK2 gene in UK melanoma families. *Human Molecular Genetics* **12**: 2061-2067.

Hayflick, L. 1965. The limited *in vitro* lifetime of human diploid cell strains. *Experimental Cell Research* **37**: 614-636.

Hayflick, L. and Moorhead, P. 1961. The serial cultivation of human diploid cell strains. *Experimental Cell Research* **25**(585-621).

Hengst, L., Gopfert, U., Lashuel, H., and Reed, S. 1998. Complete inhibition of Cdk/cyclin by one molecule of p21^{CIP1}. *Genes and Development* **12**: 3882-3888.

Herbert, B.-S., Wright, W., and Shay, J. 2002. p16^{INK4A} inactivation is not required to immortalise human mammary epithelial cells. *Oncogene* **21**: 7897-7900.

Herbig, U., Jobling, W., Chen, B., Chen, D., and Sedivy, J. 2004. Telomere shortening triggers senescence of human cells through a pathway involving ATM, p53 and p21^{CIP1}, but not p16^{INK4A}. *Molecular Cell* **14**: 501-513.

Herman, J., Merlo, A., Mao, L., Lapidus, R., Issa, J.-P., Davidson, N., Sidransky, D., and Baylin, S. 1995. Inactivation of the *CDKN2/p16/MTS1* gene is frequently associated with aberrant DNA methylation in all common human cancers. *Cancer Research* **55**: 4525-4530.

Hermeking, H., Rago, C., Schuhmacher, M., Li, Q., Barrett, J., Obaya, A., Sedivy, J., Eick, D., Vogelstein, B., and Kinzler, K. 2000. Identification of

CDK4 as a target of c-Myc. *Proceedings of the National Academy of Science* **97**(5): 2229-2234.

Herold, S., Wanzel, M., Beuger, V., Frohme, C., Beul, D., Hillukkala, T., Syvaoja, J., Saluz, H.-P., Haenel, F., and Eilers, M. 2002. Negative regulation of the mammalian UV response by Myc through association with Miz-1. *Molecular Cell* **10**: 509-521.

Hewitt, C., Wu, C., Evans, G., Howell, A., Elles, R., Jordan, R., Sloan, P., Read, A., and Thakker, N. 2002. Germline mutation of ARF in a melanoma kindred. *Human Molecular Genetics* **11**(11): 1273-1279.

Holland, E., Beaton, S., Becker, T.M., Gullet, O., Peters, B., Rizos, H., Kefford, R.F., and Mann, G.J. 1995. Analysis of the p16 gene, CDKN2, in 17 Australian melanoma kindreds. *Oncogene* **11**: 2289-2294.

Huot, T.J., Rowe, J., Harland, M., Drayton, S., Brookes, S., Gooptu, C., Purkins, P., Fried, M., Bataille, V., Hara, E., Newton-Bishop, J., and Peters, G. 2002. Biallelic mutations in p16(INK4a) confer resistance to Ras- and Ets-induced senescence in human diploid fibroblasts. *Molecular and Cellular Biology* **23**: 8135-8143.

Huschtscha, L., Noble, J., Neumann, A., Moy, E., Barry, P., Melki, J., Clark, S., and Reddel, R. 1998. Loss of p16^{INK4A} expression by methylation is

associated with lifespan extension of human mammary epithelial cells. *Cancer Research* **58**: 3508-3512.

Inoue, K., Roussel, M., and Sherr, C. 1999. Induction of *ARF* tumor suppressor gene expression and cell cycle arrest by transcription factor DMP1. *Proceedings of the National Academy of Science* **96**: 3993-3998.

Itahana, K., Bhat, K., Jin, A., Itahana, Y., Hawke, D., Kobayashi, R., and Zhang, Y. 2003a. Tumour suppressor ARF degrades B23, a nucleolar protein involved in ribosome biogenesis and cell proliferation. *Molecular Cell* **12**: 1151-1164.

Itahana, K., Zou, Y., Itahana, Y., Martinez, J., Beausejour, C., Jacobs, J., van Lohuizen, M., Band, V., Campisi, J., and Dimri, G. 2003b. Control of the replicative life span of human fibroblasts by p16 and the polycomb protein Bmi-1. *Molecular and Cellular Biology* **23**(1): 389-401.

Iwasa, H., Han, J., and Ishikawa, F. 2003. Mitogen-activated protein kinase p38 defines the common senescence signalling pathway. *Genes to Cells* **8**: 131-144.

Jacobs, J. and de Lange, T. 2004. Significant role for p16^{INK4a} in p53-independent telomere-directed senescence. *Current Biology* **14**: 2303-2308.

Jacobs, J., Keblusek, P., Robanus-Maandag, E., Kristel, P., Lingbeek, M., Nederlof, P., van Welsem, T., van de Vijver, M., Koh, E., Daley, G., and van Lohuizen, M. 2000. Senescence bypass screen identifies TBX2, which represses Cdkn2a (p19^{ARF}) and is amplified in a subset of human breast cancers. *Nature Genetics* **26**: 291-299.

Jacobs, J., Kieboom, K., Marino, S., DePinho, R., and van Lohuizen, M. 1999a. The oncogene and polycomb-group gene Bmi-1 regulates cell proliferation and senescence through the INK4A locus. *Nature* **397**: 164-168.

Jacobs, J., Scheijen, B., Voncken, J.-W., Kieboom, K., Berns, A., and van Lohuizen, M. 1999b. Bmi-1 collaborated with c-Myc in tumorigenesis by inhibiting c-Myc-induced apoptosis via INK4a/ARF. *Genes and Development* **13**: 2678-2690.

James, M. and Peters, G. 2000. Alternative product of the p16/CDKN2A locus connects the Rb and p53 tumour suppressors. *Progress in cell cycle research* **4**: 71-81.

Jarrad, D., Sarkar, S., Shi, Y., Yeager, T., Magrane, G., Kinoshita, H., Nassif, N., Meisner, L., Newton, M., Waldman, F., and Reznikoff, C. 1999. p16/Rb pathway alterations are required for bypassing senescence in human prostate epithelial cells. *Cancer Research* **59**: 2957-2964.

Kamb, A., Gruis, N., Weaver-Feldhaus, J., Liu, Q., Harshman, K., Tavitian, S., Stockert, E., Day, R., Johnson, B., and Skolnick, M. 1994. A cell cycle regulator potentially involved in genesis of many tumor types. *Science* **264**: 436-439.

Kamijo, T., Bodner, S., van de Kamp, E., Randle, D., and Sherr, C. 1999. Tumor spectrum in *ARF*-deficient mice. *Cancer Research* **59**: 2217-2222.

Kamijo, T., Zindy, F., Roussel, M., Quelle, D., Downing, J., Ashmun, R., Grosveld, G., and Sherr, C. 1997. Tumour suppression at the mouse *INK4A* locus is mediated by the alternative reading frame product p19^{ARF}. *Cell* **91**: 649-659.

Karayan, L., Riou, J.-F., Seite, P., Migeon, J., Cantereau, A., and Larsen, C.-J. 2001. Human ARF protein interacts with Topoisomerase I and stimulates its activity. *Oncogene* **20**: 836-848.

Karlseder, J., Smogorzewska, A., and de Lange, T. 2002. Senescence induced by altered telomere state, not telomere loss. *Science* **295**: 2446-2449.

Kim, S.-H., Mitchell, M., Fujii, H., Llanos, S., and Peters, G. 2003. Absence of p16^{INK4a} and truncation of ARF tumor suppressors in chickens. *Proceedings of the National Academy of Science* **100**(1): 211-216.

Kondoh, H., Lleonart, M., Gil, J., Wang, J., Degan, P., Peters, G., Martinez, D., Carnero, A., and Beach, D. 2005. Glycolytic enzymes can modulate cellular lifespan. *Cancer Research* **65**(1): 177-185.

Korgaonkar, C., Hagen, J., Tompkins, V., Frazier, A., Allamargot, C., Quelle, F., and Quelle, D. 2005. Nucleophosmin (B23) targets ARF to nucleoli and inhibits its function. *Molecular and Cellular Biology*: 1258-1271.

Kozar, K., Ciemerych, M., Rebel, V., Shigematsu, H., Zagozdzon, A., Sicinska, E., Geng, Y., Yu, Q., Bhattacharya, S., Bronson, R., Akashi, K., and Sicinski, P. 2004. Mouse development in the absence of D-cyclins. *Cell* **118**: 477-491.

Krimpenfort, P., Quon, K., Mooi, W., Loonstra, A., and Berns, A. 2001. Loss of p16^{INK4A} confers susceptibility to metastatic melanoma in mice. *Nature* **413**: 83-86.

Krishnamurthy, J., Torrice, C., Ramsey, M., Kovalev, G., Al-Regaiey, K., Su, L., and Sharpless, N. 2004. Ink4A/Arf expression is a biomarker of aging. *Journal of Clinical Investigation* **114**(9): 1299-1307.

Kuo, M.-L., den Besten, W., Bertwistle, D., Roussel, M., and Sherr, C. 2004. N-terminal polyubiquitination and degradation of the Arf tumour suppressor. *Genes and Development* **18**: 1862-1874.

LaBaer, J., Garrett, M., Stevenson, L., Slingerland, J., Sandhu, C., Chou, H., Fattaey, A., and Harlow, E. 1997. New functional activities for the p21 family of CDK inhibitors. *Genes and Development* **11**: 847-862.

Lazarov, M., Kubo, Y., Cai, T., Dajee, M., Tarutani, M., Lin, Q., Fang, M., Tao, S., Green, C., and Khavari, P. 2002. CDK4 coexpression with Ras generates malignant human epidermal tumorigenesis. *Nature Medicine* **8**(10): 1105-1114.

Lee, A., Fenster, B., Ito, H., Takeda, K., Bae, N., Hirai, T., Yu, Z.-X., Ferrans, V., Howard, B., and Finkel, T. 1999. Ras proteins induce senescence by altering the intracellular levels of reactive oxygen species. *Journal of Biological Chemistry* **274**(12): 7936-7940.

Leesard, J. and Sauvageau, G. 2003. *Bmi-1* determines the proliferative capacity of normal and leukemic stem cells. *Nature* **423**: 255-260.

Li, G.-Z., Eller, M., Hanna, K., and Gilchrest, B. 2004a. Signalling pathway requirements for the induction of senescence by telomere homolog oligonucleotides. *Experimental Cell Research* **301**: 189-200.

Li, G.-Z., M., E., Firoozabadi, R., and Gilchrest, B. 2003. Evidence that exposure of the telomere 3' overhang sequence induces senescence. *Proceedings of the National Academy of Science* **100**(2): 527-531.

Li, Y., Wu, D., Chen, B., Ingram, A., He, L., Liu, L., Zhu, D., Kapoor, A., and Tang, D. 2004b. ATM activity contributes to the tumor-suppressing functions of p14^{ARF}. *Oncogene* **23**: 7355-7365.

Lin, A., Barradas, M., Stone, J., van Aelst, L., Serrano, M., and Lowe, S. 1998. Premature senescence involving p53 and p16 is activated in response to constitutive MEK/MAPK mitogenic signalling. *Genes and Development* **12**: 3008-3019.

Lingbeek, M., Jacobs, J., and van Lohuizen, M. 2002. The T-box repressors TBX2 and TBX3 specifically regulate the tumour suppressor gene p14^{ARF} via a variant T-site in the initiator. *Journal of Biological Chemistry* **277**(29): 26120-26127.

Littlewood, T., Danielian, H., Parker, M., and Evan, G. 1995. A modified oestrogen receptor ligand-binding domain as an improved switch for the regulation of heterologous proteins. *Nucleic Acids Research* **23**(10): 1686-1690.

Liu, X., Tesfai, J., Evrard, Y., Dent, S., and Martinez, E. 2003. c-Myc transformation domain recruits the human STAGA complex and requires TRRAP and GCN5 acetylase activity for transcription activation. *Journal of Biological Chemistry* **278**(22): 20405-20412.

Llanos, S., Clark, P., Rowe, J., and Peters, G. 2001. Stabilisation of p53 by p14^{ARF} without relocation of MDM2 to the nucleolus. *Nature Cell Biology* **3**: 445-452.

Lo, K.-W., Cheung, S.-T., Leung, S.-F., van Hasselt, A., Tsang, Y.-S., Mak, K.-F., Chung, Y.-F., Woo, J., Lee, J., and Huang, D. 1996. Hypermethylation of the *p16* gene in nasopharyngeal carcinomas. *Cancer Research* **56**: 2721-2725.

Lohrum, M., Ashcroft, M., Kubbutat, M., and Vousden, K. 2000. Contribution of two independent MDM2-binding domains in p14^{ARF} to p53 stabilization. *Current Biology* **10**: 539-542.

Maeda, T., Hobbs, R., Merghoub, T., Guernah, I., Zelent, A., Cordon-Cardo, C., Teruya-Feldstein, J., and Paolo Pandolfi, P. 2005. Role of the proto-oncogene *Pokemon* in cellular transformation and *ARF* repression. *Nature* **433**: 278-285.

Maestro, R., Dei Tos, A., Hamamori, Y., Krasnokutsky, S., Sartorelli, V., Kedes, L., Doglioni, C., Beach, D., and Hannon, G. 1999. *twist* is a potential oncogene that inhibits apoptosis. *Genes and Development* **13**: 2207-2217.

Malumbres, M., Sotillo, R., Sanatamaria, D., Galan, J., Cerezo, A., Ortega, S., Dubus, P., and Barbacid, M. 2004. Mammalian cells cycle without the D-type Cyclin-Dependent kinases Cdk4 and Cdk6. *Cell* **118**: 493-504.

Martelli, F., Hamilton, T., Silver, D., Sharpless, N., Bardeesy, N., Rokas, M., DePinho, R., Livingston, D., and Grossman, S. 2001. p19ARF targets certain E2F species for degradation. *Proceedings of the National Academy of Science* **98**(8): 4455-4460.

Martin-Ruiz, C., Saretzki, G., Petrie, J., Ladhoff, J., Jeyapalan, J., Wei, W., Sedivy, J., and von Zglinicki, T. 2004. Stochastic variation in telomere shortening rate causes heterogeneity of human fibroblast replicative lifespan. *Journal of Biological Chemistry* **279**(17): 17826-17833.

Mason, S., Loughran, O., and La Thangue, N. 2002. p14^{ARF} regulates E2F activity. *Oncogene* **21**: 4220-4230.

Massague, J. 2004. G1 cell-cycle control and cancer. *Nature* **432**: 298-306.

Matheu, A., Pantoja, C., Efeyan, A., Criado, L., Martin-Caballero, J., Flores, J., Klatt, P., and Serrano, M. 2004. Increased gene dosage of *Ink4a/Arf* results in cancer resistance and normal again. *Genes and Development* **18**: 2736-2746.

Mathon, N. and Lloyd, A. 2001. Cell senescence and cancer. *Nature Reviews Cancer* **1**: 203-213.

Matsuura, I., Denissova, N., Wang, G., He, D., Long, J., and Liu, F. 2004. Cyclin-dependent kinases regulate the anti-proliferative function of Smads. *Nature* **430**: 226-231.

McConnell, B., Starborg, M., Brookes, S., and Peters, G. 1998. Inhibitors of cyclin-dependent kinases induce features of replicative senescence in early passage human diploid fibroblasts. *Current Biology* **8**: 351-354.

McMahon, S., Van Buskirk, H., Dugan, K., Copeland, T., and Cole, M. 1998. The novel ATM-related protein TRRAP is an essential cofactor for the c-MYC and E2F oncoproteins. *Cell* **94**: 363-374.

McMurray, H. and McCance, D. 2003. Human papillomavirus type 16 E6 activates TERT gene transcription through induction of the c-Myc and release of USF-mediated repression. *Journal of Virology* **77**(18): 9852-9861.

Merlo, A., Herman, J., Mao, L., Lee, D., Gabrielson, E., Burger, P., Baylin, S., and Sidransky, D. 1995. 5' CpG island methylation is associated with transcriptional silencing of the tumour suppressor *p16/CDKN2/MTS1* in human cancers. *Nature Medicine* **1**(7): 686-692.

Meuweissen, R., Linn, S., van der Valk, M., Mooi, W., and Berns, A. 2001. Mouse model for lung tumorigenesis through Cre/lox controlled sporadic activation of the K-Ras oncogene. *Oncogene* **20**(6551-6558).

Michaloglou, C., Vredeveld, L., Soengas, M., Denoyelle, C., Kuilman, T., van der Horst, C., Majoor, D., Shay, J., Mooi, W., and Peeper, D. 2005. BRAF^{E600}-associated senescence-like cell cycle arrest of human naevi. *Nature* **436**(720-724).

Monzon, J., Liu, L., Brill, H., Goldstein, A., Tucker, M.A., From, L., McLaughlin, J., Hoog, D., and Lassam, N. 2004. *CDKN2A* mutations in multiple primary mutations. *New England Journal of Medicine* **338**(13): 879-887.

Morgenstern, J. and Land, H. 1990. Advanced mammalian gene transfer: high titre retroviral vectors with multiple drug selection markers and a complementary helper-free packaging cell line. *Nucleic Acids Research* **18**(12): 3587-3596.

Morris, M., Hepburn, P., and Wynford-Thomas, D. 2002. Sequential expression of proliferative lifespan in human fibroblasts induced by over-expression of CDK4 or 6 and loss of p53 function. *Oncogene* **21**: 4277-4288.

Munro, J., Barr, N., Ireland, H., Morrison, V., and Parkinson, K. 2004. Histone deacetylase inhibitors induce a senescence-like state in human cells by a p16-dependent mechanism that is independent of a mitotic clock. *Experimental Cell Research* **295**: 525-538.

Narita, M., Nunez, S., Heard, E., Narita, M., Lin, A., Hearn, S., Spector, D., Hannon, G., and Lowe, S. 2003. Rb-mediated heterochromatin formation and silencing of E2F target genes during cellular senescence. *Cell* **113**: 703-716.

Nilsson, K. and Landberg, G. 2005. Subcellular localization, modification and protein complex formation of the cdk-inhibitor p16 in Rb-functional and Rb-inactivated tumor cells. *International Journal of Cancer*.

Nishiwaki, E., Turner, S., Harju, S., S., M., Kashiwagi, M., Koh, J., and Serizawa, H. 2000. Regulation of CDK7-Carboxy-terminal domain kinase activity by the tumor suppressor p16^{INK4a} contributes to cell cycle regulation. *Molecular and Cellular Biology* **20**(20): 7726-7734.

Nobori, T., Miura, K., Wu, D., Lois, A., Takabayashi, K., and Carson, D. 1994. Deletions of the cyclin-dependent kinase-4 inhibitor gene in multiple human cancers. *Nature* **368**: 753-756.

O'Hagan, R., Ohh, M., David, G., Moreno de Alboran, I., Alt, F., Kaelin, W., and DePinho, R. 2000. Myc-enhanced expression of Cull1 promotes ubiquitin-dependent proteolysis and cell cycle progression. *Genes and Development* **14**: 2185-2191.

Oh, S., Kyo, S., and Laimins, L. 2001. Telomerase activation by human papillomavirus type 16 E6 protein: induction of human telomerase reverse

transcriptase expression through Myc and GC-rich Sp1 binding sites. *Journal of Virology* **75**(12): 5559-5566.

Ohtani, N., Zebedee, Z., Huot, T., Stinson, J., Sugimoto, M., Ohashi, Y., Sharrocks, A., Peters, G., and Hara, E. 2001. Opposing effects of Ets and Id proteins on p16^{INK4A} expression during cellular senescence. *Nature* **409**: 1067-1070.

Okamoto, A., Demetrick, D., Spillare, E., Hagiwara, K., Hussain, S., Bennett, W., Forrester, K., Gerwin, B., Serrano, M., Beach, D., and Harris, C. 1994. Mutations and altered expression of p16^{INK4} in human cancer. *Proceedings of the National Academy of Science* **91**: 11045-11049.

Olashaw, N., Bagui, T., and Pledger, W. 2004. Cell cycle control: a complex issue. *Cell Cycle* **3**(3): 263-264.

Ortega, S., Malumbres, M., and Barbacid, M. 2002. Cyclin D-dependent kinases, INK4 inhibitors and cancer. *Biochimica et Biophysica Acta* **1602**: 73-87.

Oruetxebarria, I., Venturini, F., Kekarainen, T., Houweling, A., Zuijerduijn, L., Mohd-Sarip, A., Vries, R., Hoeben, R., and Verrijzer, P. 2004. p16^{INK4A} is required for hSNF5 chromatin remodeler-induced cellular senescence in malignant rhabdoid tumour cells. *Journal of Biological Chemistry* **279**(5): 3807-3816.

Otterson, G., Khleif, S.C., W., Coxon, A., and Kaye, F. 1995. *CDKN2* gene silencing in lung cancer by DNA hypermethylation and kinetics of p16^{INK4a} protein induction by 5-aza 2'deoxyctidine. *Oncogene* **11**: 1211-1216.

Palmero, I., McConnell, B., Parry, D., Brookes, S., Hara, E., Bates, S., Jat, P., and Peters, G. 1997. Accumulation of p16^{INK4a} in mouse fibroblasts as a function of replicative senescence and not of retinoblastoma gene status. *Oncogene* **15**: 495-503.

Palmero, I., Pantoja, C., and Serrano, M. 1998. p19^{ARF} links the tumour suppressor p53 to Ras. *Nature* **395**: 125-126.

Pardal, R., Clarke, M., and Morrison, S. 2003. Applying the principles of stem-cell biology to cancer. *Nature Reviews Cancer* **3**: 895-901.

Park, I.-K., Qian, D., Kiel, M., Becker, M., Pihaija, M., Weissman, I., Morrison, S., and Clarke, M. 2003. Bmi-1 is required for the maintenance of adult self-renewing haematopoietic stem cells. *Nature* **423**: 302-305.

Parrinello, S., Samper, E., Krtolica, A., Goldstein, J., Melov, S., and Campisi, J. 2003. Oxygen sensitivity severely limits the replicative lifespan of murine fibroblasts. *Nature Cell Biology* **5**(8): 741-747.

Parry, D., Bates, S., Mann, D., and Peters, G. 1995. Lack of cyclin D-cdk complexes in Rb-negative cells correlates with high levels of p16^{INK4/MTS1} tumour suppressor gene product. *The EMBO Journal* **14**(3): 503-511.

Parry, D. and Peters, G. 1996. Temperature sensitive mutants of p16/CDKN2 associated with familial melanoma. *Molecular and Cellular Biology* **16**: 3844-3852.

Passegue, E. and Wagner, E. 2000. JunB suppresses cell proliferation by transcriptional activation of p16^{INK4A} expression. *The EMBO Journal* **19**(12): 2969-2979.

Pear, W., Nolan, G., Scott, M., and Baltimore, D. 1993. Production of high-titer helper-free retroviruses by transient transfection. *Proceedings of the National Academy of Science* **90**: 8392-8396.

Pei, X.-H. and Xiong, Y. 2005. Biochemical and cellular mechanisms of mammalian CDK inhibitors: a few unresolved issues. *Oncogene* **24**: 2787-2795.

Perez-Roger, I., Kim, S.-H., Griffiths, B., Sewing, A., and Land, H. 1999. Cyclins D1 and D2 mediate Myc-induced proliferation via sequestration of p27^{KIP1} and p21^{CIP1}. *The EMBO Journal* **18**(19): 5310-5320.

Pollice, A., Nasti, V., Ronca, R., Vivo, M., Lo Iacono, M., Calogero, R., Calabro, V., and La Mantia, G. 2004. Functional and physical interaction of the human ARF tumor suppressor with Tat-binding protein-1. *Journal of Biological Chemistry* **279**(8): 6345-6353.

Qi, Y., Gregory, M., Li, Z., Broussai, J., West, K., and Hann, S. 2004. p19^{ARF} directly and differentially controls the functions of c-Myc independently of p53. *Nature* **431**: 712-717.

Quelle, D., Ashmun, R., Hannon, G., Rehberger, P., Trono, D., Richter, K., Walker, C., Beach, D., Sherr, C., and Serrano, M. 1995a. Cloning and characterization of murine p16^{INK4a} and p15^{INK4b} genes. *Oncogene* **11**(4): 635-645.

Quelle, D., Cheng, M., Ashmun, R., and Sherr, C. 1997. Cancer-associated mutations at the *INK4a* locus cancel cell cycle arrest by p16^{INK4a} but not by the alternative reading frame protein p19^{ARF}. *Proceedings of the National Academy of Science* **94**: 669-673.

Quelle, D., Zindy, F., Ashmun, R., and Sherr, C. 1995b. Alternative reading frames of the *INK4a* tumor suppressor gene encode two unrelated proteins capable of inducing cell cycle arrest. *Cell* **83**: 993-1000.

Radfar, A., Unnikrishnan, I., Lee, H.-W., DePinho, R., and Rosenberg, N. 1998. p19^{ARF} induces p53-dependent apoptosis during Abelson virus-mediated

pre-B cell transformation. *Proceedings of the National Academy of Science* **95**: 13194-13199.

Ranade, K., Hussussian, C., Sikorski, R., Varmus, H., Goldstein, A., Tucker, M.A., Serrano, M., Hannon, G., Beach, D., and Dracopoli, N. 1995. Mutations associated with familial melanoma impair p16^{INK4} function. *Nature Genetics* **10**: 114-116.

Rangarajan, A., Hong, S., Gifford, A., and Weinberg, R. 2004. Species- and cell type-specific requirements for cellular transformation. *Cancer Cell* **6**: 171-183.

Ries, S., Biederer, C., Wods, D., Shifman, O., Shirasawa, S., Sasazuki, T., McMahon, M., Oren, M., and McCormick, F. 2000. Opposing effects of Ras on p53: transcriptional activation of *mdm2* and induction of p19^{ARF}. *Cell* **103**: 321-330.

Rizos, H., Darmanian, A., Holland, E., Mann, G.J., and Kefford, R.F. 2001. Mutations in the *INK4a/ARF* melanoma susceptibility locus functionally impair p14^{ARF}. *Journal of Biological Chemistry* **276**(44): 41424-41434.

Rizos, H., Darmanian, A., Mann, D., and Kefford, R.F. 2000. Two arginine rich domains in the p14^{ARF} tumour suppressor mediate nucleolar localization. *Oncogene* **19**(2978-2985).

Rizos, H., Woodruff, S., and Kefford, R.F. 2005. p14ARF interacts with the SUMO-conjugating enzyme Ubc9 and promotes the sumoylation of its binding partners. *Cell Cycle* **4**(4): 597-603.

Robertson, K. and Jones, P. 1998. The human ARF cell cycle regulatory gene promoter is a CpG island which can be silenced by DNA methylation and down-regulated by wild-type p53. *Molecular and Cellular Biology* **18**(11): 6457-6473.

Rocha, S., Garrett, M., Campbell, K., Schumm, K., and Perkins, N. 2005. Regulation of NF- κ B and p53 through activation of ATR and Chk1 by the ARF tumour suppressor. *The EMBO Journal* **24**: 1157-1169.

Rodway, H., Llanos, S., Rowe, J., and Peters, G. 2004. Stability of nucleolar versus non-nucleolar forms of human p14^{ARF}. *Oncogene* **23**(37): 6186-6192.

Romanov, S., Kozakiewicz, K., Holst, C., Stampfer, M., Haupt, L., and Tlsty, T. 2001. Normal human mammary epithelial cells spontaneously escape senescence and acquire genetic changes. *Nature* **409**: 633-637.

Ruas, M. and Peters, G. 1998. The p16^{INK4A}/CDKN2A tumour suppressor and its relatives. *Biochimica et Biophysica Acta* **1378**: F115-F177.

Rubio, M., Davalos, A., and Campisi, J. 2004. Telomere length mediates the effects of telomerase on the cellular response to genotoxic stress. *Experimental Cell Research* **298**: 17-27.

Russo, A., Tong, L., Lee, J.-O., Jeffrey, P., and Pavletich, N. 1998. Structural basis for inhibition of the cyclin-dependent kinase Cdk6 by the tumour suppressor p16^{INK4a}. *Nature* **395**: 237-243.

Sage, J., Miller, A., Perez-Mancera, P., Wysocki, J., and Jacks, T. 2003. Acute mutation of retinoblastoma gene function is sufficient for cell cycle re-entry. *Nature* **424**: 223-228.

Sakamuro, D. and Prendergast, G. 1999. New Myc-interacting proteins: a second Myc network emerges. *Oncogene* **18**: 2942-2954.

Satyanarayana, A., Greenberg, R., Schaetzlein, S., Buer, J., Masutomi, K., Hahn, W., Zimmerman, S., Martens, U., Manns, M., and Rudolph, K. 2004. Mitogen stimulation cooperates with telomere shortening to activate DNA damage responses and senescence signalling. *Molecular and Cellular Biology* **24**(12): 5459-5474.

Schmitt, C., McCurrach, M., de Stanchina, E., Wallace-Brodeur, R., and Lowe, S. 1999. *INK4a/ARF* mutations accelerate lymphomagenesis and promote chemoresistance by disabling p53. *Genes and Development* **13**: 2670-2677.

Seger, Y., Garcia-Cao, M., Piccinin, S., Cunsolo, C., Doglioni, C., Blasco, M., Hannon, G., and Maestro, R. 2002. Transformation of normal human cells in the absence of telomerase activation. *Cancer Cell* **2**: 401-413.

Seoane, J., Le, H.-V., and Massague, J. 2002. Myc suppression of the *p21^{CIP1}* cdk inhibitor influences the outcome of the p53 response to DNA damage. *Nature* **419**: 729-734.

Serrano, M., Gomez-Lahoz, E., DePinho, R., Beach, D., and Bar-Sagi, D. 1995. Inhibition of ras-induced proliferation and cellular transformation by p16INK4. *Science* **267**(5195): 249-252.

Serrano, M., Hannon, G., and Beach, D. 1993. A new regulatory motif in cell-cycle control causing specific inhibition of cyclin D/CDK4. *Nature* **366**: 704-707.

Serrano, M., Lee, H.-W., Chin, L., Cordon-Cardo, C., Beach, D., and DePinho, R. 1996. Role of the *INK4a* locus in tumor suppression and cell mortality. *Cell* **85**: 27-37.

Serrano, M., Lin, A., McCurrach, M., Beach, D., and Lowe, S. 1997. Oncogenic Ras provokes premature cell senescence associated with accumulation of p53 and p16^{INK4A}. *Cell* **88**(593-602).

Sharpless, N., Bardeesy, N., Lee, K.-H., Carrasco, D., Castrillon, D., Aguirre, A., Wu, E., Horner, J., and DePinho, R. 2001. Loss of p16^{Ink4a} with retention of p19^{Arf} predisposes mice to tumorigenesis. *Nature* **413**: 86-91.

Sharpless, N. and DePinho, R. 1999. The INK4A/ARF locus and its two gene products. *Current opinion in genetics and development* **9**: 22-30.

Sharpless, N., Kannan, K., Xu, J., Bosenberg, M., and Chin, L. 2003. Both products of the mouse INK4A/ARF locus suppress melanoma formation in vivo. *Oncogene* **22**(5055-5059).

Sharpless, N., Ramsey, M., Balasubramanian, P., Castrillon, D., and DePinho, R. 2004. The differential impact of p16^{INK4A} or p19^{ARF} deficiency on cell growth and tumorigenesis. *Oncogene* **23**: 379-385.

Sherr, C. and DePinho, R. 2000. Cellular senescence: mitotic clock or culture shock? *Cell* **102**: 407-410.

Sherr, C. and McCormick, F. 2002. The RB and p53 pathways in cancer. *Cancer Cell* **2**: 103-112.

Sherr, C. and Roberts, J. 1999. CDK inhibitors: positive and negative regulators of G1-phase progression. *Genes and Development* **12**: 1501-1512.

Sherr, C. and Weber, J. 2000. The Arf/p53 pathway. *Current opinion in genetics and development* **10**: 94-99.

Smogorzewska, A. and de Lange, T. 2002. Different telomere damage signalling pathways in human and mouse cells. *The EMBO Journal* **21**(16): 4338-4348.

Soufir, N., Avril, M., Chompret, A., Demenais, F., Bombléd, J., Spatz, A., Stoppa-Lyonnet, D., Benard, J., and Bressac-de Paillerets, B. 1998. Prevalence of p16 and CDK4 germline mutations in 48 melanoma-prone families in France. The French Familial Melanoma Study Group. *Human Molecular Genetics* **7**(2): 209-216.

Sreeramaneni, R., Chaudhry, A., McMahon, M., Sherr, C., and Inoue, K. 2005. Ras-Raf-ARF signaling depends on the Dmp1 transcription factor. *Molecular and Cellular Biology* **25**(1): 220-232.

Staller, P., Peukert, K., Kiermaier, A., Seoane, J., Lukas, J., Karsunky, H., Moroy, T., Bartek, J., Massague, J., Hanel, F., and Eilers, M. 2001. Repression of p15^{INK4b} expression by Myc through association with Miz-1. *Nature Cell Biology* **3**: 392-399.

Stein, G., Drullinger, L., Soulard, A., and Dulic, V. 1999. Differential roles for the Cyclin-dependent kinase inhibitors p21 and p16 in the mechanisms of senescence and differentiation in human fibroblasts. *Molecular and Cellular Biology* **19**(3): 2109-2117.

Stewart, S., Hahn, W., O'Connor, B., Banner, E., Lundberg, A., Modha, P., Mizuno, H., Brooks, M., Fleming, M., Zimonjic, D., Popescu, N.C., and Weinberg, R. 2002. Telomerase contributes to tumorigenesis by a telomere length-independent mechanism. *Proceedings of the National Academy of Science* **99**(20): 12606-12611.

Stewart, S. and Weinberg, R. 2002. Senescence: does it all happen at the ends? *Oncogene* **21**: 627-630.

Stone, S., Jiang, P., Dayananth, P., Tavtigian, S., Katcher, H., Parry, D., Peters, G., and Kamb, A. 1995. Complex structure and regulation of the *p16* (*MTS1*) locus. *Cancer Research* **55**: 2988-2944.

Stott, F., Bates, S., James, M., McConnell, B., Starborg, M., Brookes, S., Palmero, I., Ryan, K., Hara, E., Vousden, K., and Peters, G. 1998. The alternative product from the human CDKN2A locus, p14^{ARF}, participates in a regulatory feedback loop with p53 and MDM2. *The EMBO Journal* **17**(17): 5001-5014.

Sugimoto, M., Kuo, M.-L., Roussel, M., and Sherr, C. 2003. Nucleolar arf tumour suppressor inhibits ribosomal RNA processing. *Molecular Cell* **11**: 415-424.

Suzuki, H., Kurita, M., Mizumoto, K., Moriyama, M., Aiso, S., Nishimoto, I., and Matsuoka, M. 2005. The ARF tumor suppressor inhibits BCL6-mediated

transcriptional repression. *Biochemical and Biophysical Research Communications* **326**: 242-248.

Suzuki, H., Kurita, M., Mizumoto, K., Moriyama, M., Aiso, S., Nishimoto, I., Ogata, E., and Matsuoka, M. 2003. p19^{ARF}-induced p53-independent apoptosis largely occurs through BAX. *Biochemical and Biophysical Research Communications* **312**: 1273-1277.

Tago, K., Chiocca, S., and Sherr, C. 2005. Sumoylation induced by the Arf tumor suppressor: a p53-independent function. *Proceedings of the National Academy of Science* **102**(21): 7689-7694.

Takai, H., Smogorzewska, A., and de Lange, T. 2003. DNA damage foci at dysfunctional telomeres. *Current Biology* **13**: 1549-1556.

Takaki, T., Fukasawa, K., Suzuki-Takahashi, I., Semba, K., Kitagawa, M., Taya, Y., and Hirai, H. 2005. Preferences for phosphorylation sites in the Retinoblastoma protein of D-type Cyclin-Dependent Kinases, Cdk4 and Cdk6, *In Vitro. Journal of Biochemistry* **137**(3): 381-386.

Tuveson, D., Shaw, A., Willis, N., Silver, D., Jackson, E., Chang, S., Mercer, K., Grochow, R., Hock, H., Crowley, D., Hingorani, S., Zaks, T., King, C., Jacobetz, M., Wang, L., Bronson, R., Orkin, S., DePinho, R., and Jacks, T. 2004. Endogenous oncogenic *K-ras*^{G12D} stimulates proliferation and widespread neoplastic and developmental defects. *Cancer Cell* **5**: 375-387.

van der Wetering, M., Oving, I., Muncan, V., Tjon Pon Fong, M., Brantjes, H., van Leenen, D., Holstege, F., Brummelkamp, T., Agami, R., and Clevers, H. 2003. Specific inhibition of gene expression using a stably integrated, inducible small-interfering-RNA vector. *EMBO Reports* **4**(6): 609-615.

Vance, K., Carreira, S., Brosch, G., and Goding, C. 2004. Tbx2 is overexpressed and plays an important role in maintaining proliferation and suppression of senescence in Melanomas. *Cancer Research* **65**(6): 2260-2268.

Vaziri, H. and Benchimol, S. 1998. Reconstitution of telomerase activity in normal human cells leads to elongation of telomeres and extended replicative lifespan. *Current Biology* **8**: 279-282.

Veldman, T., Liu, X., Yuan, H., and Schlegel, R. 2003. Human papillomavirus E6 and Myc proteins associate *in vivo* and bind to and cooperatively activate the reverse transcriptase promoter. *Proceedings of the National Academy of Science* **100**(14): 8211-8216.

Voorhoeve, P. and Agami, R. 2003. The tumour-suppressive functions of the human INK4A locus. *Cancer Cell* **4**: 311-319.

Vries, R., Bezrookove, V., Zuijderduijn, L., Kia, S., Houweling, A., Oruetebarria, I., Raap, A., and Verrijzer, P. 2005. Cancer associated mutations in chromatin remodeler hSNF5 promote chromosomal instability by compromising the mitotic checkpoint. *Genes and Development* **19**: 665-670.

Wadhwa, R., Suigihara, T., Hasan, K., Taira, K., Reddel, R., and Kaul, S. 2002. A major functional difference between the mouse and human ARF tumour suppressor proteins. *Journal of Biological Chemistry* **277**(39): 36665-36670.

Wagner, M., Brosch, G., Zwerschke, W., Seto, E., Loidl, P., and Jansen-Durr, P. 2001. Histone deacetylases in replicative senescence: evidence for a senescence-specific form of HDAC-2. *FEBS letters* **499**: 101-106.

Wainwright, B. 1994. Familial melanoma and p16 - a hung jury. *Nature Genetics* **8**: 3-5.

Walker, G., Gabrielli, B., Castellano, M., and Hayward, N. 1999. Functional reassessment of p16 variant using a transfection-based assay. *International Journal of Cancer* **82**: 305-312.

Wang, J., Hannon, G., and Beach, D. 2000. Risky immortalization by telomerase. *Nature* **405**: 755-756.

Wang, J., Xie, L., Allan, S., Beach, D., and Hannon, G. 1998. Myc activates telomerase. *Genes and Development* **12**: 1769-1774.

Wang, W., Chen, J., Liao, R., Deng, Q., Zhou, J. Huang, S., and Sun, P. 2002. Sequential activation of the MEK-extracellular signal-regulated kinase and MKK3/6-p38 mitogen-activated protein kinase pathways mediates oncogenic

Ras-induced premature senescence. *Molecular and Cellular Biology* **22**(10): 3389-3403.

Weber, J., Jeffers, J., Rehg, J., Randle, D., Lozano, G., Roussel, M., Sherr, C., and Zambetti, G. 2000a. p53-independent functions of the p19^{ARF} tumor suppressor. *Genes and Development* **14**: 2358-2365.

Weber, J., Kuo, M.-L., Bothner, B., DiGammarino, E., Kriwacki, R., Roussel, M., and Sherr, C. 2000b. Cooperative signals governing ARF-Mdm2 interaction and nucleolar localization of the complex. *Molecular and Cellular Biology* **20**(7): 2517-2528.

Weber, J., Taylor, L., Roussel, M., Sherr, C., and Bar-Sagi, D. 1999. Nucleolar ARF sequesters Mdm2 and activates p53. *Nature Cell Biology* **1**: 20-27.

Wei, W., Hemmer, R., and Sedivy, J. 2001. Role of p14^{ARF} in replicative and induced senescence of human fibroblasts. *Molecular and Cellular Biology* **21**(20): 6748-6757.

Wei, W., Herbig, U., Wei, S., Dutriaux, A., and J., S. 2003a. Loss of retinoblastoma but not p16 function allows bypass of replicative senescence in human fibroblasts. *EMBO Reports* **4**(11): 1061-1066.

Wei, W., Jobling, W., Chen, W., Hahn, W., and Sedivy, J. 2003b. Abolition of cyclin-dependent kinase inhibitor p16^{Ink4a} and p21^{Cip1/Waf1} functions permits Ras-induced anchorage independent growth in telomerase-immortalized fibroblasts. *Molecular and Cellular Biology* **23**(8): 2859-2870.

Wei, W. and Sedivy, J. 1999. Differentiation between senescence (M1) and crisis (M2) in human fibroblast cultures. *Experimental Cell Research* **253**: 519-522.

Wolfel, T., Hauer, M., Schneider, J., Serrano, M., Wolfel, C., Klehmann-Hieb, E., De Plaen, E., Hankeln, T., Meyer zum Buschenfelde, K., and Beach, D. 1995. A p16INK4a-insensitive CDK4 mutant targeted by cytolytic T lymphocytes in a human melanoma. *Science* **269**(5288): 1281-1284.

Wood, M., McMahon, S., and Cole, M. 2000. An ATPase/helicase complex is an essential cofactor for oncogenic transformation by c-Myc. *Molecular Cell* **5**: 321-330.

Woods, Y., Xirodimas, D., Prescott, A., Sparks, A., Lane, D., and Saville, M. 2004. p14Arf promotes small ubiquitin-like modifier conjugation of Werner's helicase. *Journal of Biological Chemistry* **279**(48): 50157-50166.

Wright, W., Pereira-Smith, O., and Shay, J. 1989. Reversible cellular senescence: implications for immortalization of normal human diploid fibroblasts. *Molecular and Cellular Biology* **9**(7): 3088-3092.

Wright, W. and Shay, J. 2002. Historical claims and current interpretations of replicative aging. *Nature Biotechnology* **20**: 682-688.

Wu, K.-J., Grandori, C., Amacker, M., Simon-Vermot, N., Polack, A., Lingner, J., and Dalla-Favera, R. 1999. Direct activation of *TERT* transcription by c-MYC. *Nature Genetics* **21**: 220-224.

Xiong, Y., Zhang, H., and Beach, D. 1993. Subunit rearrangement of the cyclin-dependent kinases is associated with cellular transformation. *Genes and Development* **7**: 1572-1583.

Xue, L., Wu, J., Zheng, W., Wang, P., Li, J., Zhang, Z., and Tong, T. 2004. Sp1 is involved in the transcriptional activation of p16^{INK4A} by p21^{WAF1} in HeLa cells. *FEBS letters* **564**: 199-204.

Yarborough, W., Buckmire, R., Bessho, M., and Liu, E. 1999. Biologic and biochemical analyses of p16^{INK4a} mutations from primary tumours. *Journal of the National Cancer Institute* **91**(18): 1569-1574.

Yeh, E., Cunningham, M., Arnold, H., Chasse, D., Monteith, T., Ivaldi, G., Hahn, W., Stukenberg, T., Shenolikar, S., Uchida, T., Counter, C., Nevins, J., Means, A., and Sears, R. 2004. A signalling pathway controlling c-Myc degradation that impacts oncogenic transformation of human cells. *Nature Cell Biology* **6**(4): 308-318.

Zhang, Y. and Xiong, Y. 1999. Mutations in human *ARF* exon 2 disrupt its nucleolar localization and impair its ability to block nuclear export of MDM2 and p53. *Molecular Cell* **3**: 579-591.

Zheng, W., Wang, H., Xue, L., Zhang, Z., and Tong, T. 2004. Regulation of cellular senescence and p16^{INK4a} expression by *Id1* and E47 proteins in human diploid fibroblasts. *Journal of Biological Chemistry* **279**(30): 31524-31532.

Zhu, J., Woods, D., McMahon, M., and Bishop, J.M. 1998. Senescence of human fibroblasts induced by oncogenic Raf. *Genes and Development* **12**: 2997-3007.

Zindy, F., Eischen, C., Randle, D., Kamijo, T., Cleveland, J., Roussel, M., and Sherr, C. 1998. Myc signaling via the ARF tumor suppressor regulates p53-dependent apoptosis and immortalization. *Genes and Development* **12**: 2424-2433.

Zindy, F., Williams, R., Baudino, T., Rehg, J., Skapek, S., Cleveland, J., Roussel, M., and Sherr, C. 2003. Arf tumour suppressor promoter monitors latent oncogenic signals in vivo. *Proceedings of the National Academy of Science* **100**(26): 15930-15935.

Zuo, L., Weger, J., Yang, Q., Goldstein, A., Tucker, M.A., Walker, G., Hayward, N., and Dracopoli, N. 1996. Germline mutations in the p16INK4a binding domain of CDK4 in familial melanoma. *Nature Genetics* **12**: 97-99.

